Drosophila Mage, a component of Smc5/6 DNA response complex, confers resistance to caffeine and genotoxic stress and plays a role in the cell cycle and cell survival

by

Xiao Li

A thesis submitted in partial fulfillment of the requirements for the degree of

Doctor of Philosophy

in
Medical Sciences – Medical Genetics

University of Alberta

Abstract

Over 50 Melanoma-associated antigen (MAGE) genes have been identified in the human genome. They share a conserved 200 amino acid MAGE-homology domain (MHD). In yeast, the only MAGE homolog (Nse3) is a component of the Smc5/6 DNA damage response complex. In humans, MAGE proteins influence cell cycle and cell survival via interaction with Rb-E2F and p53 pathways and some MAGE proteins interact with the human Smc5/6 complex as well. Only one MAGE gene (*MAGE)* exists in the genome of the fruit fly *Drosophila melanogaster*.

I hypothesize that the functions of the MAGE proteins are conserved during evolution. Drosophila Mage is part of Smc5/6 complex and plays a role in the DNA damage response. It may also regulate the cell cycle and cell survival by interacting with Drosophila p53 (Dmp53).

I found that Mage bound to Smc5/6 components (i.e. Nse1 and Nse4) in co-immuno-precipitation and *in vitro* pull-down experiments. I generated Drosophila mutants of *MAGE, Smc5, Smc6,* and *Nse1* and found that all mutants were viable, but hypersensitive to caffeine and genotoxic agents. I also studied the effects of Mage over-expression in a Drosophila cell line and found that over-expression of Mage slows cell proliferation by arresting cells in S and M phases. Further, over-expression of Mage also confers a growth advantage to cells exposed to genotoxic stress. I also found an interdependency of protein stability between Mage and its interaction partners including Smc5, Smc6, Nse4, Nse1 and p53. Finally, unlike a human MAGE homolog, Necdin, which interacts with p53 directly,

I did not detect an interaction between Mage and Dmp53, however, I did find Nse4 and Dmp53 associate.

Like other Smc5/6 gene mutants, *MAGE* mutants are also caffeine-sensitive and Mage physically interacts with the Drosophila homologs of the Nse proteins suggesting that the structure of the Smc5/6 complex is conserved in Drosophila. Although Smc5/6 proteins are required for viability in *S. cerevisiae*, they are not essential under normal circumstances in Drosophila. However, flies carrying mutations in *Smc5*, *Smc6*, *Nse1* or *MAGE* are hypersensitive to genotoxic agents, consistent with a role for the Smc5/6 complex in genome stability. Like Necdin, over-expression of Mage inhibits cell proliferation and promotes cell survival. This result could be explained by the direct interaction with the Smc5/6 complex and the indirect interaction with Dmp53.

This study reveals a conserved role of Mage as a part of Smc5/6 DNA response complex in maintaining genome stability. It also hints at a functional link between p53 and the Smc5/6 complex. Together, these data will help to uncover how this expanded protein family plays such versatile roles in cancer and development in humans.

Preface

The research work described in Chapter 2 of this thesis is published as

Li, X., Zhuo, R., Tiong, S., Di Cara, F., King-Jones, K., Hughes, S.C., Campbell, S.D., and Wevrick, R. (2013). The Smc5/Smc6/MAGE complex confers resistance to caffeine and genotoxic stress in Drosophila melanogaster. PLoS ONE *8*, e59866.

Co-first authors: XL and RZ. Conceived and designed the experiments: XL RZ ST FDC SDC SCH KK-J RW. Performed the experiments: XL RZ ST FDC. Analyzed the data: XL RZ ST FDC SDC SCH KK-J RW. Wrote the paper: XL RZ SDC SCH KK-J RW. I was responsible for experiments described in figures 2-2(B-D), 2-3B, 2-4, 2-5, 2-6, 2-7, 2-9, 2-8 (RZ prepared the samples and I carried out the confocal microscopy and data analysis) and tables 2-1, 2-2, 2-3, 2-4, 2-5.

The rest of this thesis is an original work by me and has not been published previously.

Acknowledgements

I would like to thank my mentor, Dr. Rachel Wevrick, for her guidance and support through the years. Her contribution to this work has been invaluable. I thank Dr. Sarah Hughes, who co-supervised me on my thesis work and introduced me into Drosophila genetics, for her support and encouragement. I thank my supervisory committee member Dr. Andrew Simmonds for his support and advice. I also thank the former members of my supervisory committee, Drs. Moira Glerum and Fred Berry, for their advice.

I thank the supports of the former and present members of Dr. Wevrick lab. Special thanks to Dr. Jason Bush for generously sharing his ideas and helping me set up my first few experiments, to Jocelyn Bischof and Dr. Rebecca Mercer for helping me settle down in my early days.

I thank the supports from the Drosophila community of the University of Alberta. I thank Dr. Hua Deng for sharing his expertise in Drosophila genetics and protein purification. I thank Albert Leung for his advice on the *in vitro* pull-down experiment. I thank David Primrose for his advice on culturing S2 cells. Special thanks to Dr. Shelagh Campbell, Ran Zhuo, Dr. Ellen Homola and Dr. Joseph Ayeni for their advice on a few experiments.

The friendship from my colleagues from the Hughes lab, the Simmonds lab, the Campbell lab, the King-Jones lab and the labs in the Department of Medical Genetics, has made my graduate student life more enjoyable.

I thank my family for their support and unconditional love.

I thank the University of Alberta for providing me with studentships and the *Cancer Research Society* (*CRS)* for providing the operating funding to my project.

Table of Contents

List of Tables

List of Figures

List of Abbreviations

ATM	ataxia telangiectasia mutated
ATR	ataxia telangiectasia and Rad3 related
BDSC	Bloomington Drosophila Stock Center
BSA	bovine serum albumin
CPT	camptothecin
CP3	Cleaved caspase 3
ddt	double double trouble
DGRC	Drosophila Genetic Resource Center at Kyoto
DGRC	the Drosophila Genomics Resource Center, Indiana University
DOX	doxorubicin
EID-1	E1A-like inhibitor of differentiation 1
EGUF	Ey-GAL4/UAS-FLP
EMS	Ethyl methanesulfonate
FRT	Flippase Recognition Target
HR	Homologous recombination
HU	hydroxyurea
IAP	inhibitor of apoptosis
IR	ionizing radiation
jnj	java no jive
KZNF	KRAB domain containing zinc finger transcription factor
MAGE	melanoma associated antigen
MAGE-I	Type I MAGE
MAGE-II	Type II MAGE
MHC	major histocompatibility complex
MHD	MAGE homology domain
MMS	methyl methanesulfonate
NB	nuclear body
Nse	Non SMC Element
NTR	neurotrophin receptor
RNAi	RNA interference
SEM	Scanning electron microscopy
SMC	Structural Maintenance of Chromosomes
sst	sleepness in seattle
TAP	Tandem affinity purification
TrkA	tropomyosin-related kinase A
VDRC	Vienna Drosophila RNAi Center
WH	winged-helix motifs

XIAP	X-linked inhibitor of apoptosis

Chapter 1 Introduction

Multiple *Melanoma associated antigen* (*MAGE*) genes have been identified in humans. MAGE proteins are multiple-function cellular adapters that participate in many cellular processes and play diverse roles in development and tumorigenesis. Mutations in two members of this gene family, *NDN* and *MAGEL2*, contribute to a rare genetic disorder, Prader-Willi syndrome. Over-expression of some MAGE proteins in tumors correlates with poor prognosis in many cancer types.

1.1 MAGE

1.1.1 Human MAGEs

The first *melanoma associated antigen* (*MAGE*) gene (*MAGEA1*) was identified as a gene encoding an antigen presented by the major histocompatibility complex (MHC) class I on a human melanoma and recognized by cytotoxic T lymphocytes (Van Der Bruggen *et al.* 1991). We now know that placental mammals (Eutheria) have multiple *MAGE* genes in their genomes. Based on expression patterns, human *MAGE* genes are grouped into two classes (Barker and Salehi 2002). Type I *MAGE* genes (15 *MAGEAs*, 11 *MAGEBs* and three *MAGECs*) are only expressed in germ cells, trophoblasts, and many cancers. Type II *MAGE* genes (five *MAGEDs*, two *MAGEEs*, two *MAGEFs*, *MAGEH1*, *NDNL2* (*MAGEG1*), *MAGEL2* and *NDN*) are expressed broadly in many tissues (Barker and Salehi 2002; Sasaki *et al.* 2005). The genes in the human *MAGE* gene family share a conserved MAGE homology domain (MHD) (Figure 1-1) and are derived from a single ancestral *MAGE* gene via retro transposition and gene duplication (Chomez *et al.* 2001; Katsura and Satta 2011).

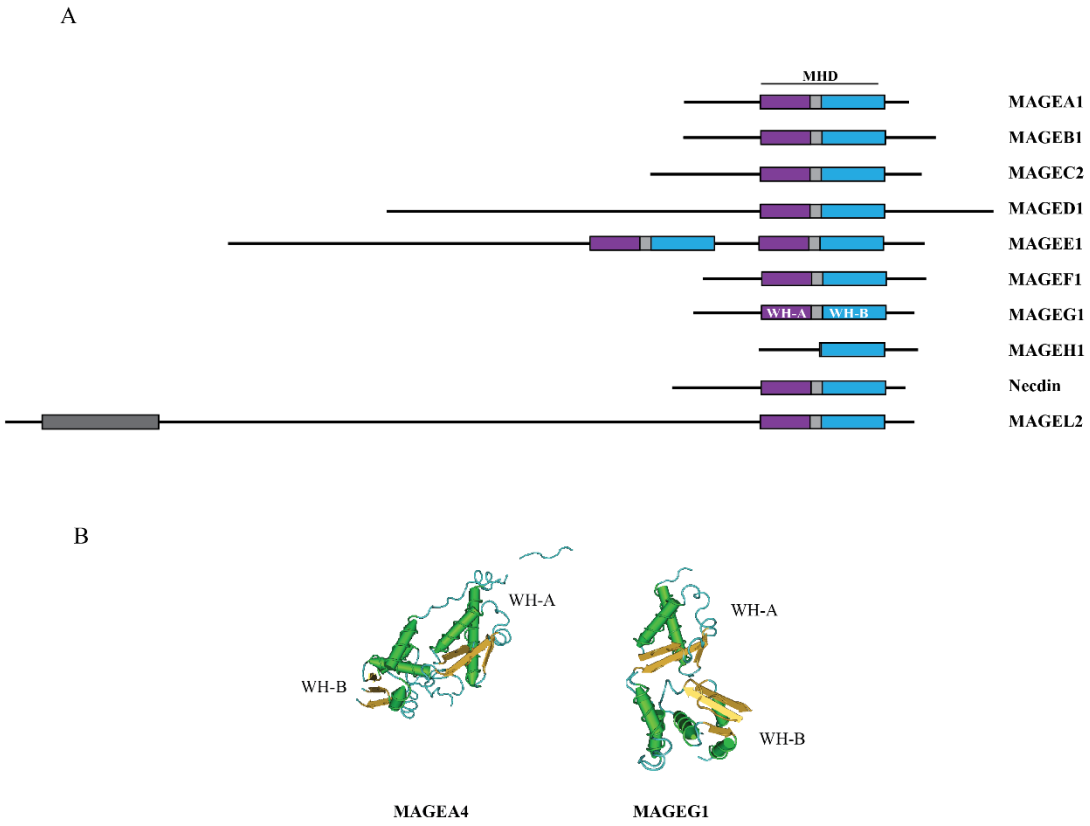

Figure 1-1 Human MAGEs and crystal structures of two MAGE proteins.

(A) One representative member from each *MAGE* gene group is shown. The MAGE homolog domain and its position in the protein sequence is identified by searching conserved homology domains in the reference protein sequences of the selected MAGE proteins using the conserved domain search from the NCBI's interface. (B) The crystal structures of free MAGEA4 and MAGEG1 in complex with NSE1 (not shown) are shown. Structures (2WA0 and MAGEG1 portion of 3NW0) are visualized in the Cn3D macromolecular structure viewer (Wang *et al.* 2000).

1.1.1.1 Type I MAGE (MAGE-I)

The three *MAGE-I* gene clusters (*A*, *B* and *C*) are located on the X chromosome (Ross *et al.* 2005). MAGE-I proteins were among a set of cancer/testis (CT) antigens that includes over 204 members (Almeida *et al.* 2009). *MAGE-I* expression is restricted in immune-privileged tissues such as testes and placenta. In many cancers, *MAGE-I* are aberrantly expressed due to global DNA hypomethylation. Short peptides derived from degraded MAGE-I proteins, presented on the cell surface by the MHC class I molecules, can be recognized by cytolytic T lymphocytes and lead to tumor rejection. For this reason, MAGE antigens are attractive targets in cancer immunological therapies (Sang *et al.* 2011a; De Carvalho *et al.* 2012; Imai *et al.* 2012). The tumor-specific expression patterns also make MAGE-I proteins diagnostic indicators and prognosis markers (Ladelfa *et al.* 2012). Aberrant *MAGE-I* expression is also important in tumorigenesis and resistance to chemotherapeutic agents. Despite the great interest from the oncology field, the physiological functions of MAGE-I proteins remain poorly researched.

1.1.1.1.1 MAGEA

MAGEA were identified more than twenty years ago, and despite extensive studies using them as targets for immunotherapy against tumors (Imai *et al.* 2012; Meek and Marcar 2012; Hartmann *et al.* 2013), their physiological roles in germ cells remain elusive. Most studies on this family of proteins have been conducted in tumor cells where their expression is high due to promoter demethylation (Bhan *et al.* 2011). Expression of *MAGEA* has been implicated in survival of multiple cancers (Atanackovic *et al.* 2010; Nardiello *et al.* 2011; Bhan *et al.* 2012).

MAGEAs interact and regulate activities of many transcriptional regulators. MAGEA1 interacts with SKIP, a transcriptional adaptor to DNA binding proteins, via its C-terminus and the deacetylase HDAC1 to repress transcription (Laduron *et al.* 2004). A cleaved form of MAGEA4 interacts with the POZ domain/zinc finger transcription factor Miz-1 to down regulate the transcription of p21 (Sakurai *et al.* 2004). A few MAGEA members have also been shown to interact with and repress p53 activities. MAGEA2 (A1, and A6) interacts with and represses p53 activity via DNA binding domain by recruiting the transcription repressor HDAC3 to p53 transcription sites (Monte *et al.* 2006). A follow

up study showed that MAGEA2, but not MAGEA4, interacts with and represses PML-induced p53 acetylation at PML-NBs to regulate cellular senescence (Peche *et al.* 2012). MAGEAs (A2, A3, and A6) and other MAGE-Is (MAGEC2) can also interact with a RING containing E3 ubiquitin ligase, TRIM28, to regulate p53 protein (Yang *et al.* 2007; Doyle *et al.* 2010) and KRAB domain containing zinc finger transcription factor (KZNF) levels (Bhatia *et al.* 2011; Xiao *et al.* 2011). In addition, MAGEAs inhibit p53 function by blocking its interaction with chromatin (Marcar *et al.* 2010). In turn, p53 can regulate MAGEA protein levels by a positive feedback loop involving the micro RNA, miR-34 (Weeraratne *et al.* 2011).

MAGEA11 is a primate-specific MAGEA gene. MAGEA11 interacts with the androgen receptor (AR) and increases its activity (Bai *et al.* 2005). Further study shows that the functional interaction is regulated by ubiquitination and phosphorylation of MAGEA11 (Askew *et al.* 2009), recruitment of the p160 steroid receptor co-activator, TIF2, and the p300 histone acetyltransferase (Askew *et al.* 2009; Askew *et al.* 2010), and bridging of AR dimers by MAGEA11 (Minges *et al.* 2012). MAGEA11 also regulates isoform-specific human progesterone receptor-B transactivation (Su *et al.* 2012)

The crystal structure of MAGEA4 has been solved (Figure 1-1; PDB: 2WA0). The MHD contains two winged-helix motifs (WH-A and WH-B).

1.1.1.1.2 MAGEB

Other than a few studies on the expression of these genes in cancer and reports of related vaccine development (Nagashima *et al.* 2001; Mou *et al.* 2004; Sypniewska *et al.* 2005; Gravekamp *et al.* 2008; Kim *et al.* 2008; Castro *et al.* 2009; Singh *et al.* 2013), we know very little about the gene family. Like MAGEAs, they interact with TRIM28 and suppress p53-dependent apoptosis (Yang *et al.* 2007).

1.1.1.1.3 MAGEC

The three *MAGEC* genes are formed by duplication of an ancestral *MAGEA* gene followed by further duplication (Katsura and Satta 2011). MAGEC1 interacts with another cancer-testis antigen, NY-ESO-1(Cho *et al.* 2006), homologous to a yeast transcription factor Pcc1p which is a component of the highly conserved KEOPS/EKC complex that has

been implicated in transcription, telomere maintenance and tRNA modification (Downey *et al.* 2006; Kisseleva-Romanova *et al.* 2006; Srinivasan *et al.* 2011). MAGEC3 interacts with TRIM28 and suppresses p53 dependent apoptosis in a few MAGE-positive cancer cell lines (Yang *et al.* 2007). The interaction of MAGEC2 with TRIM28 also leads to regulation of KZNF mediated gene repression (Xiao *et al.* 2011). MAGEC2 promotes survival of melanoma cells and forms a complex with ATM and TRIM28 and enhances TRIM28 phosphorylation by ATM in response to DNA damage (Bhatia *et al.* 2013). Very recently, the transcription co-repressor BS69 is identified as a new target for the MAGEC2-TRIM28 E3 ubiquitin ligase (Hao *et al.* 2014).

1.1.1.2 Type II MAGE (MAGE-II)

MAGE-II are broadly expressed in many tissues. They include the *MAGED* (*MAGED1-4* and *MAGED4B*) and *MAGEE* (*MAGEE1-2*) families and *MAGEF1*, *MAGEH1*, *MAGEL2*, *NDN*, *NDNL2* (*MAGEG1*) genes.

1.1.1.2.1 NDN (encoding Necdin)

Necdin is the best characterized MAGE member. Early work was primarily carried out by the Yoshikawa group, who first identified Necdin in a screen for genes involved in the neural differentiation of P19 cells (Maruyama *et al.* 1991). They determined that Necdin is expressed in postmitotic neurons (Aizawa *et al.* 1992; Hayashi *et al.* 1995; Uetsuki *et al.* 1996; Andrieu *et al.* 2003) and observed that over-expression of Necdin causes cell cycle arrest in transformed cell lines (Hayashi *et al.* 1995), presumably by interacting with E2F1 and p53 (Taniura *et al.* 1998; Taniura *et al.* 1999). They postulated that Necdin is a growth suppressor that promotes neural differentiation and survival (Kobayashi *et al.* 2002; Takazaki *et al.* 2002). By yeast-two-hybrid screen, they also identified two other Necdin interacting partners, a calcium binding protein, NEFA (Taniguchi *et al.* 2000), and a heterogeneous nuclear ribonucleoprotein U (hnRNP U) (Taniura and Yoshikawa 2002). However, the physiological significance of these interactions remains unclear.

In the late 1990s, after the *NDN* gene was localized in the *Prader-Willi* syndrome region (Macdonald and Wevrick 1997; Sutcliffe *et al.* 1997; Nakada *et al.* 1998), other

groups have identified additional interaction partners of Necdin, and established several lines of *NDN* null mice as a models for Prader-Willi syndrome (Gerard *et al.* 1999; Tsai *et al.* 1999; Muscatelli *et al.* 2000; Kuwako *et al.* 2005).

Necdin is highly expressed in the nervous system and plays roles in proliferation, differentiation, migration, and survival. Like MAGED1, *in vitro* studies show that Necdin (as well as MAGEH1 and MAGEG1) interacts with the p75 neurotrophin receptor (NTR), and p75 NTR can sequester Necdin in the cytoplasm, which reduces its association with E2F1 (Tcherpakov *et al.* 2002; Kuwako *et al.* 2004). Studies using *NDN* mice reveal that Necdin facilitates the association between p75NTR and another NTR, the tropomyosin-related kinase A (TrkA) receptor tyrosine kinase, to promote sensory neuron survival (Kuwako *et al.* 2005). Necdin also protects embryonic motor neurons from programmed cell death mediated by the TNF-receptor 1 pathway (Aebischer *et al.* 2011). Necdin's interaction with NTRs also contributes to neuronal resistance to oxidative stress (Ingraham and Schor 2009; Ingraham *et al.* 2011). *NDN* null mice have defects in axonal outgrowth and migration (Lee *et al.* 2005; Tennese *et al.* 2008). Over-expression of Necdin leads to accelerated neurite outgrowth in PC12 cells and cultured cortical neurons and this effect can be suppressed by Nogo-A, presumably by retaining Necdin in the cytoplasm (Liu *et al.* 2009a). Presumably due to its interaction with Msx/Dlx family proteins via MAGED1, Necdin is required for the proper migration of neocortical interneurons from the basal forebrain in mice (Kuwajima *et al.* 2010). Recent studies show that Necdin also has a role in neural stem cell proliferation and apoptosis (Huang *et al.* 2013; Minamide *et al.* 2014). In neural stem cells, Necdin and a Polycomb group protein Bmi1 interact and antagonize each other in regulating the cell cycle: Necdin relieves the transcriptional repression on a CDK inhibitor, p16, by Bmi1; Bmi1 counteracts the Necdin-mediated suppression of the E2F1-dependent transcription of Cdk1. The protein levels of Necdin are also regulated in neural stem cells, where Necdin is targeted to the ubiquitin proteasome for degradation by HIF-2α (Huang *et al.* 2013). Necdin forms a complex with the transcription factor Foxo1 and the HDAC Sirturin1 in hypothalamic arcuate neurons to modulate the thyroid axis by controlling Foxo1 acetylation status (Hasegawa *et al.* 2012).

Necdin has also been implicated in muscle development. Necdin interacts with the Msx2 homeodomain protein via MAGED1 to promote myogenic differentiation of C2C12

cells (Kuwajima *et al.* 2004). Necdin is expressed in myogenic precursor cells, mediates skeletal muscle regeneration, and promotes myoblast differentiation and survival (Deponti *et al.* 2007). Necdin interacts with the E1A-like inhibitor of differentiation 1 (EID-1) and promotes myoblast differentiation (Bush and Wevrick 2008). Necdin enhances myoblast survival by facilitating the degradation of the mediator of apoptosis CCAR1/CARP1(Francois *et al.* 2012). Necdin enhances muscle reconstitution of dystrophic muscle by vessel-associated progenitors, by promoting cell survival and myogenic differentiation (Pessina *et al.* 2012)

In hematopoietic stem cells (HSCs), *NDN* is a p53 target and regulates HSC quiescence and resistance to genotoxic stress (Liu *et al.* 2009b; Asai *et al.* 2012). In another study, Necdin restricts proliferation of hematopoietic stem cells during hematopoietic regeneration (Kubota *et al.* 2009).

Studies suggest that Necdin plays an inhibitory role in both white and brown adipocyte differentiation (Tseng *et al.* 2005; Goldfine *et al.* 2006; Bush and Wevrick 2012). The Insulin/IGF-I signaling pathway down-regulates Necdin to promote differentiation of brown adipocytes (Cypess *et al.* 2011). Necdin controls proliferation of white adipocyte progenitor cells (Fujiwara *et al.* 2012). Necdin also participate in hepatic stellate cell activation, a process similar to adipocyte-preadipocyte de-differentiation by targeting canonical Wnt (Zhu *et al.* 2010).

Studies also suggest that Necdin plays a role in cancer. *NDN* is hypermethylated and mutated in human cancer (De Faveri *et al.* 2013); and is also identified as a novel STAT3 target gene down-regulated in human cancer (Haviland *et al.* 2011). In principle, Necdin could contribute to tumorigenesis by negatively regulating p53 in tumors with wild-type p53 such as neuroblastoma, melanoma, and breast cancers (Papageorgio *et al.* 2007).

In summary, Necdin is a cellular adaptor which interacts with several transcription factors, HDACs, and many other proteins, and participates in diverse processes such as cell cycle regulation, promoting cell survival, migration and differentiation. Several mechanisms by which Necdin regulates its interaction partners are evident (Figure 1-2). One mechanism by which Necdin regulates transcription factor activity is to recruit HDAC to control acetylation level of transcription factors as in the cases of p53 and Foxo1

(Hasegawa and Yoshikawa 2008). Necdin could also function by altering the nucleo-cytoplasm localization of its interaction partners (Bush and Wevrick 2008). Necdin also recruits E3 ubiquitin ligases to target its interaction partners for degradation (Francois *et al.* 2012; Gur *et al.* 2014). Necdin also binds directly to DNA and affects transcription of its target genes (Matsumoto *et al.* 2001; Zhu *et al.* 2010) Finally, its own activity is also regulated by different mechanisms, including control of transcription and translation (Liu *et al.* 2009b; Haviland *et al.* 2011; Weeraratne *et al.* 2011; Lafontaine *et al.* 2012), change in cellular localization (Kuwako *et al.* 2004; Liu *et al.* 2009a; Lavi-Itzkovitz *et al.* 2012), antagonistic interplay with transcription factors (Minamide *et al.* 2014), and degradation by the proteasome pathway (Huang *et al.* 2013).

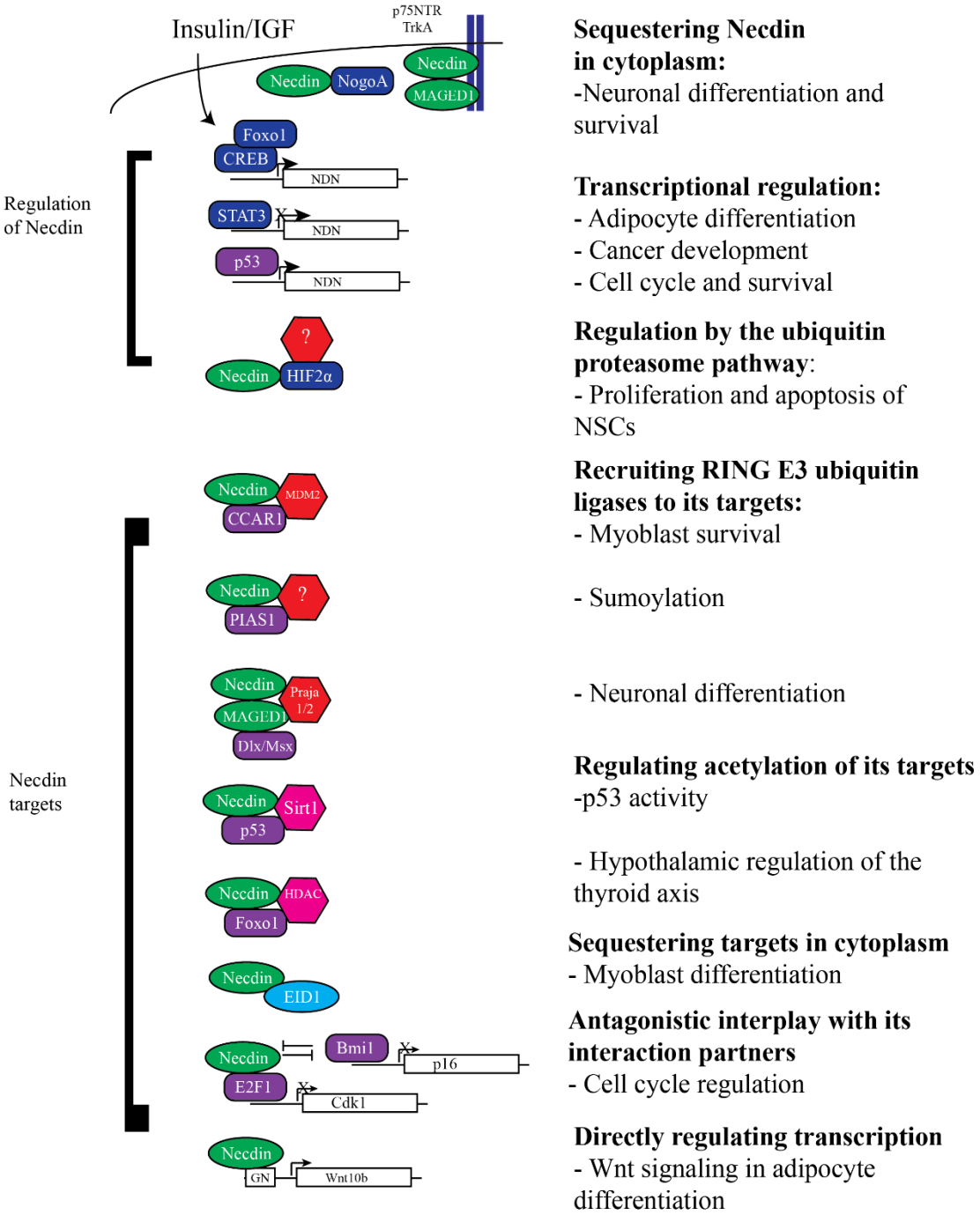

Figure 1-2 Necdin interaction partners and major pathways involved.

1.1.1.2.2 MAGED

The founding member of the *MAGED* family, *MAGED1* was identified in 1999 and was found to be expressed ubiquitously in normal tissues (Lucas *et al.* 1999; Pold *et al.* 1999; Kubu *et al.* 2000). Using yeast two-hybrid screens, several groups identified many interaction partners of MAGED1, including the p75NTR (Salehi *et al.* 2000), the X-linked inhibitor of apoptosis (XIAP) protein (Jordan *et al.* 2001), the homeodomain protein Dlx5 (Masuda *et al.* 2001), the RING finger domain containing protein Praja1 (Sasaki *et al.* 2002), the axon guidance receptor UNC5H1 (Williams *et al.* 2003), the receptor tyrosine kinase Ror2 (Matsuda *et al.* 2003), BRCA2 (Tian *et al.* 2005), and an apoptosis regulator Che-1 (Di Certo *et al.* 2007). These and some of the follow-up *in vitro* studies suggest roles in differentiation, apoptosis, and cell cycle regulation. MAGED1 works with Necdin and interacts with the Msx/Dlx homeodomain transcription factors to facilitate myogenic differentiation (Kuwajima *et al.* 2004) and GABAergic neuron differentiation (Kuwajima *et al.* 2006); The association with the cell surface signaling receptor Ror could sequester MAGED1 in the cytoplasm to modulate nuclear function of MAGED1; MAGED1 also interacts with two other cell surface signaling receptors, p75NTR and UNC5H1, to promote apoptosis. An additional study also shows that MAGED1 interacts with another NGF receptor, TrkA, and modulates NGF induced neuronal differentiation of PC12 cells (Feng *et al.* 2010; Reddy *et al.* 2010). In the cytoplasm, MAGED1 interacts with the IAPs and Che-1 to regulate apoptosis. MAGED1 can also be regulated by proteasome-dependent degradation via interaction with the E3 ubiquitin ligase PRAJA1. Like Necdin, MAGED1 was shown to have a role in the cell cycle: over-expression of MAGED1 in cancer cell lines suppressed proliferation (Salehi *et al.* 2000; Du *et al.* 2009; Reddy *et al.* 2011); BRCA2 stabilized MAGED1 thereby suppressing cell proliferation, independent of p53 (Tian *et al.* 2005). Depending on cell lines used, MAGED1 can also inhibit proliferation in a p53-dependent manner (Wen *et al.* 2004).

Studies using knockout mice confirmed that at least some of these interactions have *in vivo* relevance. MAGED1 is involved in p75NTR signaling-dependent apoptosis in the nervous system (Bertrand *et al.* 2008). MAGED1 regulates skeletal myogenic differentiation and muscle regeneration presumably by promoting p63/73-dependent $p21^{CIP1/WAF1}$ expression (Nguyen *et al.* 2010). Studies in mice also uncovered novel roles

of MAGED1 in circadian rhythm regulation involving targeting circadian clock genes via an interaction with the nuclear receptor RORα (Wang *et al.* 2010), and in the serotonergic nervous system by interacting with the serotonin transporter and promoting its ubiquitination (Mouri *et al.* 2012). Refer to Figure 1-3 for a summary of the interaction partners and major pathways involved.

Other MAGED members are much less well studied. MAGED2 is expressed ubiquitously (Langnaese *et al.* 2001) and identified as a negative regulator of p53 (Papageorgio *et al.* 2007). MAGED2 suppresses TRAIL receptor 2 expression in a p53 dependent manner, and protects against TRAIL-induced apoptosis in human melanoma cells (Tseng *et al.* 2012). Over-expression of MAGED3 (Magphinin) suppresses cell proliferation of mammalian cell lines (Saburi *et al.* 2001). Over-expression of MAGED4B increases cell migration and growth in oral squamous cell carcinoma and is associated with poor disease outcome (Chong *et al.* 2012).

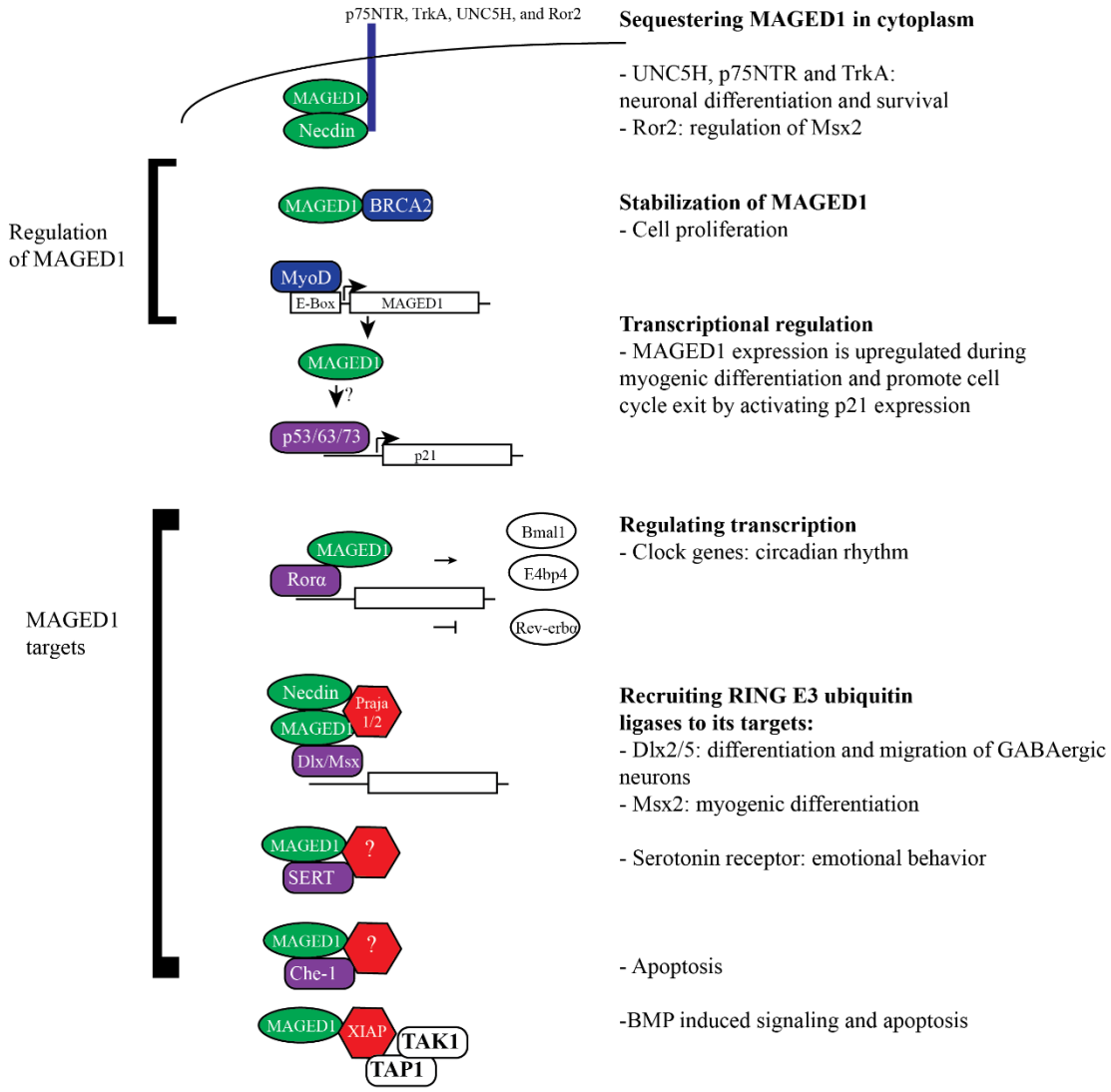

Figure 1-3 MAGED1 interaction partners and major pathways involved

1.1.1.2.3 MAGEE1/2

MAGEE1/2 contain two MHDs at the C terminus and they are poorly characterized. (not to be confused with MAGE-D4 which was originally named MAGE-E1). MAGEE1 interacts with dystrobrevin and associates with the dystrophin complex (Albrecht and Froehner 2004).

1.1.1.2.4 MAGEF1/2

MAGEF1 is localized on chromosome 3 in humans and is ubiquitously expressed in normal tissues and a few tumors (Chomez *et al.* 2001; Stone *et al.* 2001). MAGEF1 is most similar to MAGEG1 by sequence (Barker and Salehi 2002; Doyle *et al.* 2010). MAGEF1 interacts with Nse1, the E3 ubiquitin ligase from the Smc5/6 complex, another E3 ubiquitin ligase TRIM27 and the SUMO E3 ligase PIAS1 (Doyle *et al.* 2010; Gur *et al.* 2014). In addition, MAGEF1 interacts with EID family proteins, homologs of Nse4 of the Smc5/6 complex (Hudson *et al.* 2011).

1.1.1.2.5 NDNL2 (MAGEG1)

NDNL2 is located on chromosome 15 and ubiquitously expressed in embryonic and adult tissues (Chibuk *et al.* 2001). Like Necdin, it is a growth repressor, interacts with E2F1, suppresses E2F1-induced apoptosis in differentiated neuroblastoma cells and also interacts with p75NTR (Kuwako *et al.* 2004). MAGEG1 is also part of the human Smc5/6 complex (Taylor *et al.* 2008). Doyle et al. solved the crystal structure of MAGEG1-NSE1 protein complex in 2010 (Doyle *et al.* 2010) (PDB: 3NW0) The MAGEG1 MHD (amino acids 78–295) consists of WH-A and WH-B motifs that are very similar to those of MAGEA4 (Figure 1-1B). The relative orientation of WH-A and WH-B is different in the MAGEA4 and MAGEG1 structures due to a conformational change of MAGEG1 upon binding of Nse1.

1.1.1.2.6 MAGEH1

Like *NDN*, the cDNA of MAGEH1 was identified in a subtractive screen for genes differentially expressed during retinoic acid-induced differentiation of a leukemia cell line

(Zhao *et al.* 2002). The MAGEH1 only contains half of the MHD, corresponding to the WH-B motif. MAGEH1 interacts with p75NTR *in vitro* (Tcherpakov *et al.* 2002).

1.1.1.2.7 MAGEL2

MAGEL2 is the other (the other one is *NDN)* paternally expressed *MAGE* gene in the PWS region and is highly expressed in the hypothalamus (Boccaccio *et al.* 1999) (Lee *et al.* 2000). Studies on *MAGEL2* knockout mice suggest that MAGEL2 is required for normal circadian output (Kozlov *et al.* 2007), reproductive function (Mercer and Wevrick 2009), and leptin-mediated depolarization of POMC neurons in the hypothalamic arcuate nucleus (Mercer *et al.* 2013). Other phenotypes include growth abnormalities (Bischof *et al.* 2007), regionally reduced brain volume, altered serotonin neurochemistry, abnormal behavior (Mercer *et al.* 2009), and hypothalamic dysregulation of endocrine functions (Schaller *et al.* 2010; Tennese and Wevrick 2011). The mechanisms of MAGEL2 in maintenance of normal hypothalamic function are poorly understood. An *in vitro* study using cultured cells showed that a truncated version of MAGEL2 interacts with core circadian rhythm proteins and alters their sub-cellular distribution and activities (Devos *et al.* 2011). Another recent study in cultured cells showed that MAGEL2 interacts with the E3 ubiquitin ligase TRIM27 and regulates endosomal transport (Hao *et al.* 2013).

1.1.1.3 Summary

The diverse functions of MAGE proteins manifest through their ability to interact with many proteins. However, the biological significance of many reported interactions are as yet unclear. The MAGE family proteins have been studied by identifying and characterizing their interactions with other cellular proteins and they have emerged as a class of cellular adaptor proteins that regulate cell cycle, apoptosis, neuronal functions, differentiation, and regeneration in many tissue types. Only selected members have been extensively studied and the physiological roles of the majority of family members remain unknown. A few common interaction partners are shared among MAGE members, including Nse4/EIDs, RING E3 ubiquitin ligases, p53, E2F1/4, HDACs, E3 SUMO ligase PIAS1/2/4 and p75NTR (Figure 1-4).

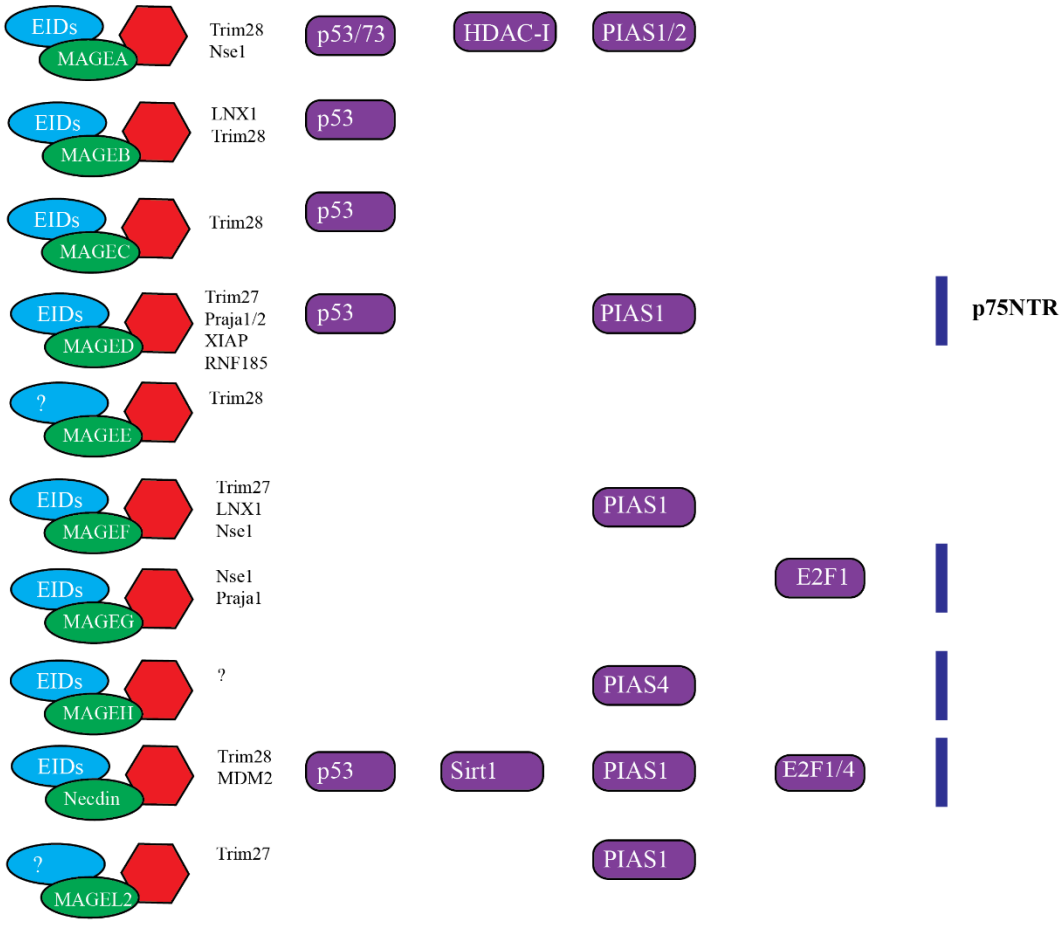

Figure 1-4 Common interaction partners shared between different MAGE families. Interactions shared by at least two MAGE groups are shown.

1.1.2 MAGE in other species

It appears that the MAGE family genes, characterized by the conserved MHD (pfam01454: MAGE) in the protein sequence, is found in all eukaryotes, including animals, fungi, green plants and protists (Barker and Salehi 2002; Lopez-Sanchez *et al.* 2007). With the exception of opossums, which have two, non-placental animals have only one MAGE gene in their genome (Figure 1-5). The zebrafish *MAGE* is expressed in the maturing central nervous system and the protein sequence is closest to the mouse MAGEG1. (Bischof *et al.* 2003). The chicken *MAGE* is weakly expressed throughout the embryo, and highly expressed in the nervous system. Similar to some MAGE-II proteins (Necdin, MAGED1, MAGEG1 and MAGEH1), *in vitro* experiments suggest that the chicken MAGE interacts with the intracellular domain of p75NTR and E2F1 to modulate apoptosis (Lopez-Sanchez *et al.* 2007). Drosophila *MAGE* (*MAGE*) is a single exon gene located on the right arm of chromosome 3 (84C7). The gene encodes a protein of 232 amino acids that contains the MHD (amino acids 33-202). The MHD shares 30%, 27%, and 26% identity with those of human MAGEB16, MAGEL2, and Necdin, respectively. Previous studies suggest that the Drosophila MAGE may play a role in cell cycle regulation and in maintaining the survival of neurons (Nishimura *et al.* 2007; Nishimura *et al.* 2008). In addition to the expression in early embryonic development and the nervous system, Mage is abundant in adult flight muscle and in the ovary (Nishimura *et al.* 2007). Though a few mammalian MAGE proteins and the chicken MAGE protein interact with E2F1 to regulate cell cycle (Taniura *et al.* 1998; Kuwako *et al.* 2004; Kurita *et al.* 2006; Lopez-Sanchez *et al.* 2007), no direct interaction between Mage and Drosophila E2F1 has been found (Nishimura *et al.* 2008).

The MHD from the yeast Nse3 to the human MAGEG1 is highly conserved (Figure 1-5). Unlike some MAGE-II proteins such as MAGEDs, MAGEEs and MAGEL2, the majority of the MAGE proteins from non-placental species have the MHD at the center of the sequence with very small flanking regions, resembling the structures of MAGEG1, Necdin, MAGEF1 and some of the type I MAGEs (Figure 1-5B).

A

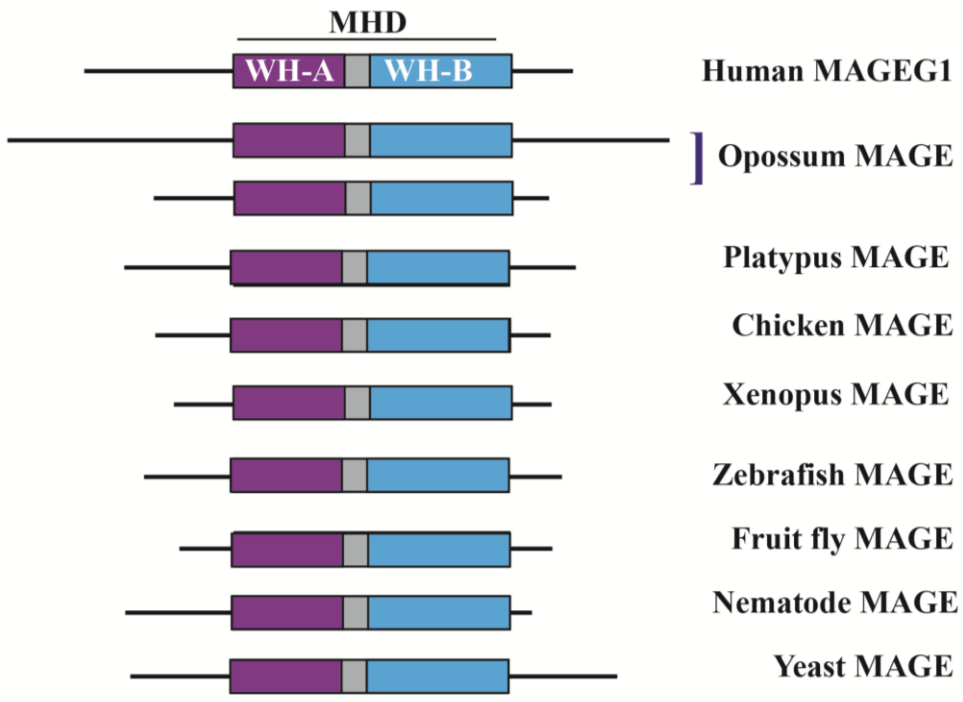
MHD
WH-A
WH-B
Human MAGEG1
Opossum MAGE
Platypus MAGE
Chicken MAGE
Xenopus MAGE
Zebrafish MAGE
Fruit fly MAGE
Nematode MAGE
Yeast MAGE

B

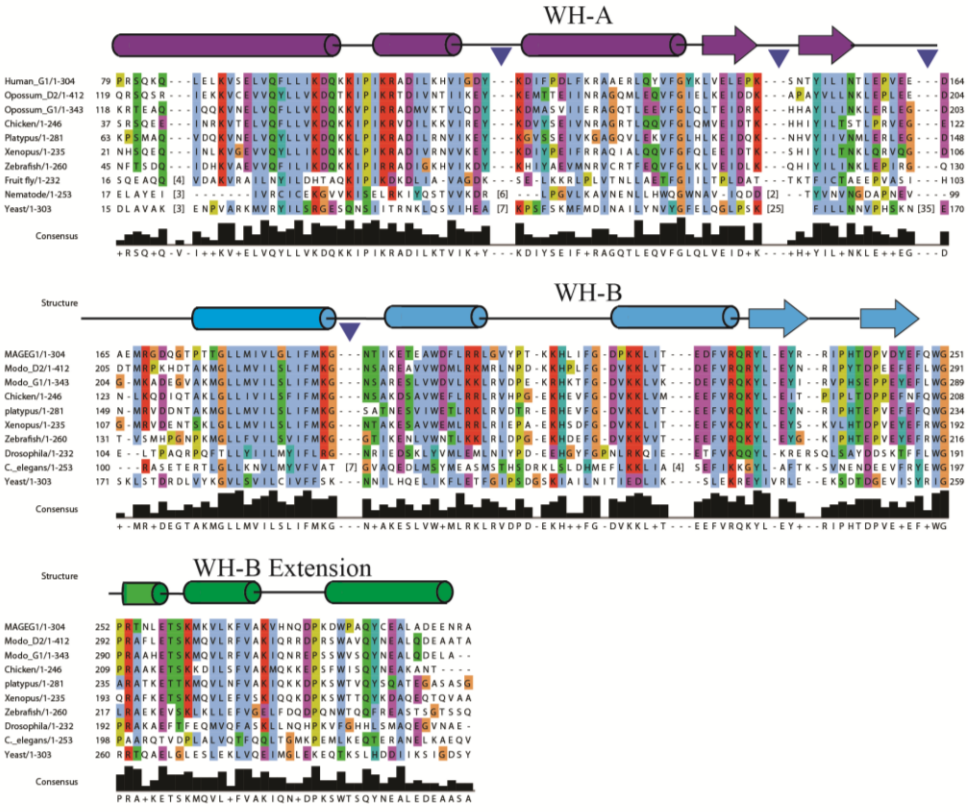
WH-A
WH-B
WH-B Extension
Structure
Consensus

-

Figure 1-5 MAGE is conserved among species.

(A) Structures of MAGE proteins from different species. The MAGE homolog domain and its position in the protein sequence is identified by searching conserved homology domains in the reference protein sequences of the selected MAGE proteins using the conserved domain search from the NCBI's interface. (B) Sequence alignment of MHDs from different species. Triangles and [ ] indicate extra nonconserved sequence regions that are not shared by other members (mainly resulted from the yeast MAGE sequence). The alignment was done using Cobalt Constraint-based Multiple Protein Alignment Tool (Papadopoulos and Agarwala 2007) and visualized using Jalview (Waterhouse *et al.* 2009). The Winged-Helix-A and B structures were redrawn based on Doyle et al. 2010

1.2 Smc5/6 complex

The Smc5/6 complex belongs to a family of evolutionarily conserved Structural Maintenance of Chromosomes (SMC) protein complexes, which are essential for the organization, segregation, and stability of the genome (Lehmann 2005; Hirano 2006; Wu and Yu 2012). Three functionally distinct SMC complexes have been defined in eukaryotes: cohesin (the Smc1/3 complex), condensin (the Smc2/4 complex), and the Smc5/6 complex. Cohesin holds sister chromatids together after DNA replication and plays important roles in regulation of gene expression and DNA repair (Dorsett and Strom 2012), while condensin is essential for mitotic chromosome organization and segregation (Cuylen and Haering 2011). The Smc5/6 complex is less well characterized but is required for proper DNA repair by homologous recombination, resolution of chromosomes during cell division, a late step during DNA replication and regulation of gene silencing (Kegel and Sjogren 2010).

The founding studies on the Smc5/6 complex, analyzing the mutant phenotypes, the architecture, and cellular function, have been mainly carried out in *Saccharomyces cerevisiae* and *Schizosaccharomyces pombe*. The yeast Smc5/6 complex consists of Smc5, Smc6, and six nonstructural maintenance of chromosome element (Nse) proteins. Similar to the other two well characterized Smc proteins (SMC1/3 in cohesin and SMC2/4 in condesin), Smc5 or Smc6 proteins consist of an amino terminus globular domain that contains a Walker A motif, a carboxyl terminus globular domain that contains a Walker B motif, and a middle hinge domain (Figure 1-6A). The protein folds back on itself in the hinge domain, which brings the Walker A motif and Walker B motif together to form an ATPase. The ATPase is connected to the hinge via an antiparallel coiled coil. Similar to the cohesin and condensin complexes, Smc5 and Smc6 heterodimerize via the hinge domains (Figure 1-6B). Nse 2 binds to Smc5 at the coiled coil domain. Nse1, Nse3, and Nse4 form a subcomplex and bridge the globular ends of Smc5 and Smc6. The Nse5/6 heterodimer associates with Smc5/6 near the globular heads for the fission yeast complex or at the hinge for the budding yeast complex (Figure 1-6B).

All components of the Smc5/6 complex are essential in *S. cerevisiae* (Zhao and Blobel 2005), and, except for Nse5 and Nse6, also in *S. pombe* (Pebernard *et al.* 2006).

Conditional mutations of any of the Smc5/6 components in yeast, confers hypersensitivity to genotoxic agents such as UV, ionizing radiation, methyl methanesulfonate, and hydroxyurea. Epistasis experiments placed the Smc5/6 genes in the Rad51- and Rad52-dependent homologous recombination (HR) DNA repair pathway. It is thought that the Smc5/6 complex functions in the late steps of HR and is required to prevent the accumulation of and/or resolve recombination structures that form between sister chromatids (Kegel and Sjogren 2010). However, the exact molecular mechanism to achieve this remains unclear. Possible mechanisms includes working with the cohesin complex to properly organize sister chromatids to facilitate DSB repair; positioning the SUMO ligase (Nse2) at the blocked replication forks; modulating the Mph1 helicase to prevent recombination at blocked forks and/or helping to resolve recombination structures formed by Mph1. In addition to a role in DNA repair by HR, to explain why Smc5/6 components are essential for viability, a non-repair topological function on replicating chromosomes is also proposed for the Smc5/6 complex (Kegel and Sjogren 2010).

Six of the human components corresponding to Smc5, Smc6, and Nse1-4 have been identified and shown to form a complex (Taylor *et al.* 2001; Harvey *et al.* 2004; Potts and Yu 2005; Palecek *et al.* 2006; Taylor *et al.* 2008; Hudson *et al.* 2011) (Figure 1-6). Human Smc5/6 proteins are highly expressed in testis and associate with meiotic sex chromosomes, suggesting a role in meiosis (Taylor *et al.* 2001). The human complex forms a stable complex *in vivo* and all the components, except Nse2, are required for the stability of the other components (Taylor *et al.* 2008).

Very little is known about the Drosophila Smc5/6 complex. During the course of my study, Chiolo et al. found that the Drosophila Smc5 and Smc6 are required for proper DNA repair of ionizing radiation-induced damage in heterochromatic regions (Chiolo *et al.* 2011). The names of the subunits vary among *Schizosaccharomyces pombe*, *Saccharomyces cerevisiae*, *Drosophila melanogaster,* and humans. Refer to Table 2-4 for species-specific names and aliases.

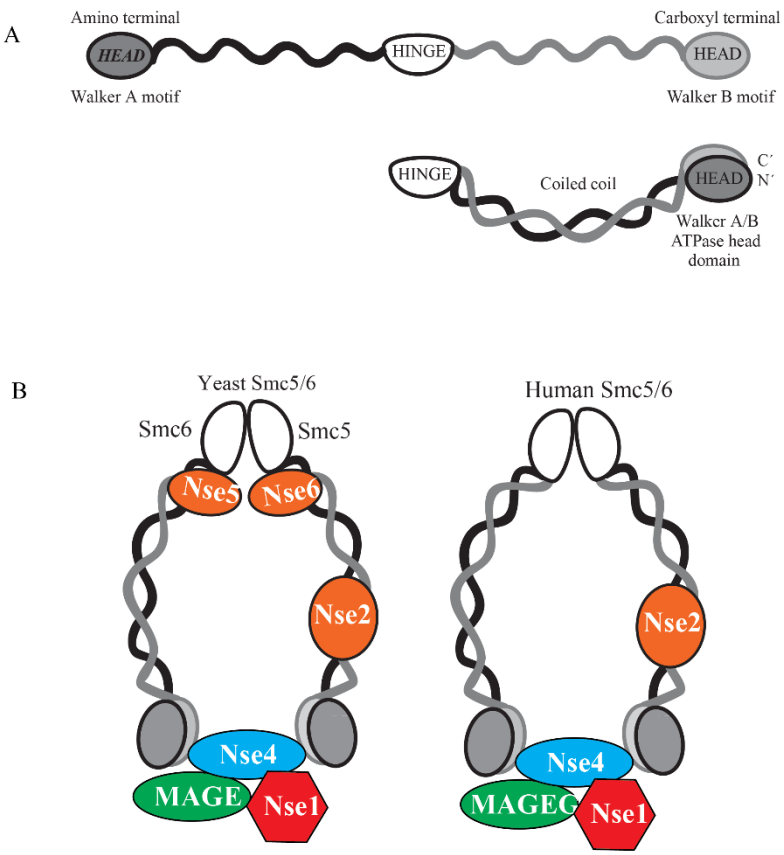

Figure 1-6 Structure of Smc5/6 complex in yeast and humans

(A) Structure of SMC proteins. (B) Structure of yeast and human Smc5/6 complex (adapted from Kegel et al. 2010)

1.3 Drosophila as a model organism for studying human diseases

The fruit fly, *Drosophila melanogaster*, is a well-established genetic model organism for studying the molecular mechanisms of human diseases. The genome is relatively small with 14,000 genes, yet covers nearly 75% of disease-related genes (Pandey and Nichols 2011). The life cycle is short and it is relatively easy to maintain lines and generate mutations. Molecular genetic tools are readily available for spatio-temporal expression of transgenes, mosaic analysis, and forward and reverse genetic screens (St Johnston 2013; Griffin *et al.* 2014). There are also primary and transformed cell lines available and many of them are amenable for taking up dsRNAs suitable for gene depletion studies *in vitro* (Bai *et al.* 2008; Rogers and Rogers 2008; Sepp *et al.* 2008; Bai *et al.* 2009; Bettencourt-Dias and Goshima 2009).

1.4 Rationale and hypotheses

The high sequence similarity, physical interactions, and overlapping expression patterns among a large number of members make it very hard to study MAGE proteins *in vivo*. Therefore, I reasoned that studying the MAGE function in a model organism where only one *MAGE* gene exists would be advantageous to revealing the *in vivo* functions of the *MAGE* gene and understanding the conserved functions of MAGE proteins among different species. I researched the feasibility to study MAGE in a few model organisms and at last chose to start the project in Drosophila because of the availability of a few potential *MAGE* mutants, transgene strains and MAGE antibodies.

Prior to the beginning of this project in early 2009, two groups had studied the Drosophila *MAGE* gene. The first group identified the gene based on sequence similarity with human and mouse MAGE proteins and determined the cDNA sequence (Pold *et al.* 2000). The second group reported expression patterns of *MAGE* during Drosophila development and a role in controlling neural precursor proliferation in postembryonic neurogenesis, based on phenotypes caused by RNAi mediated knockdown in flies (Nishimura *et al.* 2007; Nishimura *et al.* 2008). A Drosophila genome-wide yeast two-hybrid screen had previously identified a MAGE interacting protein encoded by CG13142 (Giot *et al.* 2003). CG13142 is the homolog of fission yeast Nse4 and the mammalian

EID2/EID3 (NSE4A/NSE4B). In yeast, Nse4 and the MAGE related protein Nse3 are both components of SMC5/6 complex (Pebernard *et al.* 2004; Sergeant *et al.* 2005). In 2008, MAGEG1 had been just identified as a component of the human SMC5/6 complex, along with EID2/EID3 (Taylor *et al.* 2008). As well, our laboratory had just found that Necdin interacts with EID1, another homolog of the yeast Nse4 (Bush and Wevrick 2008). Further, as described in Figure 2-6 of this thesis, MAGE and the Drosophila Nse4 (CG13142) have very similar tissue expression profiles. Based on these pieces of evidence, I hypothesized that MAGE and Nse4 interact and are in a protein complex with Smc5/6 in Drosophila. Similar to the yeast Smc5/6 components, the Drosophila MAGE/Smc5/6 complex would be essential for life and play important role in DNA repair. In addition, like some of the human MAGE proteins, the Drosophila *Mage* could have additional roles in regulating cell cycle, cell survival, and differentiation. These roles could be mediated by Smc5/6 complex, or by additional interaction partners such as E2Fs and p53.

Chapter 2 The Smc5/Smc6/MAGE complex confers resistance to caffeine and genotoxic stress in Drosophila melanogaster

2.1 Summary

The SMC5/6 protein complex consists of the Smc5, Smc6 and Non-Smc-Element (Nse) proteins and is important for genome stability in many species. To identify novel components in the DNA repair pathway, the Campbell lab carried out a genetic screen to identify mutations that confer reduced resistance to the genotoxic effects of caffeine, which inhibits the ATM and ATR DNA damage response proteins. This approach identified inactivating mutations in *CG5524* and *MAGE*, homologs of genes encoding Smc6 and Nse3 in yeasts. The fact that *Smc5* mutants are also caffeine-sensitive and that Mage physically interacts with Drosophila homologs of Nse proteins suggests that the structure of the Smc5/6 complex is conserved in Drosophila. Although Smc5/6 proteins are required for viability in *S. cerevisiae*, they are not essential under normal circumstances in Drosophila. However, flies carrying mutations in *Smc5*, *Smc6* and *MAGE* are hypersensitive to genotoxic agents such as ionizing radiation, CPT, hydroxyurea and MMS, consistent with the Smc5/6 complex serving a conserved role in genome stability. We also show that mutant flies are not compromised for pre-mitotic cell cycle checkpoint responses. Rather, caffeine-induced apoptosis in these mutants is exacerbated by inhibition of ATM or ATR checkpoint kinases but suppressed by Rad51 depletion, suggesting a functional interaction involving homologous DNA repair pathways that deserves further scrutiny. Our insights into the SMC5/6 complex provide new challenges for understanding the role of this enigmatic chromatin factor in multi-cellular organisms.

2.2 Introduction

The evolutionarily conserved Structural Maintenance of Chromosomes proteins are essential for the organization, segregation, and stability of the genome (Lehmann 2005; Hirano 2006; Wu and Yu 2012). Three functionally distinct SMC complexes have been defined in eukaryotes: cohesin (Smc1/3), condensin (Smc2/4), and the otherwise unnamed Smc5/6 complex, each accompanied by a unique set of regulatory subunits. Cohesin holds sister chromatids together after DNA replication and plays important roles in regulation of gene expression and DNA repair (Dorsett and Strom 2012), while condensin is essential for mitotic chromosome organization and segregation (Cuylen and Haering 2011). The Smc5/6 complex is less well characterized but is required for homologous DNA recombination-based processes, including repair of DNA double strand breaks, restart of stalled replication forks, ribosomal DNA maintenance, telomere elongation, and chromosome dynamics during meiosis (Pebernard *et al.* 2004; Torres-Rosell *et al.* 2005; Potts and Yu 2007; Murray and Carr 2008; Kegel and Sjogren 2010).

The Smc5/6 complex in the yeasts is made up of eight subunits that form three sub-complexes: Smc6-Smc5-Nse2, Nse1-Nse3-Nse4, and Nse5-Nse6 (Pebernard *et al.* 2006). Smc5 and Smc6 dimerize through their hinge regions to form the core. The SUMO ligase Nse2 associates with the Smc5-Smc6 heterodimer through a direct interaction with Smc5 (Sergeant *et al.* 2005; Zhao and Blobel 2005; Duan *et al.* 2009). Nse1, a RING finger protein with E3 ubiquitin ligase activity, Nse4, the kleisin component of the complex, and Nse3, a MAGE homolog, interact with each other to form the sub-complex that bridges the head domain of the Smc5-Smc6 heterodimer (Pebernard *et al.* 2004; Sergeant *et al.* 2005; Palecek *et al.* 2006; Doyle *et al.* 2010; Hudson *et al.* 2011). Nse5 and Nse6 form the third sub-complex in yeasts, but these proteins have no counterparts in higher eukaryotes (Pebernard *et al.* 2006).

In humans, the *Nse3* gene is represented by an expanded family of "*MAGE*" (melanoma antigen gene) genes with over 50 members, classified into two types. Type I MAGE genes are frequently over-expressed in human primary cancers and cancer cell lines, and may play a role in resistance to chemotherapeutic agents (Miranda 2010). In fact, 85% of cancer cell lines over-express at least one Type I MAGE gene (Sang *et al.* 2011b).

In contrast, Type II MAGE genes, such as *NDN*, *MAGEL2* and *MAGED1* are expressed in normal tissues and have important roles in mammalian development (Lee *et al.* 2000; Lee *et al.* 2005; Bertrand *et al.* 2008). MAGEG1 was identified as a component of the human Smc5/6 complex (Taylor *et al.* 2008). The crystal structure of MAGEG1 revealed its interaction with RING protein Nse1, and this interaction stimulates the ubiquitin ligase activity of Nse1 (Taylor *et al.* 2008; Doyle *et al.* 2010). Other MAGE proteins interact with the mammalian homologs of Nse1 and Nse4, suggesting a conserved role of MAGE proteins as part of distinct Smc5/6 complexes (Bush and Wevrick 2008; Taylor *et al.* 2008; Doyle *et al.* 2010; Hudson *et al.* 2011; Guerineau *et al.* 2012).

All components of the Smc5/6 complex are essential in *S. cerevisiae* (Zhao and Blobel 2005), and, except for Nse5 and Nse6, also in *S. pombe* (Pebernard *et al.* 2006). Many hypomorphic *Smc5/6* mutants are hypersensitive to genotoxic agents such as ionizing radiation (IR), the alkylating agent methyl methanesulfonate (MMS), hydroxyurea (HU) and UV light in yeasts (De Piccoli *et al.* 2009). Epistasis experiments in yeasts and vertebrate cells have placed *Smc5/6* genes in the homologous recombination-based DNA repair pathway that involves Rad51 nucleofilament proteins (Murray and Carr 2008). In Drosophila, Smc5/6 plays a role in maintaining genome stability in heterochromatin regions by repressing non-sister chromosome recombination events (Torres-Rosell *et al.* 2005; Chiolo *et al.* 2011). Drosophila Smc5/6 also serves a conserved molecular role in blocking Rad51 loading during this process and compromising Smc6 activity in S2 cells caused chromosome defects, suggesting Smc5/6 functions are essential (Chiolo *et al.* 2011). Regulation of homologous recombination-mediated repair relies largely on two kinases, ataxia telangiectasia mutated (ATM) and ataxia telangiectasia and Rad3 related (ATR). ATM and ATR are phosphoinositide 3-kinase-like kinases (PIKK) that are activated by double strand breaks, turning on a network of DNA damage response signaling pathways that coordinate cell cycle progression and DNA repair (Cimprich and Cortez 2008). Caffeine is a PIKK inhibitor commonly used to inhibit ATM and ATR (Blasina *et al.* 1999; Sarkaria *et al.* 1999). We sought to identify novel genes functioning in DNA damage response pathways that are redundant with ATM and ATR, by screening for conditional eye phenotypes in adult flies that were fed caffeine throughout larval development. We found unexpectedly that three Drosophila genes, *Smc5*, *Smc6* and *MAGE*,

are not essential under normal growth conditions, but are essential for resistance to caffeine exposure throughout development. Interestingly, these mutants are also hypersensitive to genotoxic agents, suggesting a conserved role for the Smc5/6 in DNA damage repair. Caffeine induces apoptosis in the mutant flies in a process mediated by ATM and ATR that does not involve conventional cell cycle checkpoints. We have thus identified a novel caffeine-sensitive mechanism that prevents apoptosis in cells exposed to genotoxic stress.

2.3 Materials and Methods

2.3.1 Drosophila stocks and husbandry.

All crosses were carried out at 25°C, and flies were maintained on media formulated at the Bloomington Drosophila Stock Center at Indiana University (BDSC) with *p*-Hydroxy-benzoic acid methyl ester or propionic acid as the fungicide. Stocks were obtained from the BDSC, the Vienna Drosophila RNAi Center (VDRC), or the Drosophila Genetic Resource Center at Kyoto (DGRC) or generated in our laboratories where specified. Drosophila stocks used were:

y^1 w; P{70FLP}11 P{70I-SceI}2B sna^{Sco}/CyO, S2*

*w^{1118}; P{70FLP}*10; *Sb^1/TM6, Ubx*

y^1 w^{67c23} P{Crey}1b; D/TM3, Sb^1*

P{GawB}NP2592

*w**; *Dr^1/TMS, P{Delta2-3}99B*

P{GSV1}GS3245

P{GSV6}GS14577

P{ey3.5-GAL4.Exel}2

C(1)DX, y[1] f[1] / w[1] mei-41[D3]

UAS-ATR-RNAi

UAS-ATM-RNAi

UAS-NBS1-RNAi

UAS-SpnA-RNAi

UAS-MAGE-RNAi/CyO (TRiP)

2.3.2 Ethyl methanesulfonate (EMS) screen for caffeine-sensitive mutants on chromosome 3R.

The isogenized Drosophila stock *FRT82B* carries a transgenic Flippase Recognition Target (FRT) site inserted at polytene segment 82B on chromosome 3R and was used to screen for caffeine sensitivity. Adult male flies were mutagenized by feeding with 15 mM EMS dissolved in 1% sucrose for 12 h. After a one day recovery period, mutagenized males were crossed to *EGUF; FRT82B GMR-hid, CL/TM3, Sb* virgin females. Three to five F1 progeny *EGUF/+; FRT82B/FRT82B GMR-hid, CL* males with normal eye morphology were crossed to *EGUF; FRT82B GMR-hid, CL/TM3, Sb* virgin females. The F2 progeny were raised in media with 2 mM caffeine. Individual male non-balancer F2 flies displaying abnormal eye morphology in both eyes were backcrossed to *EGUF; FRT82B GMR-hid, CL/TM3, Sb* virgin females, and the F3 progeny were raised in media without caffeine to identify any flies with caffeine-independent eye defects. Once the caffeine-dependence of the eye phenotype was confirmed, each mutation was mapped by complementation with the original jnj^{huc95E} allele (Silva *et al.* 2006) or using the Drosophila 3R deficiency kit (BDSC). Both the jnj^{R1} and sst^{RZ} lines emerged from this screen.

2.3.3 Sequencing of candidate genes.

Targeted re-sequencing of mapped caffeine-sensitive loci was used to identify mutations in candidate genes. Genomic DNA from 50 adult flies was extracted using DNAzol reagent (Invitrogen, Burlington, ON, Canada). Overlapping PCR fragments about 10 kb in size were amplified using a Long Range PCR kit (Invitrogen). These fragments covered each region predicted to contain a mutation and 10 kb on either side. The PCR products were sequenced using Illumina technology and data were analyzed with Bowtie software (Illumina Inc., San Diego, CA) (Langmead *et al.* 2009). Mutations were confirmed by Sanger sequencing with BigDye v3.1 (Applied Biosystems, Carlsbad, CA). Restriction digestion (BpmI) of a genomic PCR fragment was used to confirm the mutation in jnj^{R1}.

2.3.4 Generation of the MAGE allele sst^{XL} using gene targeting.

The "ends-out" method (Maggert *et al.* 2008) was used to produce a targeted deletion of *MAGE.* Specifically, 3 kb genomic regions upstream and downstream of the *MAGE* genomic locus were amplified by PCR from a Drosophila BAC clone (BACPAC Resources Center, RP98-3E11), using the following PCR primers 5'-ATTCATGCGGCCGCCGAAACTCAAACGCAGCGAA and 5'-ATTCTAGGTACCGAGAAGTGCTAGCCATTTCGAG or 5'-ATTCTAGGCGCGCCGGAGTAAACGCGGAGTAGAATACC and 5'-ATTCATCGTACGGGAAGGGGATCAGGATTGAA. The two PCR fragments were subcloned into the NotI-KpnI (Acc65I) or AscI-BsiWI sites of the ends-out vector *P[w25.2]* to produce a donor construct *P[w25.2]_NK_AB*. Seven transgenic lines were generated by P element transformation of a w^{1118} strain using *P[w25.2]_NK_AB* (BestGene Inc, Chino Hills. CA). The three lines in which the *P[w25.2]_NK_AB* was located on chromosome 2 were tested for efficient excision by crossing to a line carrying the *FLP* recombinase (w^{1118}*; P{ry+t7.2 70FLP}10; Sb*^{1}*/TM6, Ubx*). One of the three transgenic lines (*6030-1-6M*) with the highest excision efficiency was chosen as the donor line, and crossed to y^{1} *w*; P{70FLP}11 P{70I-SceI}2B sna*^{Sco}*/CyO, S2* (BDSC #6934). The parents were allowed to lay eggs for two days in a vial, and on the third day the larvae were heat-shocked for 1 h in a 38°C water bath. F1 virgin females were collected and crossed to w^{1118}; *P{70FLP}*10; *Sb*^{1}*/TM6*, *Ubx* (BDSC #6938) males. About 100 F2 progeny were selected by screening for nonwhite flies from about 1000 independent crosses. Each of these progeny was crossed to w^{1118}; *P{70FLP}*10; *Sb*^{1}*/TM6*, *Ubx* to make stocks. Twenty five independent lines were identified that exhibited correct targeting as detected by PCR of genomic DNA and loss of Mage protein expression by immunoblotting with a guinea pig anti-Mage antibody (Nishimura *et al.* 2007). The *white* marker of these lines was removed by crossing to a line carrying a Cre recombinase (y^{1} w^{67c23} *P{Crey}1b; D*/TM3,* Sb^{1} (BDSC #851). The resulting lines were tested for heterozygote and homozygote viability under normal conditions, yielding the line named sst^{XL}.

2.3.5 Generation of a genomic rescue construct for MAGE on chromosome 2.

Genomic DNA was isolated from the isogenized strain P{ry[+t7.2]=neoFRT}82B to PCR amplify (Sequal Prep Long PCR Kit, Invitrogen) a 4 kb fragment spanning from 3 kb upstream of the MAGE gene (genomic locus 3R:2983898, based on the predicted transcription start site), to 206 bp downstream of the MAGE stop codon (genomic locus 3R: 2979891). The PCR product was digested with the restriction enzyme XbaI and cloned into the pCasper-hs vector. Transgenic flies were generated by BestGene Inc.

2.3.6 Generation of additional Smc6 alleles by P-element mediated excision.

The *Smc6* deletion allele jnj^{X1} was generated by imprecise excision of a P element in *P{GawB}NP2592* (DGRC #104251). This insertion, hereafter referred to as *NP2592*, is located 7 bp upstream of the putative transcriptional initiation site of *CG5524* (*Smc6*) (3R:20,014,770..20,019,145). Its location was confirmed by genomic PCR using primers flanking the *NP2592* locus. To excise out *NP2592*, *NP2592* virgin females were crossed to w*; Dr^{1}*/TMS, P{Delta2-3}99B* (BDSC #1610) males carrying a Δ2-3 transposase. Single virgin F1 females of genotype *ΔNP2592/ TMS,{Δ2-3}99B* were crossed to *Ly/TM3, Sb* males. Single F2 males of genotype *ΔNP2592/TM3, Sb* were crossed to virgin *Ly/TM3, Sb* virgin females to establish balanced lines. About 200 candidate lines were produced and subsequently tested for sensitivity to 2 mM caffeine. Six lines were found to be homozygous viable but caffeine-dependent lethal. Genomic PCR was used to confirm that there were deletions around the original P insertion sites in these stocks. One of the resulting lines was renamed jnj^{X1}.

2.3.7 Molecular characterization of Smc5 alleles.

The location of *P{GSV1}GS3245* (BDSC #200582) and *P{GSV6}GS14577* (BDSC #205862) within coding exon 2 of the *Smc5* gene was confirmed by genomic PCR using primers 5'-CGTTTCCACGATTTGTTACTGACA and 5'-CGTTTTTGCTTCTTAACCAGATCAC. These lines were renamed $Smc5^{P5}$ and $Smc5^{P7}$, respectively. *Df(3L)BSC418* (BDSC #24922) is a sequence mapped chromosome deletion (78C9;78E1) that includes the *Smc5* locus and nearby genes.

2.3.8 Embryo collection, drug administration and ionizing radiation (IR) treatment.

Parental flies were allowed to lay eggs in collection cages on apple juice agar plates with yeast paste for 20 h. The eggs were gently removed from the agar plates using distilled water and a brush and collected using a small cloth-bottomed basket, and then arrayed on new apple juice agar plates. For each drug or radiation treatment, at least 100 embryos were transferred with a thin layer of agar underneath into each of 3 vials containing medium. Drug stocks were pre-added into the media to the appropriate working concentration, with the exception of methyl methanesulfonate, which was added into the medium 48 hours after transferring the embryos. For drugs dissolved in DMSO, an equal amount of DMSO alone was added into medium fed to control flies. The following drugs were used: caffeine (Sigma-Aldrich, St. Louis, MO, stock 1 M in water, final concentration 0.25-2 mM); camptothecin (Sigma-Aldrich, stock 25 mM in DMSO, final concentration 0.025 mM), methyl methanesulfonate (Sigma-Aldrich, stock 99%, final concentration 0.005-0.015%) and HU (Sigma-Aldrich, stock 1 M, final concentration 4-8 mM). For IR, third instar larvae were irradiated at doses of 20 and 40 Gray using an irradiator (Gammacell 220–Cobalt-60, Atomic Energy of Canada, 1979). The survival index (*p*) of a given genotype was calculated by dividing the number of adult survivors of the genotype resulting from media with a given reagent concentration or treatment (*n*) by the number of adult survivors of the same genotype resulting from media without that reagent or treatment (*N*).

2.3.9 Immunoblotting.

For each sample, ten 3-4 day-old adult flies were collected, frozen in liquid nitrogen and ground using a pestle in a 1.5 ml eppendorf tube. Mild lysis buffer (50 mM Tris, 150 mM NaCl, and 1% Triton X-100, pH 8.0) was then added (10 µl per fly) to solubilize the tissue. The suspension was centrifuged at 20,000*g* for 10 min. at 4°C and the supernatant was mixed and boiled with 2X Laemmli Buffer. Proteins were resolved by SDS-PAGE and transferred onto PVDF membranes for immunoblotting. A 1:2500 dilution of guinea pig anti-Mage serum was used to detect Mage protein (Nishimura *et al.* 2007).

2.3.10 Genetic interactions of ATM, ATR, NBS1 and RAD51 loss-of-function with MAGE and Smc6.

Double mutants of *ATR* and *Smc6* used *mei-41*^{D3} (Laurencon *et al.* 2003) and *Smc6* alleles *jnj*^{X1} *and jnj*$^{Df(3R)Exel6198}$. Knockdown of *ATM*, *ATR* or *NBS1* function in *MAGE* or *Smc6* homozygous mutant eye clones was achieved using the *EGUF* system, which uses the *eyeless-Gal4* driver to express transgenes throughout eye development (Stowers and Schwarz 1999). The *EGUF* system also ensures that all ommatidia of the adult eye are homozygous for either *Smc6* or *MAGE* mutant alleles, because of an eye-specific *GMR-hid* transgene that eliminates non-mutant ommatidia. RNAi knockdown of *MAGE* alone or double RNAi of *MAGE* and *Rad51* ortholog *SpnA* in the eye was achieved by crossing appropriate RNAi constructs containing males to *UAS-Dcr2/CyO; ey-Gal4/TM3,Ser* virgin females. For each genotype, five to nine specimens were photographed, and representative phenotypes are shown.

2.3.11 cDNA clones, cell culture, transfections, and co-immunoprecipitation.

Full-length cDNA clones for *Nse1* (GM14348) and *Nse4* (IP09347) were obtained from the Canadian Drosophila Microarray Centre, the *MAGE* (RE25453) clone was obtained from the Drosophila Genomics Resource Center (DGRC, Indiana University). Drosophila S2 cells (from the DGRC) were grown at 25°C in TNM-FH medium (SH30280.02, Thermo Scientific, Waltham, MA) supplemented with 10% fetal bovine serum. Expression constructs for transfection of S2 cells were created by inserting relevant full-length coding sequences into the Drosophila Gateway destination vectors (obtained from the DGRC). S2 cells were transfected with relevant expression constructs using dimethyldioctadecyl-ammonium (Han 1996). Cells were harvested 24 h after transfection, washed once in phosphate buffered saline, pH 7.2, and re-suspended in the mild lysis buffer supplemented with a protease inhibitor cocktail (Roche Applied Science, Indianapolis, IN). The lysate was centrifuged for 10 min. at 20,000*g* at 4°C, and the supernatant transferred to a fresh tube. 200 µl of supernatant was mixed with 20 µl of protein G agarose beads (GE Healthcare Life Sciences, Piscataway, NJ) pre-bound with 5 µg of antibody in 800 µl mild lysis buffer. The agarose beads were then incubated for 1 h at 4°C with rocking, washed six times using mild lysis buffer and the bound proteins analyzed on immunoblots.

2.3.12 In vitro pulldown assays.

pMBP-Mage was previously described (Nishimura *et al.* 2007) and the control pMBP construct was supplied with a Maltose binding protein (MBP) purification kit (New England Biolabs, Ipswich, MA). Expression constructs were produced by inserting relevant full-length coding sequences into a Gateway pDEST-14 expression vector. MBP fused Mage (MBP-Mage) was expressed in *Escherichia coli* (ER2523, New England Biolabs) and immobilized onto amylose resin (E8200S) according to the manufacturer's directions. ^{35}S labeled proteins were expressed from Gateway pDest14 vectors using the TNT-coupled *in vitro* transcription-translation system (Promega, Madison, WI). For the *in vitro* binding assay, ^{35}S-labeled proteins were incubated with immobilized MBP-Mage proteins in 500 µl of buffer (20 mM Tris, 100 mM NaCl, 0.5 mM EDTA, 10% glycerol, and 1% Tween-20, pH 7.6) containing 0.25% bovine serum albumin (BSA) and protease inhibitor cocktail (Deng *et al.* 2009) overnight at 4°C with end-over-end mixing. The resin was washed six times in 500 µl of the same buffer, and the bound proteins were resolved by SDS-PAGE and detected by autoradiography.

2.3.13 Scanning electron microscopy (SEM) and immunohistochemistry.

Adult heads were prepared for SEM according to the HMDS method described in Drosophila *Protocols* (Sullivan *et al.* 2000) and imaged using a Scanning Electron Microscope (FEI (XL30), Philips, Hillsboro, OR). Dissection, fixation, BrdU labeling, and antibody staining of third larval instar eye-antennal discs were also carried out as described in *Drosophila Protocols.* Antibodies for immunohistochemistry included anti-cleaved caspase 3 (1:1600 dilution, Cell Signaling Technologies, Beverly, MA), anti-BrdU (1:200 dilution, Pharmingen San Jose, CA), and anti-phospho-histone H3 (Cell Signaling, 1:1000 dilution). Secondary antibodies were used at a dilution of 1:1000 (Alexa Fluor 488 and 586, Invitrogen). For the detection of apoptosis in third instar imaginal discs with an anti-cleaved caspase 3 antibody, embryos were collected at one hour intervals on grape juice plates and larvae were reared on yeast paste plates until the L3 molt. They were then transferred to 2 mM caffeine medium 32 h after the L3 molt and allowed to develop for a further 12 h before dissection. Images of the dissected discs were acquired using a LSM 700 confocal microscope (Carl Zeiss Inc., Thornwood, NY) and processed using Zen (Carl Zeiss). A maximum projection of all stacks of a confocal image was used to quantify the

signal intensity of staining using a lower threshold to eliminate background staining. This value was divided by the area of each eye disc to obtain a ratio representing the relative amount of immunostaining. Data represent at least 7 eye discs per genotype per treatment.

2.3.14 Quantitative RT-PCR.

Total RNA was extracted from adult flies using Trizol reagent (Invitrogen). RNA concentration and integrity were determined by a Nanodrop ND-1000 (NanoDrop products, Wilmington, DE) and Agilent 2100 Bioanalyser (Agilent Technologies, Santa Clara, CA), respectively. One µg of total RNA per reaction was used for double strand cDNA synthesis (Applied Biosystems). Then, 2.5 µl of 1/20 diluted cDNA was used for each qPCR reaction with quantification based on SYBR Green incorporation (Applied Biosystems).

2.4 Results

2.4.1 A screen for caffeine-sensitive eye mutants reveals three loci on chromosome 3R.

The compound eyes of Drosophila are ideal tissues to detect defects in proliferation and apoptosis as they are not essential for survival, but they are sensitive to developmental perturbations and easy to score for mutant phenotypes. To identify novel genes functioning in DNA damage response pathways that are redundant with ATM and ATR, the laboratory of Dr. Shelagh Campbell (University of Alberta) previously performed a genetic screen to identify conditional eye phenotypes in adult flies fed 2 mM caffeine and 3 mM hydroxyurea (HU) throughout larval development (Silva *et al.* 2006). While caffeine inhibits ATM and ATR, HU stalls replication forks through inhibition of dNTP production, eventually generating single strand or double strand DNA breaks, thereby activating DNA damage responses regulated by ATM and ATR. At the drug concentrations used, there were no phenotypic effects in wildtype flies. In this screen, they used the "*EGUF, GMR-hid*" (*EGUF*) system to produce homozygous mutant clonal cells in the entire adult eye of an otherwise heterozygous fly (Stowers and Schwarz 1999). This screen identified a single caffeine-sensitive locus (*huc95E*) on chromosome arm 3R, here renamed *java no jive* (*jnj*),

which they mapped to cytological region 95E by complementation testing with chromosomal deficiencies (Silva *et al.* 2006). Flies that were mosaic hemizygous for *jnj* in the eye exhibit caffeine-dependent small, rough eyes associated with increased apoptosis. To identify novel DNA damage pathway components, the Campbell group has now carried out a new screen of chromosome arm 3R for conditional caffeine-sensitive eye phenotypes. By screening 9098 males, they identified three loci on chromosome arm 3R including six additional alleles of *jnj*, two mutant alleles of a locus called *sleepless in seattle* (*sst*), and one allele of a novel locus called *double double trouble* (*ddt*), that has not yet been linked to a specific gene (Figure 2-1, Figure 2-2A). All hemizygous *jnj, sst* and *ddt* mutants exhibit caffeine-dependent pupal lethality (Figure 2-2B-D).

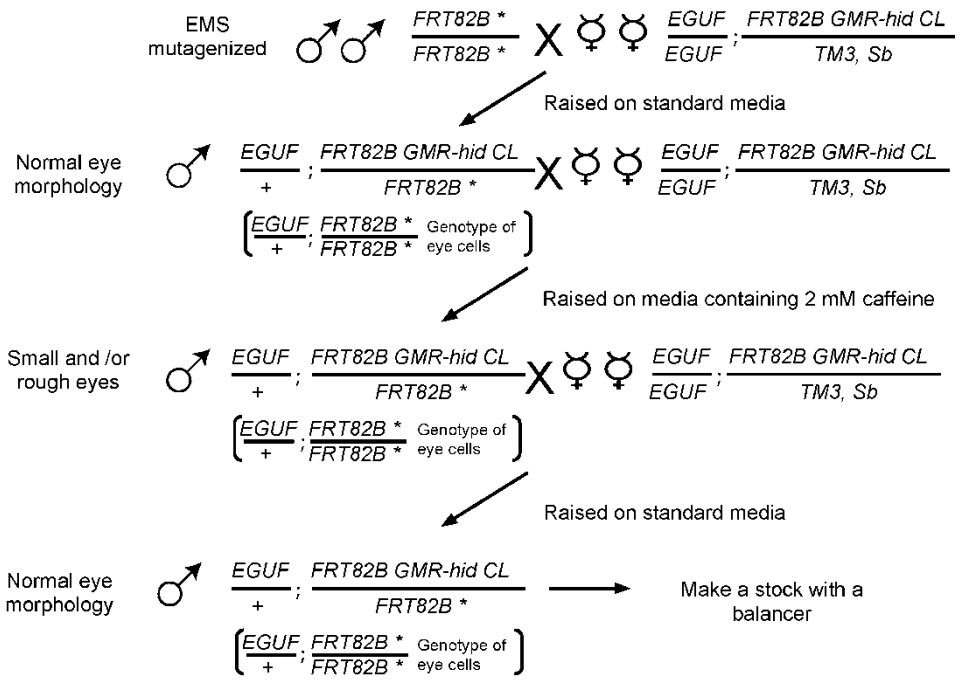

Figure 2-1 An ethyl methanesulfonate (EMS) screen for caffeine-sensitive mutants on chromosome 3R.

Ethylmethane sulfonate (EMS) mutagenized male flies carrying transgenic *FRT82B* sites were crossed en masse to *y,w; EGUF; FRT82B GMR-hid/TM3, Sb* virgin females in standard media. Non-*TM3, Sb* progeny males containing normal looking eyes were then collected and crossed in pools of 3-5 males to 3-5 *y,w; EGUF; FRT82B GMR-hid/TM3, Sb* virgin females in molasses and cornmeal media containing 2 mM caffeine. Non-*TM3, Sb* progeny males containing developmental defects in both eyes were selected and individually tested with *y,w; EGUF; FRT82B GMR-hid/TM3, Sb* virgin females in normal media to eliminate any false positive caffeine-independent mutations that might have arisen in the male germline. Once a caffeine-dependent phenotype was confirmed, the mutant was then crossed to *y,w; EGUF; FRT82B GMR-hid/TM3, Sb* virgin females to establish balanced stocks. "*" indicates a putative mutation.

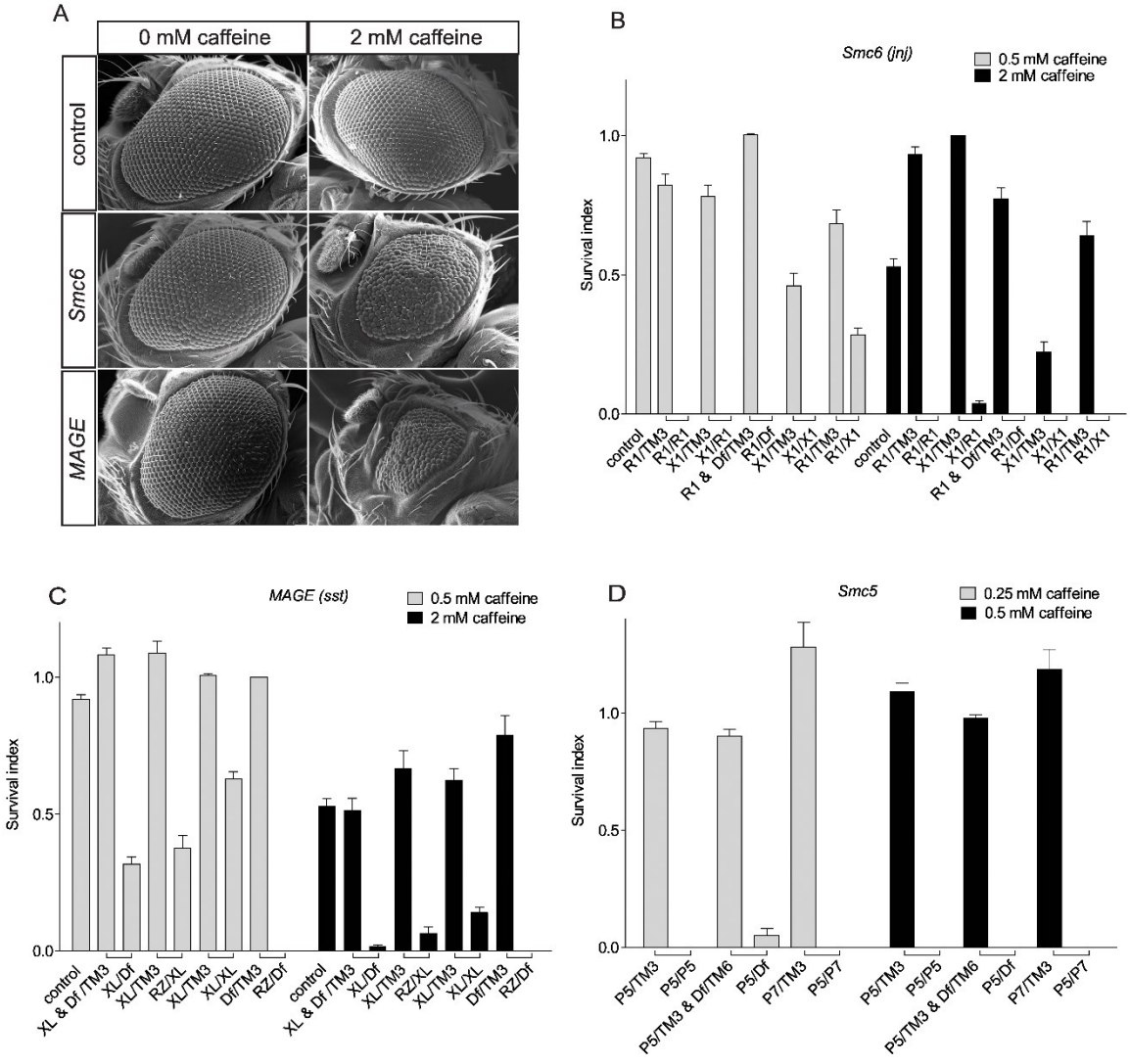
A
0 mM caffeine
2 mM caffeine
control
Smc6
MAGE
B
Smc6 (jnj)
0.5 mM caffeine
2 mM caffeine
Survival index
1.0
0.5
0.0
control
R1/TM3
R1/R1
X1/TM3
X1/R1
R1 & Df/TM3
R1/Df
X1/TM3
X1/X1
R1/TM3
R1/X1
C
MAGE (sst)
0.5 mM caffeine
2 mM caffeine
Survival index
control
XL & Df /TM3
XL/Df
XL/TM3
RZ/XL
XL/TM3
XL/XL
Df/TM3
RZ/Df
D
Smc5
0.25 mM caffeine
0.5 mM caffeine
Survival index
P5/TM3
P5/P5
P5/TM3 & Df/TM6
P5/Df
P7/TM3
P5/P7

Figure 2-2 Eye phenotypes in caffeine-sensitive mutant flies.

(A) Caffeine-dependent eye phenotype of *Smc6 (jnj)* and *MAGE (sst)* mutants. Drosophila genotypes are as follows. Control: *EGUF/+; FRT82B +/FRT82B GMR-hid*. *Smc6* (loss of *Smc6* in eye cells): *EGUF/+; FRT82B* jnj^{R1}*/FRT82B GMR-hid. MAGE* (loss of *MAGE* in eye cells): *EGUF/+; FRT82B* sst^{RZ}*/FRT82B GMR-hid*. (B-D) *Smc6, MAGE* or *Smc5* homozygous, trans-heterozygous or hemizygous mutants have reduced survival when raised in media with caffeine. Bars represent the survival index (*p*) and error bars represent SEM. "␣" indicates flies eclosed from the same cross. Absence of a bar indicates no surviving flies. Wildtype control flies are w^{1118}. (B) *Smc6* mutants are sensitive to caffeine. *R1* (jnj^{R1}) is an allele from the caffeine screen, *X1* (jnj^{X1}) was generated by an imprecise excision of a P-element adjacent to the 5'UTR of *Smc6*, and *Df* (*Df(3R)Exel6198*) is a deficiency chromosome uncovering the *Smc6* locus. (C) *MAGE* mutants are sensitive to caffeine. *RZ* (sst^{RZ}) is an allele from the caffeine screen, *XL* (sst^{XL}) is a targeted knockout, and *Df* ($Df(3R)Antp^{1}$) is a deficiency chromosome uncovering the *MAGE* locus. (D) *Smc5* mutants are sensitive to caffeine. Both *P5* ($Smc5^{P\{GSV1\}GS3245}$) and *P7* ($Smc5^{P\{GSV6\}GS14577}$) contain P-element insertions in a coding exon of *Smc5*, and *Df* (*Df(3L)BSC418*) is a deficiency chromosome uncovering the *Smc5* locus.

2.4.2 Mutations in Smc6 cause caffeine-dependent defects in java no jive mutant flies.

Deletion mapping indicated that all of the caffeine-sensitive *jnj* alleles were viable in hemizygous combinations with deletions uncovering region 95E, indicating that the homozygous lethality of most *jnj* alleles was caused by second site mutation(s). Homozygotes for one allele, jnj^{R1}, were viable on regular media, but died at the pupal stage when raised in media containing caffeine (Figure 2-2B). Sequencing of candidate genes in the *jnj* region identified a four base pair deletion in exon two of the FlyBase annotated gene *CG5524* (del_ATCT at position 334-337 bp from the presumptive start codon), creating a frameshift resulting in a stop codon at position 133 of the presumptive 1122 amino acid protein (Figure 2-4A). The predicted CG5524 protein has highest amino acid identity with SMC6 (Structural Maintenance of Chromosomes 6) in other species. SMC6 regulates chromosome stability in yeasts (Pebernard *et al.* 2004; Torres-Rosell *et al.* 2005; Murray and Carr 2008), and is implicated in heterochromatic DNA repair in Drosophila (Chiolo *et al.* 2011). We tested *CG5524* (hereafter called *Smc6*) and four neighboring genes for levels of expression by quantitative RT-PCR of RNA from whole flies. Levels of *Smc6* RNA were greatly reduced with all seven alleles of *jnj*, ranging from 9% to 24% of control levels (Figure 2-3A) whereas nearby genes showed little change in expression. Despite extensive sequencing efforts, we were not able to identify the nature of *jnj* alleles other than jnj^{R1}, suggesting that these unmapped mutations reside in as yet unidentified regulatory regions of *Smc6*. To be certain that our *jnj* alleles corresponded to *Smc6*, we generated additional *Smc6* lines by imprecise excision of the P-element present in line *NP2592*, including the new line jnj^{X1} that lacks exon 1 and sequences up- and downstream of this exon (Figure 2-4A). We tested caffeine sensitivity in all of the *jnj* allelic combinations and found that raising larvae on 0.5 mM caffeine resulted in almost complete lethality (Figure 2-2B). Using RNAi to deplete *Smc6* expression in developing eye discs also resulted in a caffeine-dependent rough eye phenotype (Figure 2-3B). Collectively, the presence of a frame shift mutation in *Smc6* in jnj^{R1}, the reduced expression levels of *Smc6* in all seven alleles of *jnj*, the caffeine-dependent lethality of the deletion allele jnj^{X1}, and caffeine-dependent eye phenotypes induced by *Smc6* RNAi all implicate *CG5524/Smc6* as the relevant gene in *jnj* mutants.

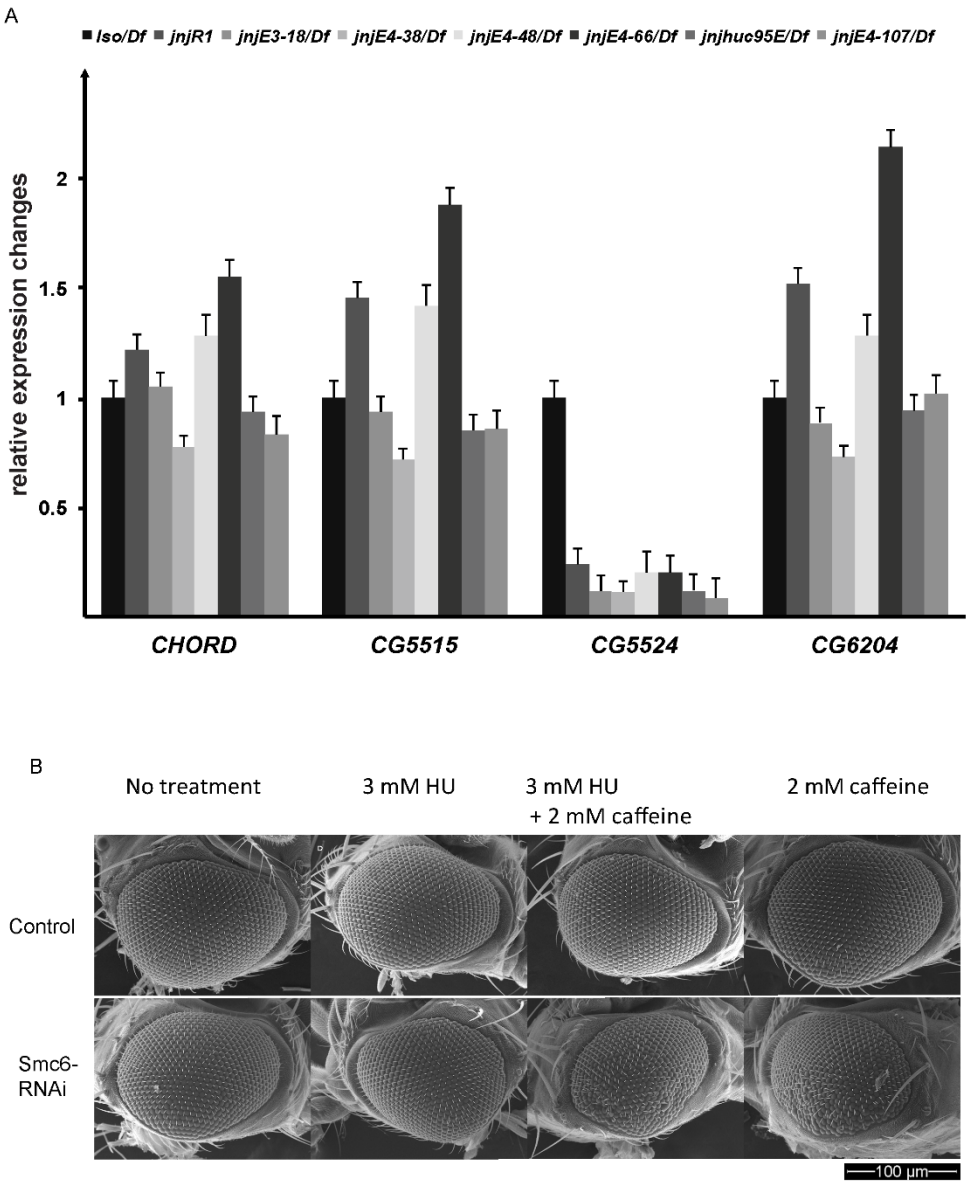
A
Iso/Df
jnjR1
jnjE3-18/Df
jnjE4-38/Df
jnjE4-48/Df
jnjE4-66/Df
jnjhuc95E/Df
jnjE4-107/Df
relative expression changes
2
1.5
1
0.5
CHORD
CG5515
CG5524
CG6204
B
No treatment
3 mM HU
3 mM HU
+ 2 mM caffeine
2 mM caffeine
Control
Smc6-
RNAi
100 µm

Figure 2-3 Caffeine sensitivity of *jnj* alleles is caused by loss of *Smc6*.

(A) mRNA transcript levels of *Smc6* (*CG5524*) and its neighboring genes *CHORD, CG5515* and *CG6204* in control and *jnj* mutant flies were measured by quantitative RT-PCR. All seven *jnj* alleles tested had reduced *Smc6* transcript levels ranging from 7% to 24% of the control level, while the transcript levels of the neighboring genes were comparable to the control level. The caffeine screen starting stock "Iso" carrying the transgenic *FRT82B* site crossed to Df to normalize the *Smc6* level was used to generate control flies. "Df" is the deficiency chromosome *Df(3R)Exel6198*. (B) Knocking-down *Smc6* expression using RNAi in developing eye discs resulted in a caffeine-dependent adult rough eye phenotype. Control, *Eyeless-Gal4/+* was from a cross of *Eyeless-Gal4/Eyeless-Gal4* X w^{1118} and *Smc6*-RNAi, *Eyeless-Gal4/+; UAS-Smc6-RNAi/+* resulted from the cross *Eyeless-Gal4/Eyeless-Gal4* X *UAS-Smc6-RNAi/+*. *UAS-Smc6-RNAi* was obtained from VDRC (#107055).

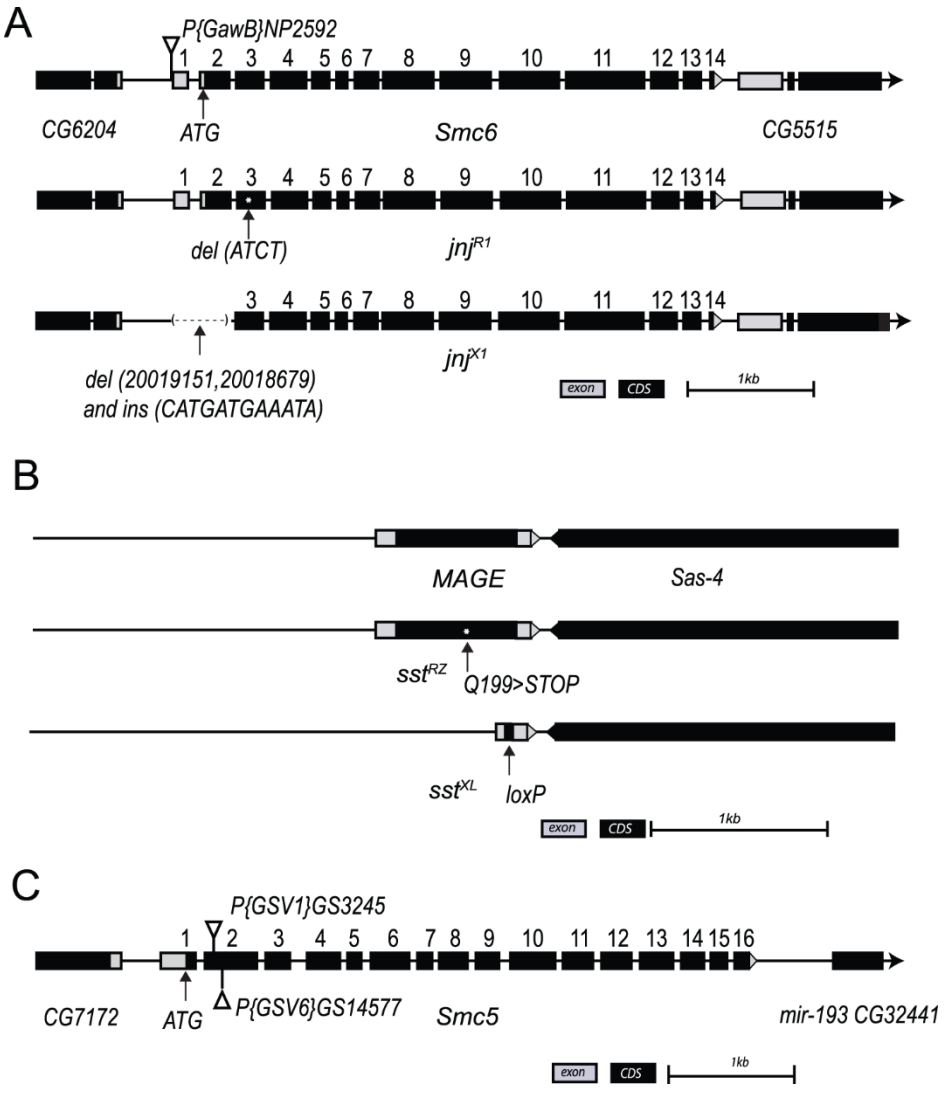
A
P{GawB}NP2592
1 2 3 4 5 6 7 8 9 10 11 12 13 14
CG6204
ATG
Smc6
CG5515
del (ATCT)
jnj^R1
jnj^X1
del (20019151,20018679)
and ins (CATGATGAAATA)
exon
CDS
1kb
B
MAGE
Sas-4
sst^RZ
Q199>STOP
sst^XL
loxP
C
P{GSV1}GS3245
1 2 3 4 5 6 7 8 9 10 11 12 13 14 15 16
CG7172
ATG
P{GSV6}GS14577
Smc5
mir-193 CG32441

Figure 2-4 Overview of *Smc6, MAGE*, and *Smc5* gene location, structural organization and mutant alleles.

(A) *Smc6* is a 14 exon gene located on 3R:95E8-95F1. jnj^{R1} contains a 4 bp deletion in the 2nd coding exon. jnj^{X1} contains a 473 bp deletion of sequences upstream of exon 1 (196 bp), the entire exon 1 (252 bp), and a portion of intron 1 (25 bp), with a 12 bp vestige of the original P element remaining. *Smc6* genomic locus (3R:20,014,770..20,019,145 [-]) is shown. (B) *MAGE* is a single exon gene located on the right arm of the 3rd chromosome at position 84C7-84C7. sst^{RZ} has a point mutation that converts a glutamine at position 109 to a stop codon. sst^{XL} carries a targeted deletion of the entire coding sequence of *MAGE*. *MAGE* genomic locus (3R:2,979,960..2,980,898 [-]) is shown. (C) *Smc5* is a 16 exon gene located in 78D6-78D7 of the left arm of the 3rd chromosome. Exons encoding the longest transcripts are shown. Both *P{GSV1}GS3245* and *P{GSV6}GS14577* are inserted in the second coding exon. The *Smc5* genomic locus (3L:21,562,309..21,566,623 [+]) is shown. CDS, coding sequence.

2.4.3 Caffeine-sensitivity in sleepless in seattle mutants is due to mutations in the MAGE gene.

The sst^{RZ} mutation exhibits caffeine-dependent pupal lethality in combination with a chromosomal deficiency (*Df(3R)Antp*^{1}, Figure 2-2C) but sst^{RZ} homozygotes are not viable on regular media, presumably because of a second site mutation. Further deletion mapping refined the position of the caffeine-sensitive *sst* locus to a region containing seven candidate genes, each of which were sequenced. Campbell and colleagues identified a glutamine to stop mutation affecting the *MAGE* gene (Pold *et al.* 2000) in sst^{RZ}, at position 109 of the 232 amino acid Mage protein (Figure 2-4B). In previous studies, depletion of *MAGE* mRNA using double strand RNA injection suggested that *MAGE* was essential for viability during early embryogenesis, whereas conditional knockdown at later developmental stages suggested a role in postembryonic neuronal cell survival and proliferation (Nishimura *et al.* 2008). Moreover, DNA fibers connecting mitotic cells were observed after RNAi-mediated depletion of *Smc5* or *Smc6* in *S2* cells, suggesting that the Smc5/6 complex could be essential for mitosis in Drosophila (Chiolo *et al.* 2011). We therefore initially reasoned that sst^{RZ} was a partial loss-of-function allele, since hemizygous sst^{RZ} flies were viable. To test this idea we synthesized a knockout allele by homologous recombination (Maggert *et al.* 2008). In this new allele (sst^{XL}) the complete coding sequence of *MAGE* was deleted (Figure 2-4B). Surprisingly, homozygous sst^{XL} flies displayed no increased lethality or obvious mutant phenotype when raised on media without caffeine. As with sst^{RZ} hemizygotes, sst^{XL} flies reared in caffeine media were inviable, but they were less sensitive to a lower dose of caffeine (0.5 mM) than *jnj* mutants (Figure 2-2C). About 15% of predicted sst^{XL} homozygous flies survived 2 mM caffeine exposure and the surviving flies often had small or rough eyes, similar to sst^{RZ} mutants (Figure 2-2A). Transheterozygous sst^{RZ}/sst^{XL} progeny were also viable on normal media, but only 6% survived on 2 mM caffeine (Figure 2-2C). Using polyclonal antibodies directed against Mage (Nishimura *et al.* 2007) we found that Mage was absent from protein lysates derived from *sst* adult flies (Figure 2-5). In addition, caffeine-dependent lethality of sst^{XL} can be complemented by a genomic *MAGE* transgene (Table 2-1) that includes the full coding region of *MAGE* and 3 kb sequence upstream and expresses Mage protein at normal levels (Figure 2-5). Collectively, the identification of a stop mutation in the *MAGE*

gene (sst^{RZ}), the caffeine-sensitivity of a *MAGE* knockout allele sst^{XL}, the loss of Mage protein in *sst* flies and the rescue of caffeine sensitivity by a *MAGE* transgene all implicate *MAGE* as the mutated gene in *sst* flies.

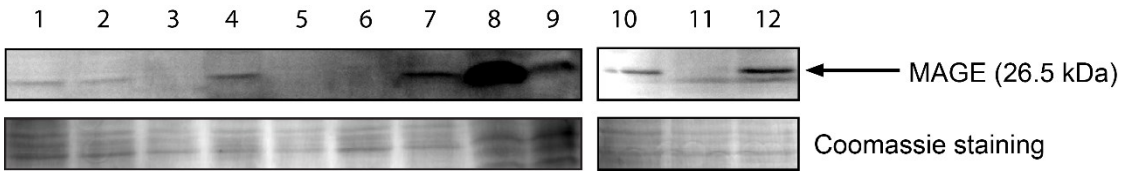

Figure 2-5 Immunoblot for Mage.

Levels of endogenous Mage were measured in protein lysates from whole flies derived from various lines, immunoblotted with anti-Mage antibody. Genotypes were as follows: Lane 1: sst^{XL}/*TM3,Sb*, 2: sst^{RZ}/*TM3,Ser,ActGFP*, 3: sst^{XL}/sst^{RZ}, 4: *Df(3R)Antp1/TM3,Sb*, 5: *Df(3R)Antp1*/sst^{RZ}, 6: *Df(3R)Antp1*/sst^{XL}, 7. w^{1118}, 8: *S2* cells, 9: *S2* cells dMAGE RNAi, 10: sst^{XL}/TM3,Ser,ActGFP, 11: sst^{XL}/sst^{XL}, 12: *3Kb+MAGE transgene/CyO;* sst^{XL}/sst^{XL}.

Genotype	0 mM caffeine	2 mM caffeine
3Kb+MAGE/+;sst^{XL}/sst^{XL}	64	118
3Kb+MAGE/+; sst^{XL}/TM3, Ser, ActGFP	59	77
CyO/+; sst^{XL}/sst^{XL}	52	0
CyO/+; sst^{XL}/TM3, Ser, ActGFP	77	30

Table 2-1 *sst* caffeine sensitivity can be rescued by a *MAGE* transgene.

All genotypes were produced from cross *sst^{XL}/sst^{XL}* X *3Kb+dMAGE/CyO;sst^{XL}/TM3, Ser, ActGFP*.

2.4.4 Smc5 mutant flies are also caffeine sensitive.

In yeasts and mammalian cells, all known SMC6 functions involve SMC5 (Fujioka *et al.* 2002; Taylor *et al.* 2008), so we predicted that loss of *Smc*5 activity would also cause caffeine sensitivity in flies (Figure 2-7A). We tested two P insertion alleles predicted to affect *Smc5* for caffeine sensitivity, namely $Smc5^{P\{GSV1\}GS3245}$, referred to as $Smc5^{P5}$, and $Smc5^{P\{GSV6\}GS14577}$, referred to as $Smc5^{P7}$ (Toba *et al.* 1999). As predicted, both *Smc5* mutants were sensitive to caffeine (Figure 2-2D). Both of these alleles have P-element insertions within the second exon of *Smc5* and the insertion sites are very close to the putative start codon (Figure 2-4C). Therefore, they are very likely to be null alleles. To rule out the possibility that caffeine-sensitivity of *Smc5* flies was caused by second site mutations, we generated Drosophila lines in which the P-elements in both alleles were excised by a transposase, either restoring the wild-type sequence or resulting in an insertion or deletion of the original P element insertion in the coding exon of *Smc5*. We therefore predicted that some excision lines would no longer be caffeine-sensitive while others would retain the mutant phenotype. As expected, of 13 independent Drosophila lines produced by the excision of *P7*, seven lines were no longer caffeine sensitive (Table 2-2A). Similar results were obtained from the excision of *P5* (Table 2-2B). In conclusion, as with *Smc6* and *MAGE*, loss of *Smc5* function results in caffeine-dependent lethality.

Table 2-2 A									
Excision alleles	Caffeine sensitive?	*Smc5*^{P14577}/Smc5^{P14577} X Smc5^{exP14577}/TM3,Sb				*Smc5*^{exP14577}/Smc5^{exP14577} X Smc5$^{Df(3L)BSC418}$/TM6,Sb			
		Standard media		Caffeine 1mM		Standard media		Caffeine 1mM	
		Smc5^{exP14577} /Smc5^{P14577}	*Smc5*^{P14577} */TM3,Sb*	*Smc5*^{exP14577} */Smc5*^{P14577}	*Smc5*^{P14577} */TM3,Sb*	*Smc5*^{exP14577} */Smc5*$^{Df(3L)BSC418}$	*Smc5*^{exP14577} */TM6,Sb*	*Smc5*^{exP14577} */Smc5*$^{Df(3L)BSC418}$	*Smc5*^{exP14577} */TM6,Sb*
1	No	50	56	18	27	61	97	51	57
2	No	28	33	14	18	60	81	30	47
3	Yes	58	79	0	16	51	30	0	11
4	No	62	101	19	35	30	33	29	36
5	Yes	N/A	N/A	N/A	N/A	42	56	0	12
7	Yes	52	77	0	22	39	40	0	8
9	Yes	24	19	N/A	N/A	41	56	1	24
10	Yes	29	40	0	2	45	47	0	16
11	Yes	57	53	0	43	38	47	1	24
12	No	17	30	15	13	63	77	26	39
13	No	54	90	28	35	33	43	14	35
14	Yes	54	61	0	21	29	32	0	33
15	Yes	52	74	0	20	82	84	11	27
Original Allele		*Smc5*^{P14577}/Smc5^{P14577} X Smc5^{P14577}/TM3,TM3,Ser,ActGFP				*Smc5*^{P14577}/Smc5^{P14577} X Smc5$^{Df(3L)BSC418}$/TM6,Sb			
		Smc5^{P14577}/Smc5^{P14577}	*Smc5*^{P14577}*/TM3,Ser,ActGFP*	*Smc5*^{P14577}/*Smc5*^{P14577}	*Smc5*^{P14577}*/TM3,Ser,ActGFP*	*Smc5*^{P14577}/*Smc5*$^{Df(3L)BSC418}$	*Smc5*^{P14577}*/TM6,Sb*	*Smc5*^{P14577}/*Smc5*$^{Df(3L)BSC418}$	*Smc5*^{P14577}*/TM6,Sb*
	Yes	58	77	0	33	44	56	0	7

Table 2-2 B

Excision alleles	Caffeine sensitive?	$Smc5^{F3245}$/$Smc5^{F3245}$ X $Smc5^{exF3245}$/TM3,Sb				$Smc5^{exF3245}$/TM3,Sb X $Smc5^{Df(3L)BSC418}$/TM6,Sb			
		Standard media		Caffeine 1mM		Standard media		Caffeine 1mM	
		$Smc5^{exF3245}$ /$Smc5^{F3245}$	$Smc5^{F3245}$ /TM3,Sb	$Smc5^{exF3245}$ /$Smc5^{F3245}$	$Smc5^{F3245}$ /TM3,Sb	$Smc5^{exF3245}$ /$Smc5^{Df(3L)BSC418}$	$Smc5^{exF3245}$ $Df(3L)BSC418$/TM6 or TM3,Sb or	$Smc5^{exF3245}$ /$Smc5^{Df(3L)BSC418}$	$Smc5^{exF3245}$ $Df(3L)BSC418$/TM6 or TM3,Sb or
1	No	10	32	13	34	46	82	27	45
2	No	15	72	17	41	57	119	22	45
3	No	19	53	6	46	N/A	N/A	N/A	N/A
4	No	39	115	6	39	29	64	12	44
5	No	37	128	17	49	30	117	15	48
6	No	50	108	25	40	56	109	18	28
7	No	20	72	31	52	43	64	24	28
8	No	34	106	0	69	37	95	0	34
9	Yes	27	155	0	73	55	116	0	36
10	Yes	44	105	26	30	57	87	16	50
11	No	42	127	22	56	35	147	10	39
12	Yes	20	77	0	51	30	110	0	30
13	Yes	34	84	0	48	11	33	0	33
Original Alleles		$Smc5^{F3245}$/$Smc5^{F3245}$ X $Smc5^{F3245}$/TM3,TM3,Ser,ActGFP				$Smc5^{F3245}$/TM3,Sb X $Smc5^{Df(3L)BSC418}$/TM6,Sb			
		$Smc5^{F3245}$ /$Smc5^{F3245}$	$Smc5^{F3245}$ /TM3,Ser Act GFP	$Smc5^{F3245}$ /$Smc5^{F3245}$	$Smc5^{F3245}$/TM 3,Ser,Act GFP	$Smc5^{F3245}$ /$Smc5^{Df(3L)BSC418}$	$Smc5^{F3245}$ $Df(3L)BSC418$/TM6 or TM3,Sb or	$Smc5^{F3245}$ /$Smc5^{Df(3L)BSC418}$	$Smc5^{F3245}$ $Df(3L)BSC418$/TM6 or TM3,Sb or
	Yes	30	71	0	52	39	96	0	46

Table 2-2 P-element excision of *P{GSV1}GS3245* and *P{GSV6}GS14577* produces both caffeine-sensitive and -insensitive lines.

2.4.5 Caffeine sensitivity is mediated through Smc5/6.

At the whole organismal level, a higher proportion of *MAGE* mutants were able to survive exposure to 0.5 mM caffeine throughout larval development than *Smc6* and *Smc5* mutants. Indeed all genetic combinations of *MAGE* mutant flies had some survivors on media containing 2 mM caffeine, while there were essentially no survivors among the *Smc5* or *Smc6* mutants raised on 2 mM caffeine (Figure 2-2B-D). This suggests that the Mage protein is less important for caffeine resistance than the Smc5 and Smc6 proteins. To further test this hypothesis, we measured the viability of flies carrying mutations in two different components of the protein complex (Smc6 and Mage) when raised on media containing caffeine. Flies deficient for both Mage and Smc6 were more sensitive to caffeine than flies deficient for Mage alone, but were similar in sensitivity to flies deficient for Smc6 alone (Table 2-3). This suggests that the Smc5/6 heterodimer has a more critical role in caffeine resistance than does the sub-complex containing Nse1-Mage, consistent with observations in yeasts (Lehmann 2005).

Cross	Genotype	Mutant status	No caffeine	Caffeine	Sensitivity ratio
1	*sst^{XL}, jnj^{X1}/sst^{XL}, jnj^{R1}*	Double Mutant	104	9	0.07
	sst^{XL}, jnj^{R1} or *X1 /TM3,Ser,ActGFP*	Double Het	226	267	
2	*+, jnj^{X1}/sst^{XL}, jnj^{R1}*	Smc6 Mutant	224	8	0.05
	+, jnj^{X1}/TM3,Ser,ActGFP	Smc6 Het	238	189	
3	*sst^{XL}, +/sst^{XL}, jnj^{R1}*	MAGE Mutant	279	83	0.34
	sst^{XL}, +/TM3,Ser,ActGFP	MAGE Het	310	274	

Table 2-3 . Caffeine sensitivity of *MAGE* and *Smc6* double mutants is similar to sensitivity of flies mutant for *Smc6* alone.

Caffeine sensitivity of *MAGE* and *Smc6* double mutants or single mutants was tested using media with 0.25 mM caffeine. A Sensitivity ratio was calculated by dividing the ratio of the homozygous versus the heterozygous flies surviving on media containing caffeine by the ratio of homozygous to heterozygous flies surviving on standard media. A Sensitivity ratio of 1 indicates that caffeine has no effect. Double Mutant: both *sst*/*MAGE* and *jnj/Smc6* inactivated; Double Het: *MAGE* and *Smc6* heterozygous mutant; Smc6 Mutant: *Smc6* inactivated; MAGE Mutant: *MAGE* inactivated; Het: heterozygous for either *MAGE* or *Smc6*.

component	Drosophila CG	*Drosophila* symbol in FlyBase	*Schizosacchromyces pombe* gene	*Saccharomyces cerevisiæ* gene	Human gene
Smc5	CG32438	Dmel*Smc5*	Spr18	YOL034W/SMC5	SMC5L1 (alias KIAA0594, SMC5L1)
Smc6	CG5524	Dmel\CG5524	Rad18	YLR383W/SMC6 Rhc18	SMC6L1 (alias FLJ22116, FLJ35534, SMC-6, SMC6L1, hSMC6)
Nse1	CG11329	Dmel\CG11329	NSE1	YLR007W/NSE1	NSMCE1 (alias HSPC333, NSE1)
Nse2	CG13732 CG15645	*Dmel\qjt Dmel\cerv	NSE2	YEL019C/MMS21	NSMCE2 (alias C8orf36, FLJ32440, MMS21, NSE2)
Nse3	CG10059	Dmel*MAGE* (alias dMAGE)		YDR288W/NSE3	All MAGE genes NDNL2 (alias HCA4, MAGEG1, MAGEL3, NSE3, NSMCE3)
Nse4	CG13142	Dmel\CG13142	Rad 62	YDL105W/NSE4 (alias Qri2)	NSMCE4A (alias NSE4APP4762, C10orf86, FLJ20003, NSE4A) NSMCE4B (alias NSE4B, EID3)/EID1

Table 2-4 Genes encoding Smc5/6 complexes in different model organisms.

* used by Chiolo I, Minoda A, Colmenares SU, Polyzos A, Costes SV, Karpen GH. 2011. Double-strand breaks in heterochromatin move outside of a dynamic HP1a domain to complete recombinational repair. Cell 144:732-744. Nse= Non-SMC (structural maintenance of chromosomes) element 1 protein; SMC= structural maintenance of chromosomes

2.4.6 Drosophila Smc5/6 components form a protein complex.

In yeasts, the Smc5/6 complex consists of Smc5, Smc6 and six Nse (non-Smc element) subunits (Sergeant *et al.* 2005), four of which were also identified in humans (Taylor *et al.* 2008; Hudson *et al.* 2011). In searches of Drosophila genome databases, we uncovered a set of putative transcription units that appear to correspond to SMC5/6 complex subunits in yeasts (Table 2-4). Of these, *MAGE* has previously been described as a homolog of yeast *Nse3* and human *MAGEG1* (Taylor *et al.* 2008). In Drosophila, Mage protein was shown to interact with Drosophila Nse4 (Nse4) using a yeast two-hybrid system (Giot *et al.* 2003). When we examined the Gene Expression Omnibus (GEO, (Chintapalli *et al.* 2007)) to compare gene expression profiles, we found that these two genes have very similar expression patterns across different tissues, supporting the idea that the encoded proteins function in a complex (Figure 2-6). Fission yeast Nse1 has been detected in the same sub-complex as Nse3 and Nse4, as part of the larger Smc5/6 complex (Figure 2-7) (Pebernard *et al.* 2006). We first tested for a physical interaction between Drosophila Mage and Nse4 in cell culture, by generating epitope-tagged plasmid constructs that produce HA-tagged Nse4 or FLAG-tagged Mage, and co-transfecting them into Drosophila Schneider 2 (S2) cells. We were able to co-immunoprecipitate HA-Nse4 and FLAG-Mage from S2 cell lysates (Figure 2-7B). We then performed *in vitro* pull down experiments to show that this interaction is likely direct, and that Mage also interacts with Nse1 directly (Figure 2-7C). These results indicate that the three Drosophila proteins (Nse1, Mage and Nse4) form a sub-complex analogous to that found in yeast, consistent with conservation of structure across species.

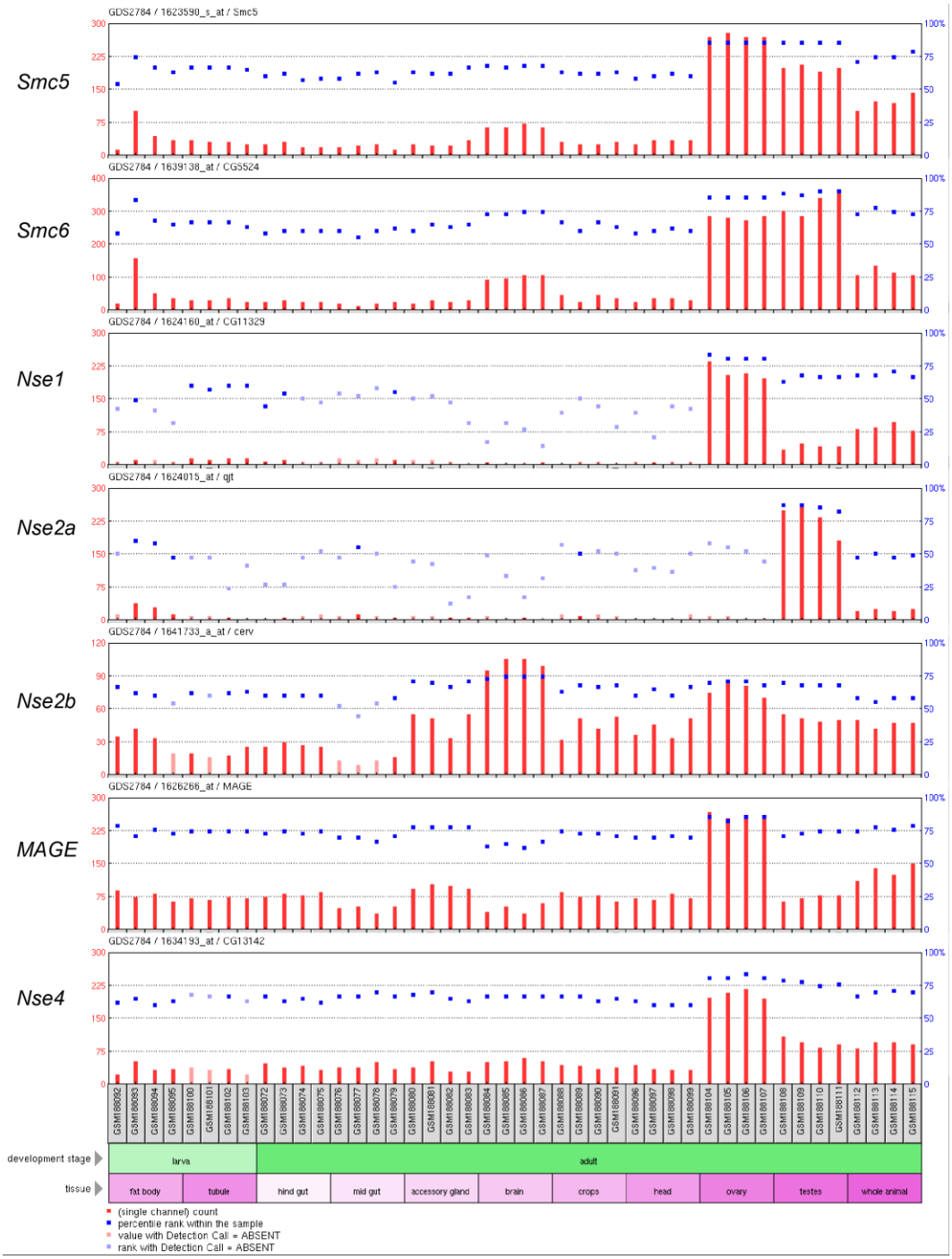

Figure 2-6 Expression profiles of genes encoding *Smc5/6* complex proteins.

The expression profile figure for each gene was obtained from GEO Profiles database at NCBI (GDS2784) from the original data of Chintapalli *et al.*(Chintapalli *et al.* 2007)

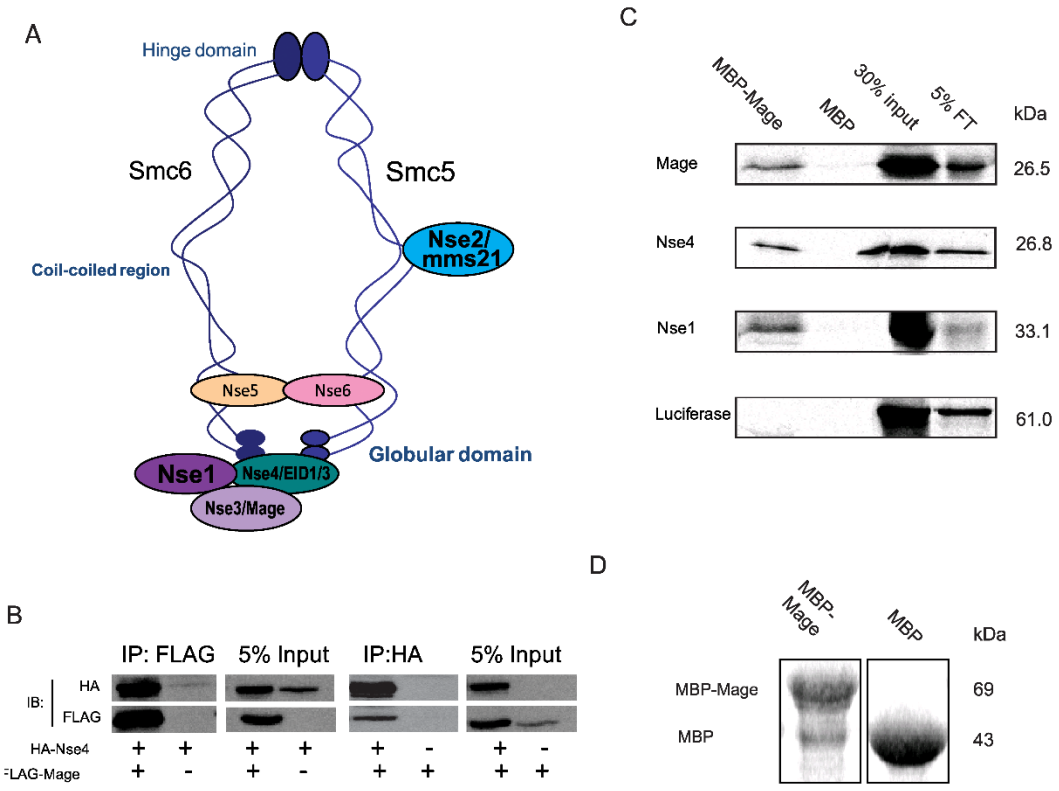

Figure 2-7 Mage is part of the Drosophila Smc5/6 complex.

(A) Diagram of a generic Smc5/6 complex in *S. pombe* (adapted from (Stephan *et al.* 2011c)). The structure in *S. cerevisiae* is different in that Nse5/6 were found to bind at the hinge. (B) Mage interacts with Nse4 when both proteins are co-expressed in *S2* cells. HA-Nse4 co-immunoprecipitated (co-IP) with FLAG-Mage from an *S2* cell lysate when two proteins were co-expressed; FLAG-Mage co-IPed with HA-Nse4 from the *S2* cell lysate when two proteins were co-expressed. (C) Recombinant Mage interacts with Nse4 and Nse1 directly. Immobilized maltose binding protein (MBP)-fused MAGE or MBP were incubated with ^{35}S-methionine labeled Mage, Nse4, Nse1, or luciferase (as a negative control), respectively. Proteins that were associated with immobilized MBP-Mage or MBP were resolved with SDS-PAGE and visualized by autoradiography. Results show that Mage, Nse4, and Nse1 each interact with MBP-Mage but not with MBP and luciferase does not interact with either of these proteins. (D) Coomassie staining of protein immobilized on 10 µl of amylose beads showed that approximately equal amounts of MBP-Mage and MBP proteins were immobilized on resin beads.

2.4.7 Loss of function for Smc6 or MAGE sensitizes imaginal cells to caffeine-induced apoptosis.

Previous examinations of *jnj*^{huc95E} hemizygous mutants were based on the EGUF eye mosaic system (Silva *et al.* 2006). In this experiment, Campbell and colleagues observed caffeine-dependent defects in ommatidial patterning and increased apoptosis in the eye discs. Larvae mutant for *Smc6* or *MAGE* die at the pupal stage when raised long term on caffeine-containing media. Remarkably, upon dissection of these larvae we noticed that the imaginal discs were severely damaged or altogether absent, suggesting increased cell death as the cause of this defect. To test this hypothesis, we dissected eye imaginal discs from late third instar larvae and labeled them with antibodies against activated caspase 3 to mark apoptotic cells. We detected minimal labeling of apoptotic foci in eye discs of control larvae, regardless of caffeine exposure (Figure 2-8). In contrast, dramatically increased labeling of apoptotic foci were seen in the eye discs of *Smc6* or *MAGE* mutant third instar larvae after short term (12 hours) caffeine exposure. Apoptotic labeling was markedly enhanced in a band of cells immediately anterior to the morphogenetic furrow, where cells become synchronized in G1 phase (Thomas and Zipursky 1994). These results suggest that caffeine-induced apoptosis in developing imaginal discs likely underlies caffeine-dependent pupal lethality in *MAGE* and *Smc6* mutant flies.

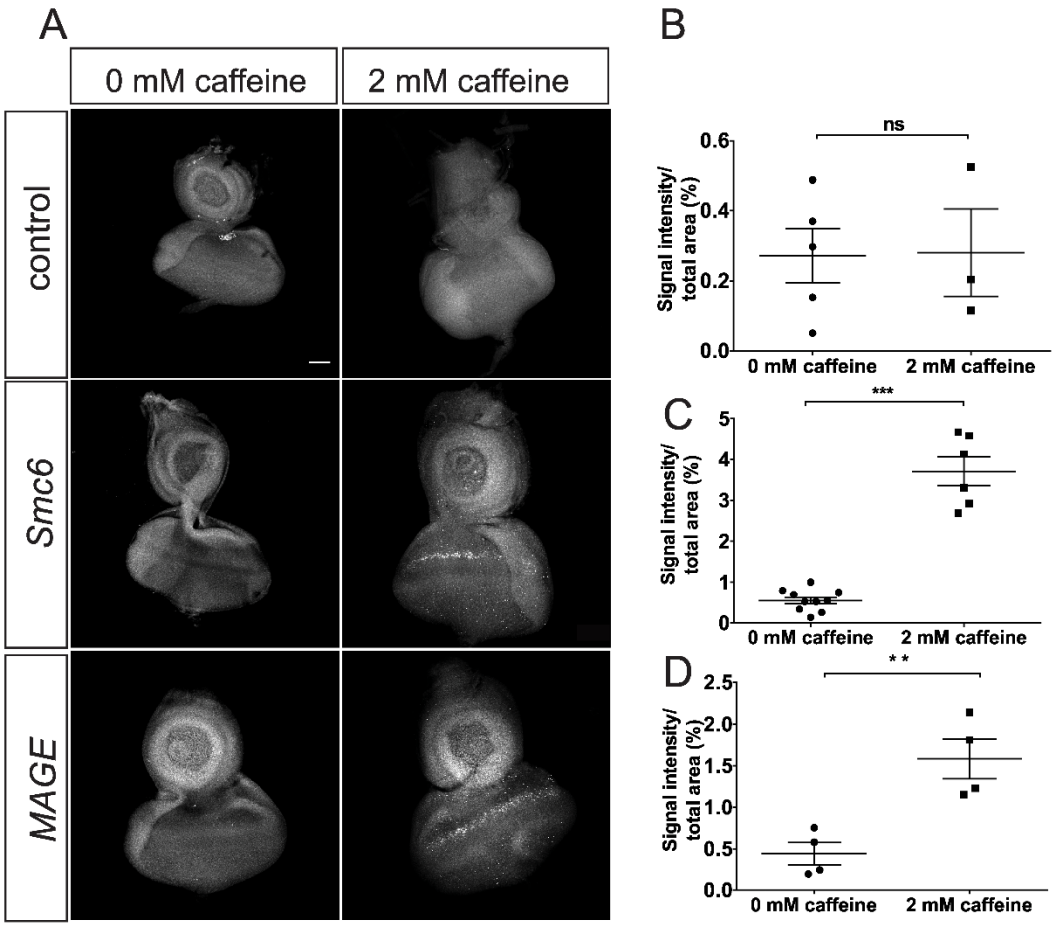
A
0 mM caffeine
2 mM caffeine
control
Smc6
MAGE
B
ns
Signal intensity/ total area (%)
0.6
0.4
0.2
0.0
0 mM caffeine
2 mM caffeine
C
***
Signal intensity/ total area (%)
5
4
3
2
1
0
0 mM caffeine
2 mM caffeine
D
**
Signal intensity/ total area (%)
2.5
2.0
1.5
1.0
0.5
0.0
0 mM caffeine
2 mM caffeine

Figure 2-8 Caffeine exposure results in apoptosis in eye discs of *MAGE* and *Smc6* mutants.

(A) Anti-cleaved-caspase-3 antibody staining of eye discs from third instar larvae of control (*WT*, *FRT82B*), *MAGE* (sst^{RZ}/sst^{XL}), and *Smc6* (jnj^{X1}/jnj^{R1}) genotypes raised in either standard media (0 mM caffeine) or media supplemented with 2 mM caffeine for 12 hours before dissection. Images are single stacks of confocal images. More cleaved-caspase-3 foci in eye discs of sst^{RZ}/sst^{XL} and jnj^{X1}/jnj^{R1} larvae were observed after caffeine exposure. A narrow band of apoptotic cells (white arrow heads) anterior to the presumptive morphogenetic furrow are most noticeable. Scale bar represents 50 μM. (B-D) Quantification and comparison of cleaved caspase-3 staining levels in *WT* (B), *MAGE* (C) or *Smc6* (D) eye discs, comparing the no caffeine and 2 mM caffeine groups. Data represent mean area stained from multiple eye discs for each genotype per treatment. A maximum projection of all stacks of a confocal image was used to quantify the signal intensity of staining. This value was divided by the area of each eye disc to obtain a ratio representing the relative amount of immunostaining. Error bars represent SEM. A non-paired two-tailed *t*-test was used to determine statistical significance. **, $P=0.006$, ***, $P<0.0001$.

2.4.8 Smc5/6 mutant flies are hypersensitive to genotoxic stress.

The DNA damage response is a multi-step process that involves sensing of damage, cell cycle arrest, and repair of the damaged DNA. Yeast with hypomorphic mutations affecting *Smc6*, *Nse1*, *Nse2*, *Nse3* or *Nse4* are hypersensitive to gamma irradiation, UV light, MMS, camptothecin (a topoisomerase I inhibitor), and inhibition of DNA replication by HU (De Piccoli *et al.* 2009). All of these genotoxic stresses directly or indirectly generate DNA single-stranded or double-stranded breaks. To explore whether Drosophila Smc5/6 provides similar responses to genotoxic stress, we analyzed the effects of ionizing radiation, camptothecin, HU or MMS on viability. Exposure to 40 Gy ionizing radiation caused increased lethality in *MAGE*, *Smc6* and *Smc5* mutants compared to controls (Figure 2-9). Moreover, all three mutants were hypersensitive to camptothecin, HU and MMS, compared to controls (Figure 2-10).

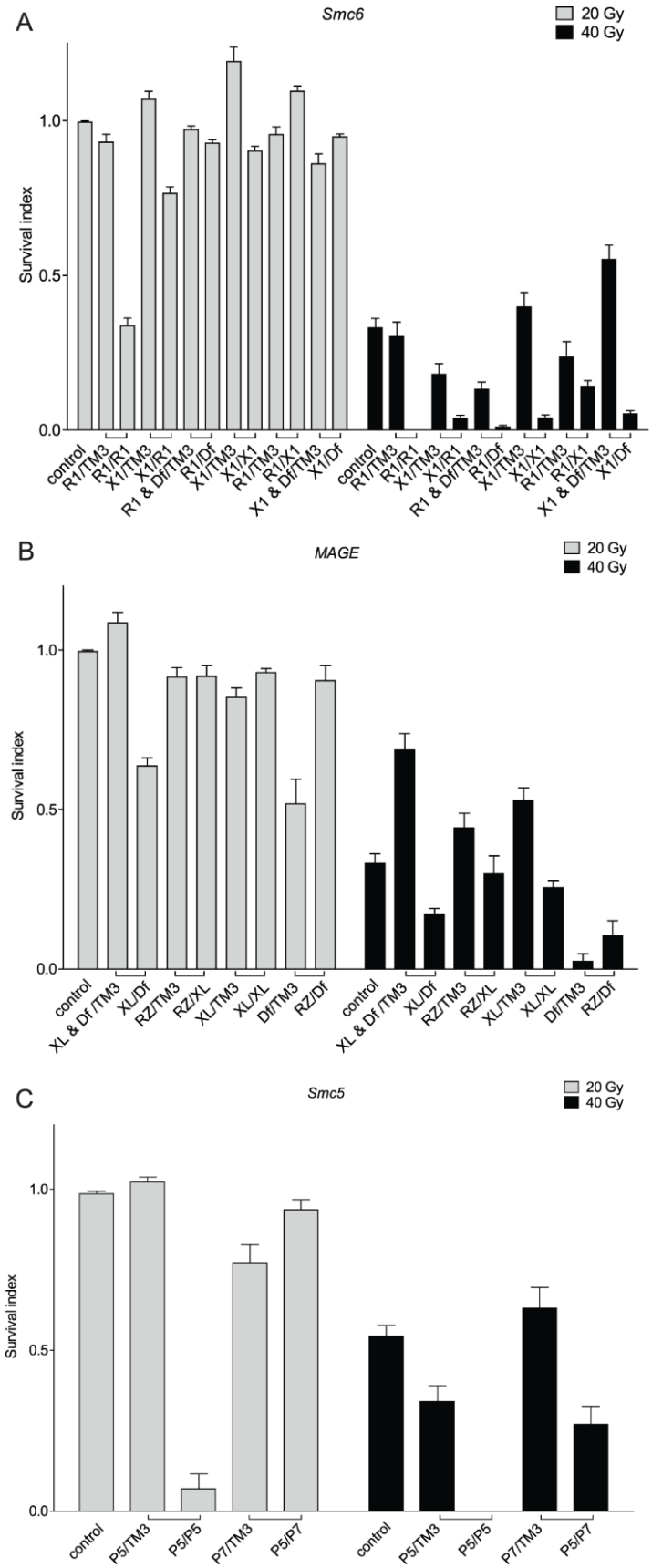
A
Smc6
20 Gy
40 Gy
Survival index
1.0
0.5
0.0
control
R1/TM3
R1/R1
X1/TM3
X1/R1
R1 & Df/TM3
R1/Df
X1/TM3
X1/X1
R1/TM3
R1/X1
X1 & Df/TM3
X1/Df
B
MAGE
20 Gy
40 Gy
Survival index
1.0
0.5
0.0
control
XL & Df /TM3
XL/Df
RZ/TM3
RZ/XL
XL/TM3
XL/XL
Df/TM3
RZ/Df
C
Smc5
20 Gy
40 Gy
Survival index
1.0
0.5
0.0
control
P5/TM3
P5/P5
P7/TM3
P5/P7

Figure 2-9 *Smc5/6* mutants are hypersensitive to ionizing radiation.

(A-C) *Smc6, MAGE* or *Smc5* homozygous, trans-heterozygous or hemizygous mutants have reduced survival when exposed to 40 Gy of IR. Bars represent the survival index (*p*) ± SEM. "␣" indicates flies eclosed from the same cross. Absence of a bar indicates that no flies survived at that IR dose. (A) *Smc6* mutants are hypersensitive to IR. *R1* (jnj^{R1}) and *X1* (jnj^{X1}) are *Smc6* alleles. *Df* (*Df(3R)Exel6198*) is a deficiency chromosome uncovering the *Smc6* locus. (B) *MAGE* mutants are hypersensitive to IR. *RZ* (sst^{RZ}) and *XL* (sst^{XL}) are *MAGE* alleles. *Df* ($Df(3R)Antp^{1}$) is a deficiency chromosome uncovering the *MAGE* locus. (C) *Smc5* mutants are hypersensitive to IR. *P5* ($Smc5^{P\{GSV1\}GS3245}$) and *P7* ($Smc5^{P\{GSV6\}GS14577}$) are *Smc5* alleles. *Df* (*Df(3L)BSC418*) is a deficiency chromosome uncovering the *Smc5* locus.

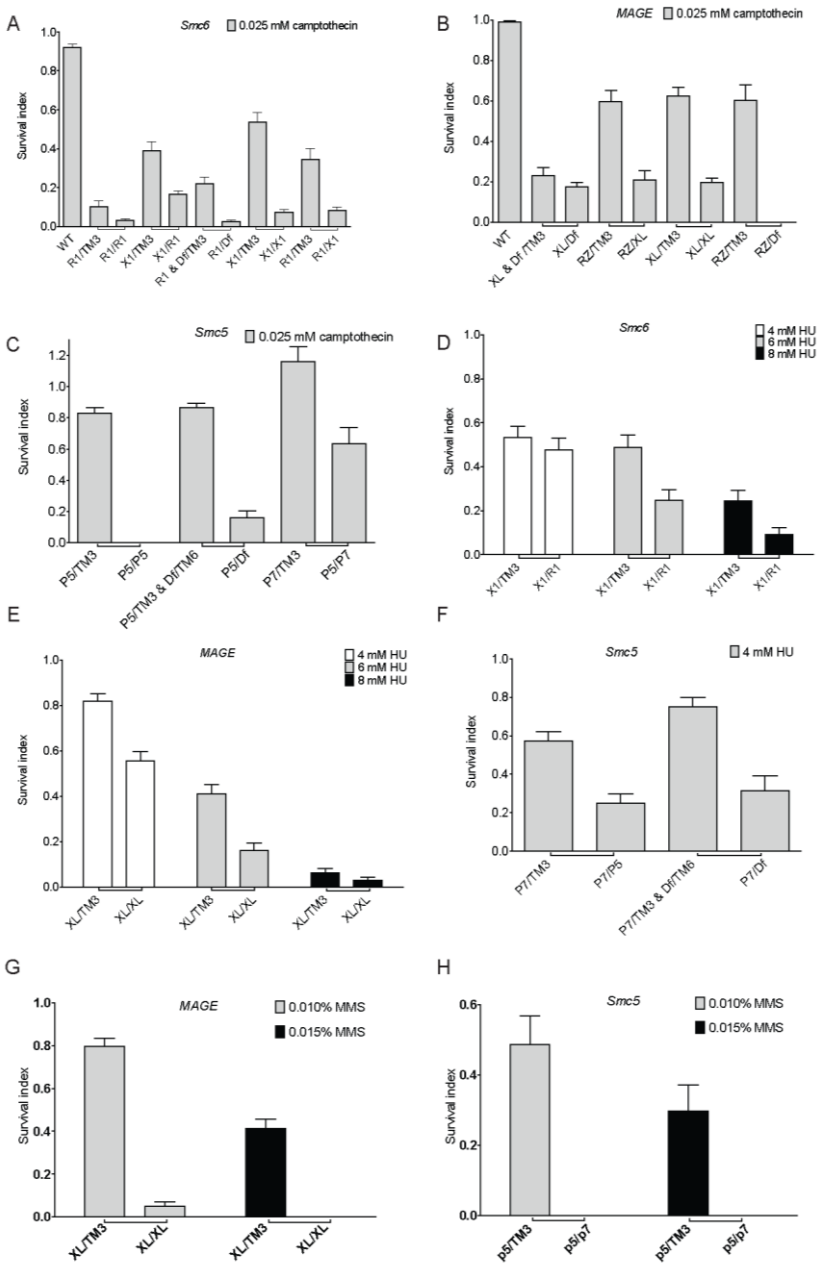
A
Smc6
0.025 mM camptothecin
Survival index
WT
R1/TM3
R1/R1
X1/TM3
X1/R1
R1 & Df/TM3
R1/Df
X1/TM3
X1/X1
R1/TM3
R1/X1
B
MAGE
0.025 mM camptothecin
Survival index
WT
XL & Df /TM3
XL/Df
RZ/TM3
RZ/XL
XL/TM3
XL/XL
RZ/TM3
RZ/Df
C
Smc5
0.025 mM camptothecin
Survival index
P5/TM3
P5/P5
P5/TM3 & Df/TM6
P5/Df
P7/TM3
P5/P7
D
Smc6
4 mM HU
6 mM HU
8 mM HU
Survival index
X1/TM3
X1/R1
X1/TM3
X1/R1
X1/TM3
X1/R1
E
MAGE
4 mM HU
6 mM HU
8 mM HU
Survival index
XL/TM3
XL/XL
XL/TM3
XL/XL
XL/TM3
XL/XL
F
Smc5
4 mM HU
Survival index
P7/TM3
P7/P5
P7/TM3 & Df/TM6
P7/Df
G
MAGE
0.010% MMS
0.015% MMS
Survival index
XL/TM3
XL/XL
XL/TM3
XL/XL
H
Smc5
0.010% MMS
0.015% MMS
Survival index
p5/TM3
p5/p7
p5/TM3
p5/p7

Figure 2-10 *Smc6, MAGE* and *Smc5* mutants are sensitive to camptothecin, HU and MMS.

Flies eclosed from the same cross are indicated with a '␣' . Embryos (n=360, expected to be half homozygous or transheterozygous mutants and half heterozygous mutants) were collected from a given cross for each drug concentration and allowed to develop in media without or with each drug. Bars represent the survival index (*p*) ± SEM. Absence of a bar indicates that no flies survived at that drug concentration. The survival index was calculated by normalizing the number of eclosed adults from each drug treatment against the number of eclosed adults from the no treatment control.

(A-C) *Smc6, MAGE* or *Smc5* homozygous, trans-heterozygous or hemizygous mutants have reduced survival when raised in media supplemented with 0.025 mM camptothecin;

(D-F) *Smc6, MAGE* or *Smc5* homozygous, trans-heterozygous or hemizygous mutants have reduced survival when raised in media supplemented with hydroxyurea (HU); (G) *MAGE* mutants are sensitive to MMS; (H) *Smc5* mutants are sensitive to MMS. *Smc6* mutants are also sensitive to MMS (data not shown). *Smc6*: *R1* (jnj^{R1}) and *X1* (jnj^{X1}) are *Smc6* alleles. *Df* (*Df(3R)Exel6198*) is a deficiency chromosome uncovering the *Smc6* locus; *MAGE*: *RZ* (sst^{RZ}) and *XL* (sst^{XL}) are *MAGE* alleles. *Df* ($Df(3R)Antp^{1}$) is a deficiency chromosome uncovering the *MAGE* locus. *Smc5*: *P5* ($Smc5^{P\{GSV1\}GS3245}$) and *P7* ($Smc5^{P\{GSV6\}GS14577}$) are *Smc5* alleles. *Df* (*Df(3L)BSC418*) is a deficiency chromosome uncovering the *Smc5* locus.

2.4.9 Loss of Smc5/6 function does not compromise G2/M and S phase checkpoints induced by genotoxic agents.

Studies in Drosophila have proven to be valuable for the study of proteins and pathways controlling DNA repair and checkpoint responses, which are remarkably well conserved among flies and other organisms (Sekelsky *et al.* 2000; Chiolo *et al.* 2011). In *S. pombe*, *nse3-1* hypomorphic mutants activate a DNA damage checkpoint that arrests cells in late S phase/G2 (Pebernard *et al.* 2004), and *Smc6 (Rad18)* is required for maintenance but not activation of the G2 checkpoint (Verkade *et al.* 1999; Miyabe *et al.* 2006). We therefore tested whether cell cycle checkpoints important for DNA damage response pathways were perturbed in caffeine-sensitive *MAGE* or *Smc6* mutant flies. To assess G2/M checkpoint function we used ionizing radiation (IR) to determine if IR exposure decreased the number of mitotic cells (Brodsky *et al.* 2000). We dissected eye imaginal discs from late third instar larvae and labeled them with anti-phospho histone H3 antibodies to mark mitotic cells. The number of mitotic cells in un-irradiated eye imaginal discs of jnj^{R1} *(Smc6)* or sst^{XL} *(MAGE)* larvae was comparable to that of control eye discs (Figure 2-11A). Larvae were exposed to 40 Gy of IR and dissected eye discs were examined from 15 to 120 min. after exposure. Phospho-histone H3 foci disappeared after 30 or 60 min in wild-type (*Iso)* controls, $jnj^{R1/X1}$ *(Smc6)* and $sst^{XL/RZ}$ *(MAGE)* eye discs (Figure 2-11A), demonstrating that neither Mage nor Smc6 is required for activation of the G2/M checkpoint.

The caffeine sensitive ATM/ATR kinases are important mediators of DNA damage checkpoints (Cimprich and Cortez 2008). In *S. pombe*, the SMC5/6 complex is recruited to and stabilizes stalled replication forks after Rad3 (ATR homolog) activation (Irmisch *et al.* 2009). To investigate whether the S phase checkpoint was intact in $jnj^{R1/X1}$ *(Smc6)* and $sst^{XL/RZ}$ *(MAGE)* mutant flies, we monitored BrdU incorporation pattern in eye imaginal discs before and after treatment with HU, which induces the S phase checkpoint (Klovstad *et al.* 2008). We observed many S-phase cells incorporating BrdU in control untreated eye discs, however incorporation was abolished upon exposure to HU. BrdU incorporation was also abolished by HU treatment in $jnj^{R1/X1}$ and $sst^{XL/RZ}$ mutant discs (Figure 2-11B), demonstrating that Mage and Smc6 are also not essential for S phase checkpoint activity in Drosophila.

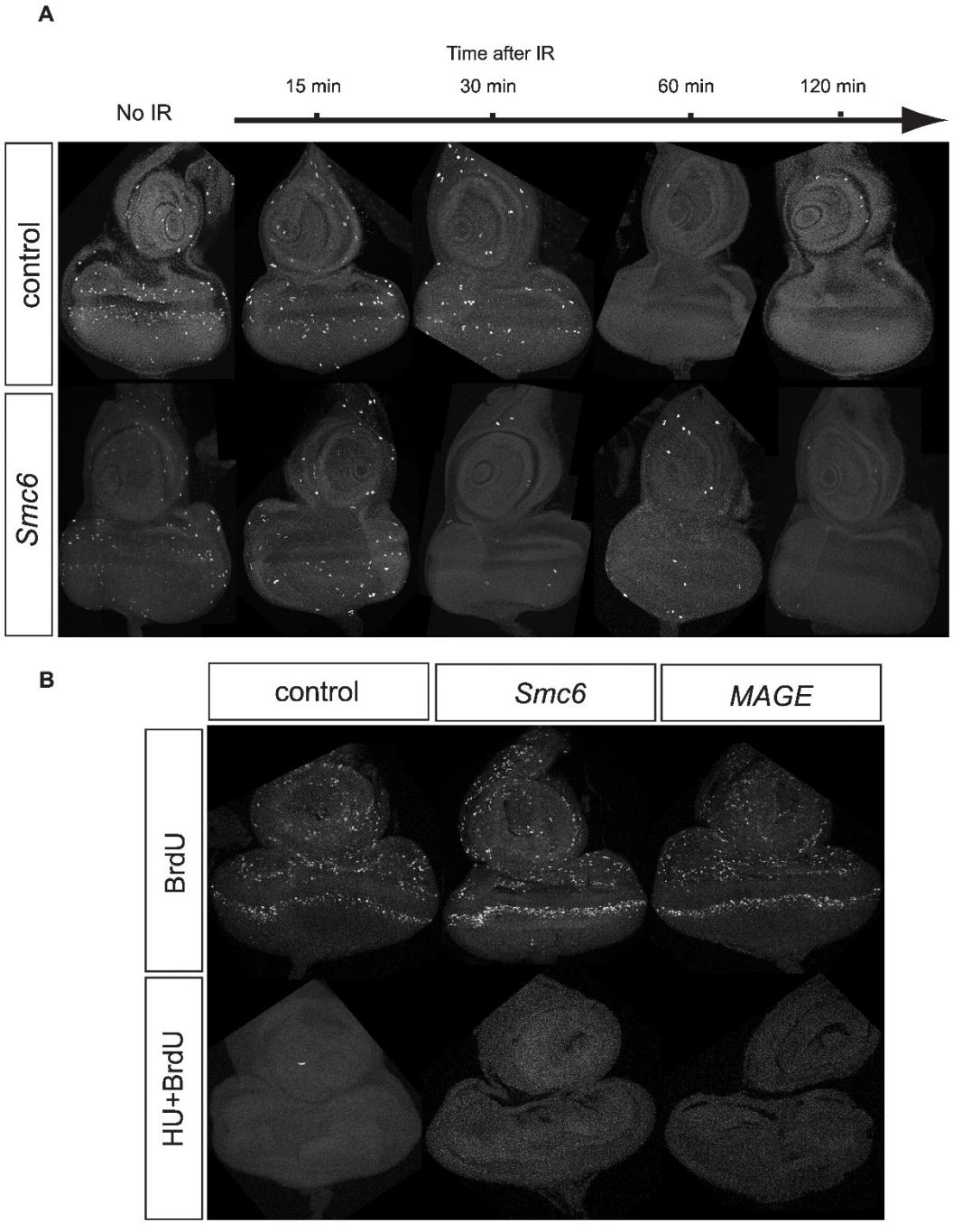
A
Time after IR
15 min
30 min
60 min
120 min
No IR
control
Smc6
B
control
Smc6
MAGE
BrdU
HU+BrdU

Figure 2-11 *Smc5/6* genes are not required for G2/M and S phase checkpoints induced by genotoxic agents.

(A) Wandering third instar larvae were irradiated with 40 Gy of ionizing radiation and the eye-antenna discs were dissected and fixed 15 minutes, 30 minutes, 1 hour or two hours after radiation, with discs from unirradiated larvae serving as controls. Representative images of PH3 staining for mitotic cells in eye-antenna discs from control (*WT, FRT82B*) and *Smc6*, (jnj^{R1}/jnj^{X1}) transheterozygous larvae are shown. (B) Eye-antenna discs from wandering third instar larvae were incubated with or without HU before adding BrdU to the incubation solution. Representative images of BrdU staining for cells in S phase in eye-antenna discs from control (*WT, FRT82B*), transheterozygous *Smc6* (jnj^{R1}/jnj^{X1}) or transheterozygous *MAGE* (sst^{RZ}/sst^{XL}) eye-antenna discs are shown.

2.4.10 Smc6 and MAGE genetically interact with proteins required for DNA damage responses.

Caffeine inhibits ATR and ATM kinase activity (Blasina *et al.* 1999; Sarkaria *et al.* 1999), raising the possibility that partial loss of ATM or ATR function could be contributing to the caffeine-induced defects that we observed in *Smc5/6* mutant flies. We therefore examined whether genetically reducing ATM or ATR function in an *Smc6* mutant background would cause synthetic lethality. The Drosophila homolog of ATR is Mei-41 (Laurencon *et al.* 2003) and *mei-41* mutants are homozygous viable but not caffeine-sensitive on their own (Silva *et al.* 2006). To test for genetic interactions between *mei-41* and *Smc6*, we generated double mutants and measured the proportion that survived to adulthood when raised on caffeine-free media. There was no increased lethality associated with *mei-41;Smc6* double mutants (Table 2-5), implying that the inhibition of ATR alone by caffeine was not the main cause of caffeine-dependent lethality of *Smc6* homozygotes. To further examine genetic interactions between *ATR* and *MAGE* or *Smc6*, we used the EGUF system as a more sensitive system for detecting mutant phenotypes than lethality. Raised on standard media, adult flies with homozygous *MAGE* mutant eyes were indistinguishable from control flies (Figure 2-12). Raised on 2 mM caffeine, however, *MAGE* mutant eyes were moderately rough relative to control eyes. *ATR* RNAi alone caused no observable roughness in the eye but when *ATR* RNAi was expressed in MAGE-deficient eyes, moderate to severely rough caffeine-dependent eye defects were observed that were not seen on caffeine-free media (Figure 2-12, quantification in Figure 2-13). We then tested whether ATM plays a role in caffeine sensitivity. Drosophila *ATM* (*tefu*) null mutants are non-conditional pupal lethal (Silva *et al.* 2004), so we used the *EGUF* system to examine these interactions as well. *ATM*-RNAi knockdown alone produced a normal looking eye, either in the absence or presence of caffeine. When *MAGE* mutant eyes were combined with *ATM*-RNAi, however, we observed a range of caffeine-dependent rough eye phenotypes, similar to eye defects caused by *ATR*-RNAi in *MAGE*-deficient eyes (Figure 2-12, Figure 2-13). We noted differences in expressivity between the *MAGE*-deficient eyes (compare Figure 2-2A and Figure 2-12A) that could be caused by slight differences in the genetic background (the genetic interaction study used *CyO* balancers while the original screen had wild type chromosomes) or the accumulation of genetic

modifiers. We propose that the caffeine-induced partial loss of function of both ATM and ATR causes the rough eye phenotype in the *MAGE*-deficient background, and that further loss of either ATM or ATR increases the severity of this phenotype, We also examined interactions with *NBS1*, a component of the MRN (Mre11, Rad50 and Nbs1) complex that collaborates with ATM in DNA repair and telomere maintenance (Czornak *et al.* 2008). While *NBS1*-knockdown alone produced no effect, a dramatic caffeine-dependent enhancement of the rough eye phenotype was observed when *NBS1*-RNAi was combined with eye-specific *MAGE* mutants (Figure 2-14). These striking caffeine-dependent genetic interactions between *MAGE* and *ATR, ATM,* and *NBS1* suggest that these proteins act together in maintaining genome stability. Similar genetic interactions were observed between *ATR* and *ATM* in *Smc6* eye-specific mutants, supporting this conclusion (Ran Zhuo, personal communications).

	$jnj^{X1}/jnj^{Df(3R)Exel6198}$	$jnj^{X1}/TM3,Ser,ActGFP$
$mei\text{-}41^{D3}/Y$	99^{ns}	79^{ns}
FM7/Y	22^{***}	35^{***}
$mei\text{-}41^{D3}/+$	118^{ns}	110 (double heterozygotes)
FM7/+	118^{ns}	105^{ns}

Table 2-5 *mei-41/ATM* and *jnj/Smc6* double mutants have normal viability.

jnj^{X1} homozygous males were crossed to $mei\text{-}41^{D3}/FM7;\ jnj^{Df(3R)Exel6198}/TM3,Ser,ActGFP$. The progeny representing the eight possible genotypes were counted. The number of progeny for each genotype was compared with the number of progeny heterozygotes for *mei41* and *Smc6* ($mei41^{D3}/+$; $jnj^{X1}/TM3,Ser,ActGFP$) using a chi-square test, with equal numbers expected in each category. "ns" indicates the number of progeny was not significantly different from the number of double heterozygotes ($P > 0.05$) while "***" indicates the number of progeny was significantly different from the number of double heterozygotes ($P < 0.001$). Fewer *FM7/Y* progeny survived, independent of *jnj* genotype, presumably because of non-balanced mutations on the *FM7* chromosome that reduce viability.

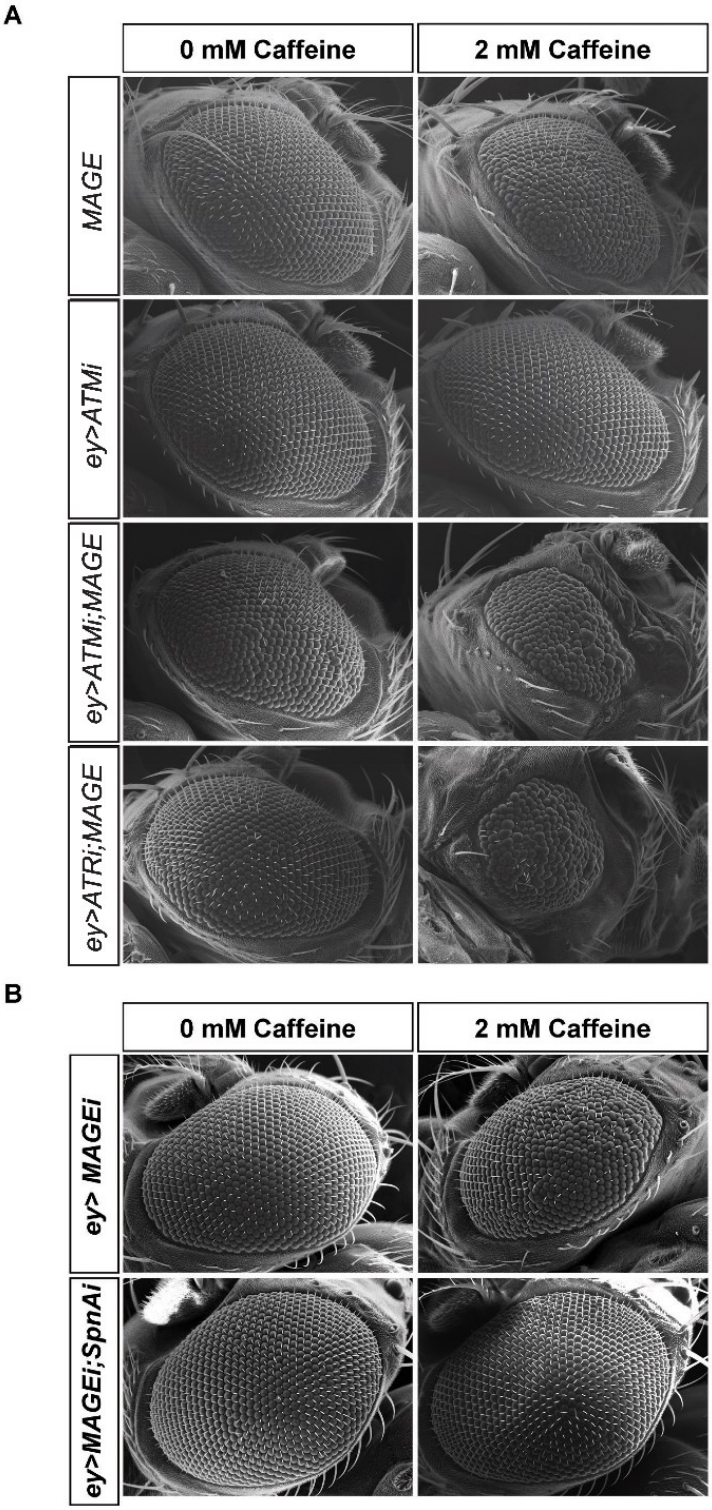
A
0 mM Caffeine
2 mM Caffeine
MAGE
ey>ATMi
ey>ATMi;MAGE
ey>ATRi;MAGE
B
0 mM Caffeine
2 mM Caffeine
ey> MAGEi
ey>MAGEi;SpnAi

Figure 2-12 Caffeine-dependent genetic interaction of *MAGE* with *ATM*, *ATR* and *Rad51*(*SpnA*).

(A) Representative eye phenotypes of *MAGE* (*EGUF/+; FRT82B sst^{RZ}/FRT82B GMR-hid*, loss of *MAGE* in eye cells), *ey>ATMi* (knockdown of *ATM* in eye cells), *ey>ATMi;MAGE* (*EGUF/UAS-ATM-RNAi;FRT82B sst^{RZ}/FRT82B GMR-hid,* loss of *MAGE* and knockdown of ATM in eye cells) and *ey>ATRi;MAGE* (*EGUF/UAS-ATR-RNAi;FRT82B sst^{RZ}/FRT82B GMR-hid,* loss of *MAGE* and knockdown of ATR in eye cells) flies that were reared on either standard media or media containing 2 mM caffeine. The EGUF system carrying the *eyeless-Gal4* driver was used to drive the UAS-RNAi transgenes in the eye and also makes the eye homozygous for *MAGE* (*sst^{RZ})*. Controls for the effects of each eyeless-driven RNAi alone were carried out for *ATM* and *ATR* resulting in wild type appearing eyes, but only the results of *ATM* RNAi are shown here as an example. (B) Representative eye phenotypes of *MAGE* knockdown (*eyeless-Gal4/+;UAS-MAGE-RNAi/UAS-Dicer2,* knockdown of *MAGE* in eye cells) and *MAGE Rad51* double knockdown (*eyeless-Gal4/UAS-SpnA-RNAi;UAS-MAGE-RNAi/UAS-Dicer2*, knockdown of *MAGE* and *Rad51* in eye cells) flies that were reared on either standard media or media containing 2 mM caffeine.

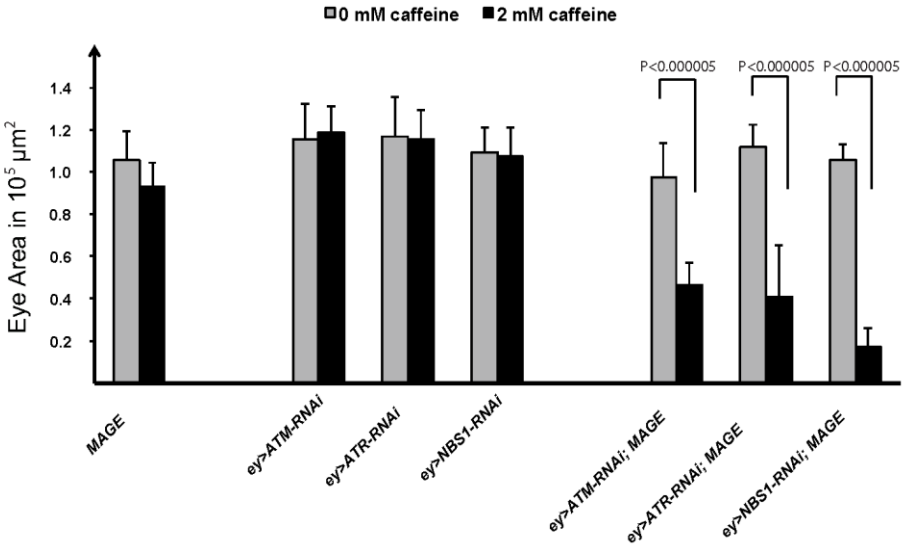

Figure 2-13 Quantification of the area of the adult eye as a measure of the genetic interaction of *MAGE* with *ATM*, *ATR* or *NBS1*.

MAGE (*EGUF/+; FRT82B sst^{RZ}/FRT82B GMR-hid*, loss of *MAGE* in eye cells), *ey>ATM-RNAi* (knockdown of *ATM* in eye cells), *ey>ATR-RNAi* (knockdown of *ATR* in eye cells), *ey>NBS1-RNAi* (knockdown of *NBS1* in eye cells), *ey>ATM-RNAi;MAGE* (*EGUF/UAS-ATM-RNAi;FRT82B sst^{RZ} /FRT82B GMR-hid,* loss of *MAGE* and knockdown of ATM in eye cells), *ey>ATR-RNAi;MAGE* (*EGUF/UAS-ATR-RNAi;FRT82B sst^{RZ} /FRT82B GMR-hid,* loss of *MAGE* and knockdown of ATR in eye cells), and *ey>NBS1-RNAi;MAGE* (*EGUF/UAS-NBS1-RNAi;FRT82B sst^{RZ}/FRT82B GMR-hid,* loss of *MAGE* and knockdown of *NBS1* in eye cells) flies were reared on either standard media or media containing 2 mM caffeine. A Student two-tailed *t*-test was performed to compare between genotypes.

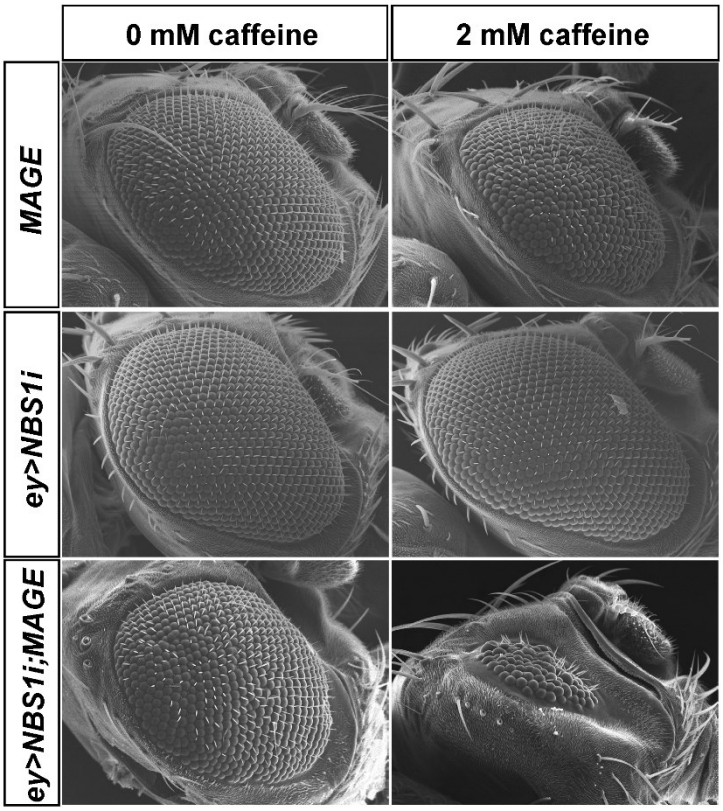

Figure 2-14 *NBS1* interacts with *MAGE*.

Representative eye phenotypes of *MAGE* (*EGUF/+; FRT82B sst^{RZ}/FRT82B GMR-hid*, loss of *MAGE* in eye cells) and *ey>NBS1i* (knockdown of *NBS1* in eye cells) and *ey>NBS1i;MAGE* (*EGUF/UAS-NBS1-RNAi;FRT82B sst^{RZ}/FRT82B GMR-hid,* loss of *MAGE* and knockdown of *NBS1* in eye cells) flies that were reared on either standard media or media containing 2 mM caffeine. The *EGUF* system carrying the *eyeless-Gal4* driver was used to drive the *UAS*-RNAi transgene in the eye and was also made the eyes homozygous for *sst^{RZ}*.

2.4.11 Drosophila MAGE RNAi caffeine sensitive phenotype is rescued by Rad 51 knockdown.

In Drosophila and other organisms, Smc5/6 functions in the homologous recombination repair pathway in DNA double strand break repair (De Piccoli *et al.* 2009; Watanabe *et al.* 2009; Stephan *et al.* 2011b). Rad51 is a key component of the homologous recombination pathway, regulating the rate-limiting step of homology searching and strand invasion. In Drosophila, Smc5/6 prevents precocious Rad51 loading onto irradiation damaged heterochromatin region before it moves outside of the HP1a domain for proper repair (Chiolo *et al.* 2011). In yeast, *Smc5/6* mutants accumulate unresolved DNA structures, and Smc5/6 actively resolves DNA mediated sister chromatin linkages (Ampatzidou *et al.* 2006; Branzei *et al.* 2006; Sollier *et al.* 2009). We therefore tested whether the caffeine-dependent rough eye phenotype of *Smc5/6* mutants is related to deregulated Rad51 activity. Knocking down *Rad51* in the *MAGE*-RNAi background rescued the rough eye phenotype of *MAGE*-RNAi flies in 80% of the double RNAi flies raised on 2 mM caffeine (Figure 2-12B, Figure 2-15). Taken together, these data indicate that the caffeine sensitivity of the Smc5/6 complex or at least of *MAGE* mutants is largely attributable to improper Rad51 activity. It is also possible that Rad51 action is normal during HR, but the Smc5/6 complex mutants are unable to complete HR repair or resolve HR intermediates.

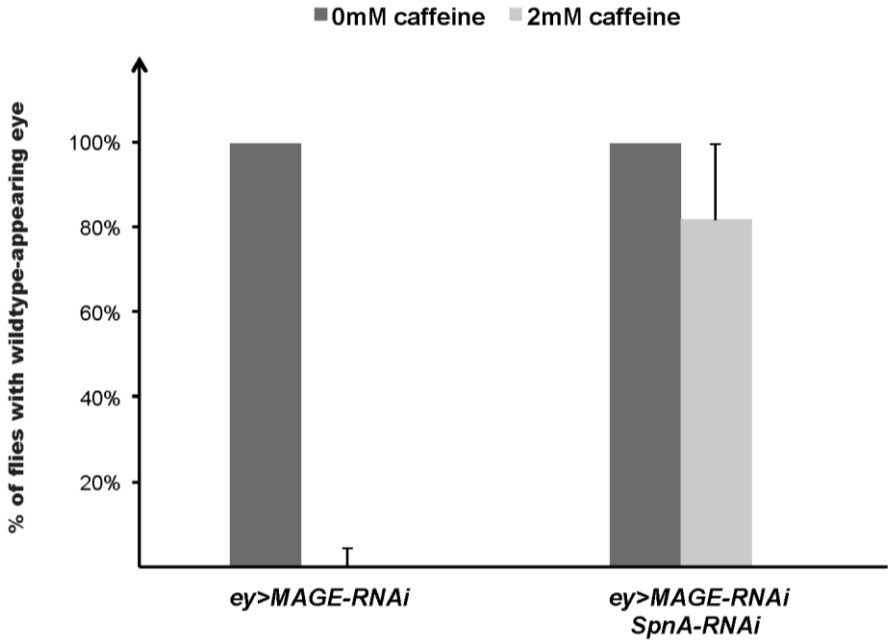

Figure 2-15 *Rad51 (SpnA-RNAi)* depletion rescues the *MAGE-RNAi* caffeine-sensitive eye phenotype.

Bars represent the percentage of flies with wildtype eye phenotypes among *MAGE* knockdown (*UAS-Drc2/+; UAS-MAGE-RNAi/+*) and *MAGE Rad51* double knockdown (*Drc2/+; UAS-MAGE-RNAi/UAS-SpnA-RNAi*) flies that were reared on either standard media or media containing 2 mM caffeine. Data were collected from 4 replicates of each cross. Absence of error bar indicates flies of this genotype had consistent phenotypes.

2.5 Discussion

In a genetic screen for mutations conferring caffeine sensitivity in flies, Campbell et al. identified viable alleles of Drosophila *Smc6* (*jnj*; *CG5524*) and *MAGE* (*sst; CG10059*) as well as an unknown gene (*ddt*). Additional loss-of-function alleles created by imprecise P-element excision of *Smc6* (jnj^{X1}) or targeted knockout of *MAGE* (sst^{XL}) were also viable under normal conditions, but exhibited caffeine-sensitive lethality. Although no molecular lesions were identified for most *jnj* (*Smc6)* alleles, transcript levels were dramatically reduced in all these mutants when hemizygous, implying that either mutations in regulatory regions affected expression, or that, like jnj^{R1}, transcripts were subjected to nonsense-mediated decay. There was no detectable *MAGE* expression in homozygous, transheterozygous, or hemizygous *sst* mutants. Furthermore, a genomic *MAGE* transgene restored expression and rescued the caffeine-dependent lethality of *sst* mutants. Loss of *Smc5* by P-element insertion also resulted in caffeine sensitivity. These genetic results as well as biochemical data showing physical interactions among SMC6, MAGE, Nse1 and Nse4 indicate that the Drosophila Smc5/6 complex is structurally and functionally conserved between yeast and flies. The Campbell screen only covered one chromosome arm (3R) to obtain seven alleles of *Smc6* and two alleles of *MAGE*, representing ~20% of the genome. Homologs of the remaining SMC5/6 components reside on chromosome arms 2L and 3L (Table 2-4) and were thus not discovered in the screen. As there are no known *Smc5/6* homologs mapping to the *ddt* locus, identifying this gene and screening remaining chromosome arms for mutations conferring caffeine sensitivity may lead to novel Smc5/6 components or other pathways in which *Smc5/6* is involved.

The SMC5/6 complex has been intensively studied in yeasts and human cells for its roles in chromosome replication, segregation and repair of DNA double strand breaks by homologous recombination (Kegel and Sjogren 2010). Depletion of Smc5 or Smc6 in Drosophila tissue culture cells resulted in heterochromatin bridges in 50% of mitotic cells (Chiolo *et al.* 2011), suggesting that the *Smc5* or *Smc6* genes would be essential for viability. On the contrary, we found that the loss of *Smc5, Smc6*, or *MAGE* did not result in lethality *in vivo*, and indeed homozygous mutant flies have been maintained for generations. There was a slight reduction in hatching rates among null eggs from null mothers in some of the mutant lines, so we cannot rule out a contribution of the maternal

RNA to viability in early development. We also did not observe DNA links between sister chromatids, excess aneuploidy, or translocations in mitotic chromosomes of neuroblast squashes from Smc5/6 mutant flies. Homologs of *Smc5* and *Smc6* in *Caenorhabditis elegans* are also dispensable for viability, however the homozygous mutant strains were prone to sterility and germ cell defects because of compromised inter-sister chromatid recombinational repair and excessive germ cell apoptosis (Bickel *et al.* 2010).

In both *S. cerevisiae* and *S. pombe*, genes encoding SMC5/6 and Nse1-4 are essential and hypomorphic mutants are sensitive to genotoxic agents (Pebernard *et al.* 2004). In *C. elegans*, *smc-5* and *smc-6* mutant germ cells are also hypersensitive to IR and exhibit increased germ cell apoptosis even without IR exposure (Bickel *et al.* 2010). In vertebrates, *Smc5*-deficient chicken DT40 cells are sensitive to MMS and IR (Stephan *et al.* 2011b). Interfering with the function of human *NSE2* by RNAi sensitizes HeLa cells to MMS-induced DNA damage (Potts and Yu 2005). The *Smc5, Smc6* and *MAGE* mutants described here are also sensitive to IR (40 Gy), HU (4 mM to 8 mM), camptothecin (0.025 mM) and MMS (0.05-0.015%), consistent with an evolutionarily conserved role in resistance to genotoxic agents. Components of the Smc5/6 complex may be responsible for existing Drosophila mutagen sensitive (*mus*) mutants (e.g. (Boyd *et al.* 1976)) or may not yet be represented among these collections so constitute novel genes important for mutagen resistance.

Our experiments suggested that cells located just before the morphogenetic furrow in the imaginal eye discs of larvae lacking Smc5/6 components were most sensitive to caffeine (Figure 2-8). Many of these cells normally become synchronized in G1 phase by being forced through mitosis through induction of the $Cdc25^{stg}$ gene suggesting that the *Smc5/6* and *MAGE* mutants described here are particularly sensitive to mitotic kinase Cdk1 activity when treated with caffeine (Thomas and Zipursky 1994). G2/M checkpoint responses to DNA damage and the S-phase checkpoint induced by stalled replication forks were both intact in Drosophila *Smc6* or *MAGE* mutants, however. These results may be explained by accumulating evidence that yeast *Smc5/6* mutants undergo normal initiation of the checkpoint response but then fail to complete repair before entering mitosis leading to the formation of DNA bridges and aberrant mitosis (Verkade *et al.* 1999; Harvey *et al.* 2004; Torres-Rosell *et al.* 2005; Bermudez-Lopez *et al.* 2010). Consistent with this

explanation, Drosophila MAGE and Smc6 mutants genetically interact with ATM and ATR to increase the severity of the caffeine-induced rough eye phenotypes (Figure 2-12). Similar dependencies were also recently reported for *S. cerevisiae,* where *Nse2* mutants deficient in SUMO ligase activity were viable but needed Mec1 kinase (ATR) to survive, even in the absence of genotoxic stress (Rai *et al.* 2011).

Studies of protein complexes that are critical for cellular responses to genotoxic stress are also highly relevant to cancer therapy in humans. It is increasingly apparent that the gene expression signature of each tumor dictates in part the success or failure of chemotherapeutic treatment or radiotherapy (Wong *et al.* 2011). The expression of human Type I MAGE genes is commonly dysregulated in cancer cells. Moreover, studies have correlated the levels of expression of particular MAGE genes with therapeutic response, prognosis and probability of metastasis (Miranda 2010). The unexpected synergy between caffeine and loss of SMC5/6 activity could potentially be exploited for new therapeutic strategies where one could preferentially sensitize checkpoint-compromised cancer cells to apoptosis. Although the therapeutic potential of caffeine for causing premature chromosome condensation in G1 checkpoint-compromised cancer cells has long been recognized, the concentrations needed to fully inhibit ATR kinases are toxic (Nghiem *et al.* 2001). In cells exposed to UV-light, caffeine inhibits rescue of stalled replication forks by translesion DNA synthesis, causing a switch to homologous recombination that can result in chromosomal aberrations (Johansson *et al.* 2006; Han *et al.* 2011). Further studies are needed to elucidate the relationships among MAGE proteins, Smc5/6 components, and proteins such as ATM and ATR that are also important for resistance to genotoxic agents in normal and cancer cells. In turn, mechanistic understanding of how cells respond to genotoxic stress will aid in the selection and dose of chemotherapeutic agents that target specific disruptions to DNA damage response pathways, in order to improve cancer prognosis and survival.

Chapter 3 Drosophila Mage plays a role in the cell cycle and in cell survival

3.1 Summary

Over 50 Melanoma-associated antigen (MAGE) genes have been identified in humans. The proteins share a conserved 200 amino acid MAGE-homology domain (MHD). MAGE members play diverse roles in development and cancer progression by interacting with a variety of proteins. Some members regulate cell cycle and cell survival by interacting with the pRb-E2F and/or the p53 pathways. Other members are implicated in DNA damage repair as a component of the structural maintenance of chromosomes (SMC) 5/6 protein complex. The only Mage (encoded by *MAGE)* in the fruit fly, *Drosophila melanogaster*, is also a component of the Smc5/6 complex. Mutations in *MAGE* confer sensitivity to caffeine and genotoxic stress to flies. In this chapter, we hypothesized that MAGE's roles in regulating cell cycle and cell survival are conserved between flies and humans, and we studied the effects of *MAGE* depletion and over-expression in Drosophila S2 cells. *MAGE* depletion, resembling *Smc5* or *Smc6* depletion, leads to G1 and S phase accumulation. *MAGE* over-expression slows cell proliferation by arresting cells in S and M phases and promoting polyploidy. Furthermore, *MAGE* over-expression also confers a survival advantage to cells exposed to genotoxic stress. We also found an interdependency of protein stability between Mage and its interaction partners including Smc5, Smc6, Nse4, and Nse1. Finally, we found a functional link between p53 and Mage. p53 levels were reduced by Mage over-expression. Nse4, the interaction partner of Mage, but not Mage itself, interacts with p53.

3.2 Introduction

Melanoma-associated antigen (MAGE) proteins were first identified as antigens expressed by human melanomas. Over 50 MAGE genes have been identified in the human genome. Type I MAGE proteins (MAGEA, MAGEB and MAGEC) are expressed only in male germ cells, placental tissues and tumors, while Type II MAGE proteins (MAGED, MAGEE, MAGEL2, NDN and NDNL2 (MAGEG1)) are expressed in the nervous system and other tissues. The majority of cancer cell lines over-express type I MAGE proteins due to global DNA hypomethylation. Type I MAGE over-expression correlates with cancer development, drug resistance, and poor prognosis (Li *et al.* 2014). The MAGE proteins

share a conserved 200 amino acid MAGE-homology domain (MHD) and most members are 300-400 amino acid long (Barker and Salehi 2002).

Previous studies suggest that mammalian MAGE proteins influence cell cycle and cell survival by interacting with Rb-E2F and/or p53 pathways. Some MAGE proteins, such as Necdin, MAGEG1, MAGED1 and MAGED3 strongly inhibit cell proliferation when they are over-expressed in cancer cell lines (Hayashi *et al.* 1995; Salehi *et al.* 2000; Kuwako *et al.* 2004; Wen *et al.* 2004; Nishimura *et al.* 2008). Some of them interact with the E2F1 transcription factor and repress its transcriptional activation in reporter assays (Taniura *et al.* 1998; Kuwako *et al.* 2004). E2F1 promotes the progression of the cell cycle from G1 to S phase by inducing expression of the G1 cyclins, including cyclin D and E. Therefore, MAGE proteins can induce cell cycle arrest by repressing E2F1 activity. MAGE proteins could also regulate the cell cycle by interacting with p53. For example, MAGE-D1 represses cell cycle progression in a p53 dependent manner (Kuwako *et al.* 2004; Wen *et al.* 2004). MAGE proteins repress apoptosis by regulating p53 activities (Kuwako *et al.* 2004; Ladelfa *et al.* 2012). MAGE can recruit histone deacetylases (HDACs) to target p53 and repress its activity (Kuwako *et al.* 2004; Monte *et al.* 2006; Yang *et al.* 2007). MAGE can also target p53 by interacting with RING domain E3 ubiquitin ligases and enhancing their ligase activities (Doyle *et al.* 2010; Feng *et al.* 2011). In addition, MAGE can repress p53 transcriptional activity directly by blocking p53 interaction with chromatin (Marcar *et al.* 2010). Finally, MAGE can also influence cell survival when cells encounter DNA damage agents as some MAGE proteins are part of the Smc5/6 complex that functions in DNA damage repair (De Piccoli *et al.* 2009; Li *et al.* 2013).

The Smc5/6 complex is formed by the association of four conserved Non-Smc-Elements (Nse1-4) proteins with the core Smc5/6 heterodimer (De Piccoli *et al.* 2009). Nse1, a RING domain-containing protein with E3-ubiquitin ligase activity, Nse3, encoded by *MAGE* genes in humans and flies, and Nse4, a kleisin domain containing protein, together form a tight sub-complex that bridges the core Smc5/6 head domains.

Only one MAGE gene exists in the Drosophila genome (*MAGE*). We previously showed that the Drosophila Mage protein is part of the Smc5/6 complex and homozygous *MAGE* mutant flies are viable but sensitive to DNA damaging agents (Li *et al.* 2013). In

this chapter, we asked whether *MAGE* plays a role in proliferation, resistance to genotoxic agents, and regulation of p53 in Drosophila S2 cells. We found that *MAGE*, *Smc5* or *Smc6* depletion changes the cell cycle profile. Over-expression of *MAGE* slows cell proliferation by arresting cells in S and M phases and promotes polyploidy. Furthermore, over-expression of *MAGE* confers a growth advantage to cells exposed to genotoxic stress. We also found an interdependency of protein stability between Mage and its interaction partners including Smc5, Smc6, Nse4, and Nse1. Finally, although p53 level was reduced by Mage over-expression, it associated with Nse4 but not Mage.

3.3 Materials and Methods

3.3.1 DNA constructs and dsRNAs

Full-length cDNA clones were obtained from the Canadian Drosophila Microarray Centre (*Nse1* (GM14348), *Nse4* (IP09347), *Smc5* (RE65864), *Smc6* (SD25546), *E2f* (GH16721)*, Dp* (LD24245), *CycE* (LD22682)*, cdc2c (cdk2)* (LD22351)*, Cdk4* (LD31205), *Rbf* (LD02906), *dm(dMyc)* (LD32539), *Myt1* (GH08848), *Wee1* (LD27552), *cdk1(cdc2)* (LD38718), *CycB* (LD23613), *Myb (*LD22943*)*, *tefu (ATM)* (AT01448), and *p53* (GH11591)) or the Drosophila Genomics Resource Center (DGRC, Indiana University) (*MAGE* (RE25453)). Expression constructs for transfection of S2 cells were created by inserting relevant full-length coding sequences into Drosophila Gateway destination vectors (pHWH (hsp70::C-3XHA), pHWF ((hsp70::C-3XFLAG) pTWH (UAST::C-3XHA) obtained from the DGRC) or pMT-DEST48 (C-terminal V5 epitope; Invitrogen, Burlington, ON, Canada). Ubiquitin-GAL4 (ubi-GAL4) was a gift from Dr. Sarah Hughes. dsRNAs were synthesized using the MEGAscript T7 Transcription Kit (AM1334, Invitrogen). T7 promoter anchored PCR products amplified from the cDNA clones were used as templates for dsRNA synthesis. dsRNA treatment of S2 cells was described previously (Rogers and Rogers 2008).

3.3.2 Culture and transfection of S2 cells

S2 cells (Invitrogen) were cultured in SFX medium (SH3027801, Thermo Scientific, Waltham, MA) without serum, at 25℃. Transfection was performed using

dimethyldioctadecylammonium bromide (DDAB) according to an adapted protocol (Han 1996). For transfections, 2×10^6 cells/ml were plated in SFX medium. For 1 ml of culture, a DDAB/medium mixture (35 µl of DDAB (250 µg/ml) and 70 µl of SFX medium) was prepared and 0.5 µg of plasmid was added 5 minutes later. The DDAB/medium/DNA mixture was incubated for 15 minutes and added to the cells. Cells were collected for analysis two days after transfection.

3.3.3 Generation of Mage expressing lines

S2 cells were co-transfected with an expression construct (e.g. pMT-MAGE-V5) and pCoHygro (Invitrogen) at a ratio of 19:1. On day 3 following transfection, the cell media were replaced with fresh media, and on day 5 the media were replaced with fresh media containing 300 µg/ml hygromycin B (H0654-250MG, Sigma-Aldrich, Oakville, Ontario, Canada). From then on, the media were replaced with fresh hygromycin B-containing media every 5 days until a hygromycin resistant culture was established. Cell lines were maintained in hygromycin B-containing media. All experiments were carried out in media without hygromycin.

3.3.4 Drug treatment

Drug stocks were prepared according to a previously described method (Li *et al.* 2013). Drugs were added into media 24 hours after induction of Mage-V5 expression by addition of $CuSO_4$ to the concentration of 500 µM. After 24 hours, cells were collected, washed once with PBS and fixed in a solution of 2% paraformaldehyde in PBS for 10 min. V5-tagged Mage was detected with an anti-V5 antibody (R960-25, Invitrogen, 1:1000 ~ 1:2000) by immunofluorescence.

3.3.5 Cell labeling and flow cytometry of S2 cells.

S2 cells were fixed and immunostained for flow cytometry analysis using an adapted protocol (Bettencourt-Dias and Goshima 2009). S2 cells were suspended in the culture media and pelleted by centrifugation at 300 *g*. Cells were resuspended in 200 µl PBS and fixed by adding 2 ml 70% ice-cold ethanol drop-by-drop and mixed by vortexing.

After allowing at least 30 minutes of ethanol fixation, cells were re-hydrated by washing two times in PBS.

For cell cycle analysis of dsRNA-treated S2 cells, cells were treated with RNase A (100 µg/ml) and incubated at 37℃ for 30 min. Cells were then stained with propidium iodide (PI, 100 µg/ml, P3566, Invitrogen) for 30 min. Three replicates of the dsRNA transfections were performed for each gene. About 40,000 cells were analyzed for each replicate by a FACSCalibur (BD Biosciences, San Jose, CA). Data were analyzed using the FlowJo software (Tree Star, Ashland, OR). DNA content (PI staining) was presented in the FL2-H channel instead of the more conventional FL2-A channel to show the >2N population (>2N is outside FL2-A range). Cell size was measured in the FSC (Forward Scatter) -A channel. Cell cycle shifts were examined by overlapping DNA content profiles of experimental and control samples.

For examination of DNA content and mitotic index in MAGE over-expressing cells, cells were resuspended in PBS with 1% BSA and 0.25% Triton X-100 and incubated on ice for 15 min. Immunostaining was carried out in PBS with 1% BSA. Mage-V5 was labelled with a mouse anti-V5 antibody (R960-25, Invitrogen, 1:1000) followed by Alexa 488-conjugated anti-mouse antibody (A-10680, Invitrogen, 1: 1000) and detected in the FITC-A channel or with a mouse anti-V5-Cy3 antibody (V4014, Sigma-Aldrich, 1:1000) and detected in the PE-Texas Red-A channel. Phospho-histone H3 was labelled with a rabbit anti-phospho histone H3 antibody (sc-8656-R, Santa Cruz, 1:1000) followed by Alexa 647-conjugated anti-rabbit antibody (Invitrogen) and detected in the APC-A channel. DNA was labeled with FxCycle Violet (F-10347, Invitrogen) and detected in the Indo-1(violet)-A channel. Flow cytometry was carried out using a LSR Fortessa Cell Analyzer (BD Biosciences). Data were analyzed using the FlowJo software (Tree Star).

3.3.6 Quantification of the proportion of Mage+ or CP3 + cells in the samples.

Transfected cell cultures were fixed and immunostained with the mouse anti V5 antibody (1:1000 ~ 1:2000). The following approaches were used to minimize artificially derived variations between samples in a given comparison. First, aliquots of antibodies from a master mix were always used to carry out immunostaining for all the samples. For

confocal imaging, pinhole size, laser power, and gains were adjusted so that captured signals for each channel were within a proper dynamic range. Images were always captured in one session to insure the same conditions for confocal imaging. Fixed number of stacks (usually 3~5 middle stacks) in a confocal image were used to produce a maximum projected image for quantification. To quantify the total number of cells (DAPI stained nuclei) or the number Mage+ cells (*i.e.* V5 positive cells), a control reference image was opened in ImageJ software (1.48v). The threshold and particle size were set so that the number of particles counted by the software reflected the actual number of cells or Mage+ cells in the reference image. A typical particle size is "5 pixel units ~ infinity". A typical threshold of "25-255" or "50-255" was used for nuclei or Mage+ cells, respectively. Particle numbers were then counted for each image for the number of total cells or of Mage+ cells. At least 5 images were counted for each sample and the proportion of Mage+ cells (*p)* was calculated by dividing the total number of Mage+ cells by the number of total cells (*N*). Standard error of the mean (SE) was calculated using the equation $\frac{\sqrt{p(1-p)}}{\sqrt{N}}$. The proportion of CP3+ cells was determined by the same approach using a rabbit anti-activated caspase 3 antibody (Millipore, Billerica, MA, 1:1000).

3.3.7 Co-expression, co-immunoprecipitation (Co-IP) and immunoblots

S2 cells ($3x10^6$ per well) were transfected with relevant expression constructs as described above. Induction of protein expression was carried out by adding $CuSO_4$ to a final concentration of 500 μM 24h after transfection for constructs with metallothionein promoters (pMT-p53-V5, pMT-Smc5-V5, pMT-Nse1-V5, and pMT-Nse4-V5), or by incubating the cells at 37℃ for 30 min 4h prior to harvest for constructs with heat shock promoters (Hsp70-MAGE-FLAG and Hsp70-Nse4-HA), or constitutive co-expression of Gal4 for UAS construct (ubi-GAL4 and UAST-Nse4-HA). For co-immunoprecipitation, cells were harvested 48 hours after transfection and re-suspended in ice-cold mild lysis buffer (50 mM Tris-HCl, 150 mM NaCl, 1% Triton X100, pH 7.4) supplemented with a protease inhibitor cocktail and a phosphatase inhibitor cocktail (Roche Applied Science, Indianapolis, IN). The lysate was centrifuged for 10 minutes at 20,000 *g* at 4 ℃. The supernatant was transferred to a fresh tube and mixed with 20 μl of protein G sepharose beads (GE Healthcare Life Sciences, Piscataway, NJ) pre-bound with 5 μg of a mouse

monoclonal antibody (anti-FLAG or anti-HA (Sigma-Aldrich)) or 15 µl of an anti-V5 agarose beads (Sigma-Aldrich). This mixture was then incubated overnight at 4℃ with rocking. The beads were washed six times in mild lysis buffer. Bound proteins were released by boiling beads in a sample buffer (20% glycerol, 4% SDS, 130 mM Tris-HCl pH 6.8, and 2% β-mercaptoethanol) and analyzed by immunoblots. For the experiments to determine the effect of *MAGE* over-expression on protein levels of Smc5/6 complex proteins and p53, cells were collected and boiled directly in the sample buffer and analyzed using immunoblots. Antibodies used on immunoblots included rabbit anti-FLAG (Sigma-Aldrich, 1:1000), rabbit anti-HA (Sigma-Aldrich, 1:1000), and rabbit anti-V5 (Millipore, Billerica, MA, 1:1000). Rabbit or guinea pig anti-Mage antibodies (gifts from Dr. K. Yoshikawa from Osaka University, 1:200~ 1:1000) were used to determine the endogenous Mage in S2 or Drosophila lysates. A mouse anti-β-tubulin antibody (E7, the Developmental Studies Hybridoma Bank at the University of Iowa, 1:2000) was used to determine the amount of β-tubulin in S2 cell or Drosophila lysates for normalizing variations in sample loading.

3.4 Results

3.4.1 Depletion of endogenous MAGE alters cell cycle

MAGE, *Smc5,* and *Smc6* are not required for cell viability during Drosophila development (Li *et al.* 2013). However, knocking down *MAGE* expression by RNA interference in neural stem cells leads to increased proliferation (Nishimura *et al.* 2008). we hypothesized that the Smc5/6 complex may nonetheless contribute to cell cycle progression when tested in cells cultured *ex vivo*. To examine the robustness of the cell cycle when Smc5/6 components are reduced, we used *in vitro* synthesized double strand RNA (Rogers and Rogers 2008) to deplete gene expression in the embryonic, spontaneously immortalized Drosophila Schneider 2 (S2) cell line. The *MAGE* gene is expressed in S2 cells as measured by immunoblotting for endogenous Mage protein (Figure 3-1a) and by RT-PCR detecting *MAGE* RNA (Figure 3-1b). Expression of *MAGE* was effectively reduced by treatment of S2 cells with dsRNA (Fig 1c).

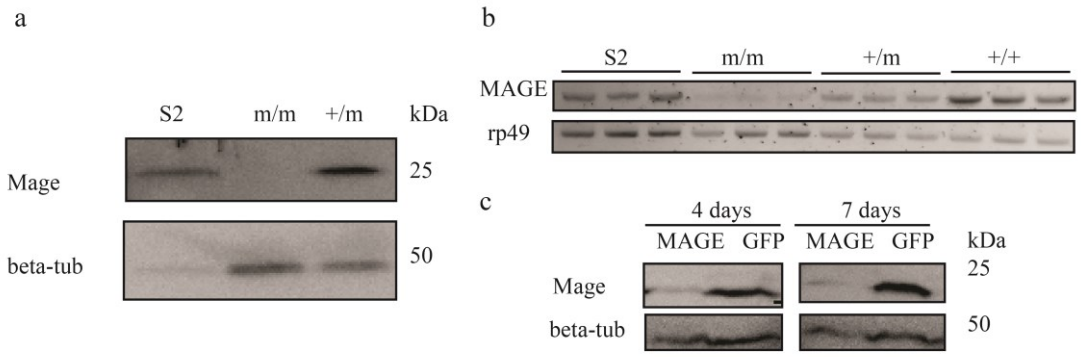

Figure 3-1 *MAGE* is expressed in S2 cells.

a. Immunoblot analysis of Mage protein in S2 cell lysates. Ovary protein lysates derived from homozygous MAGE mutant (m/m) or heterozygous mutant (+/m) flies were used as controls for Mage expression.

b. Semi-quantitative RT-PCR analysis of MAGE expression in S2 cells compared to RT-PCR of total RNAs from ovaries of homozygous mutant (m/m), heterozygous MAGE mutant (+/m) and wild type (+/+) flies.

c. Immunoblot analysis of Mage protein in lysates of S2 cells treated with MAGE dsRNA showing loss of Mage protein. Cells treated with GFP dsRNA were used as a control.

We predicted that knocking down *MAGE* expression in S2 cells would produce cell cycle profile changes that could be determined by flow cytometry. For comparison with *MAGE* depletion, we analyzed the effect of depletion of a variety of cell cycle regulatory genes within the same system. The genes we analyzed include genes in the Cdk/E2f pathway (*Dmel\E2f, \Dp, \CycE, \cdc2c (cdk2), \Cdk4,* and *\Rbf*), the myc/max pathway (*Dmel\dm (dMyc)*), the cdk1 pathway (*Dmel\Myt1, \Wee1, \cdk1 (cdc2),* and *\CycB*), *Dmel\Myb*, and the DNA damage repair gene *Dmel\tefu (ATM)*. We also included *Dmel\Smc5* and *Dmel\jnj (Smc6),* genes encoding the core heterodimer of the Smc5/6 complex in the experiment. Indeed, obvious cell cycle profile shifts were observed in cells in which cell cycle regulatory genes were depleted compared to control S2 cells (Figure 3-2a and Figure 3-3). For *MAGE*, *Smc5*, and *Smc6* knockdowns, small but consistent increases in the G1 (0 to 3%) and S (2-4%) fractions and decreases in the G2 fraction (3-7%) were observed. The small increases in G1 and S and decreases in G2 fractions also resembled the profiles of *Rbf* (G1 +4%, S +5% and G2 -7%) and *ATM* (G1 +3%, S +2% and G2 -7%) knock-downs.

Loss of MAGE/Smc5/6 complex function confers caffeine sensitivity *in vivo*, especially in proliferating cells (Li *et al.* 2013). S2 cells accumulate in the G1 stage (10% increase) when 2 mM caffeine is present in the medium (Figure 3-2b and Figure 3-3). We explored whether caffeine could modify the cell cycle profile shifts for cells with depleted *MAGE, Smc6,* or *Smc5*. Caffeine altered cell cycle profiles of S2 cells when *MAGE*, *Smc5* or *Smc6* was depleted. However, we did not observe any significant difference in cell cycle shift in *MAGE*, *Smc5,* or *Smc6* depleted cells compared to the control cells (dsRNA GFP with caffeine) when caffeine was present in the culture medium (Figure 3-2b and Figure 3-3). Therefore, caffeine treatment masks the effect of the *MAGE, Smc6,* or *Smc5* depletion on the cell cycle profiles observed previously.

We conclude that depletion of *MAGE, Smc6,* or *Smc5* in S2 cells increases the G1 and S phase population and decreases the G2 population. Caffeine treatment increases the G1 phase population but masks the effect from the depletion of *MAGE, Smc6,* or *Smc5*.

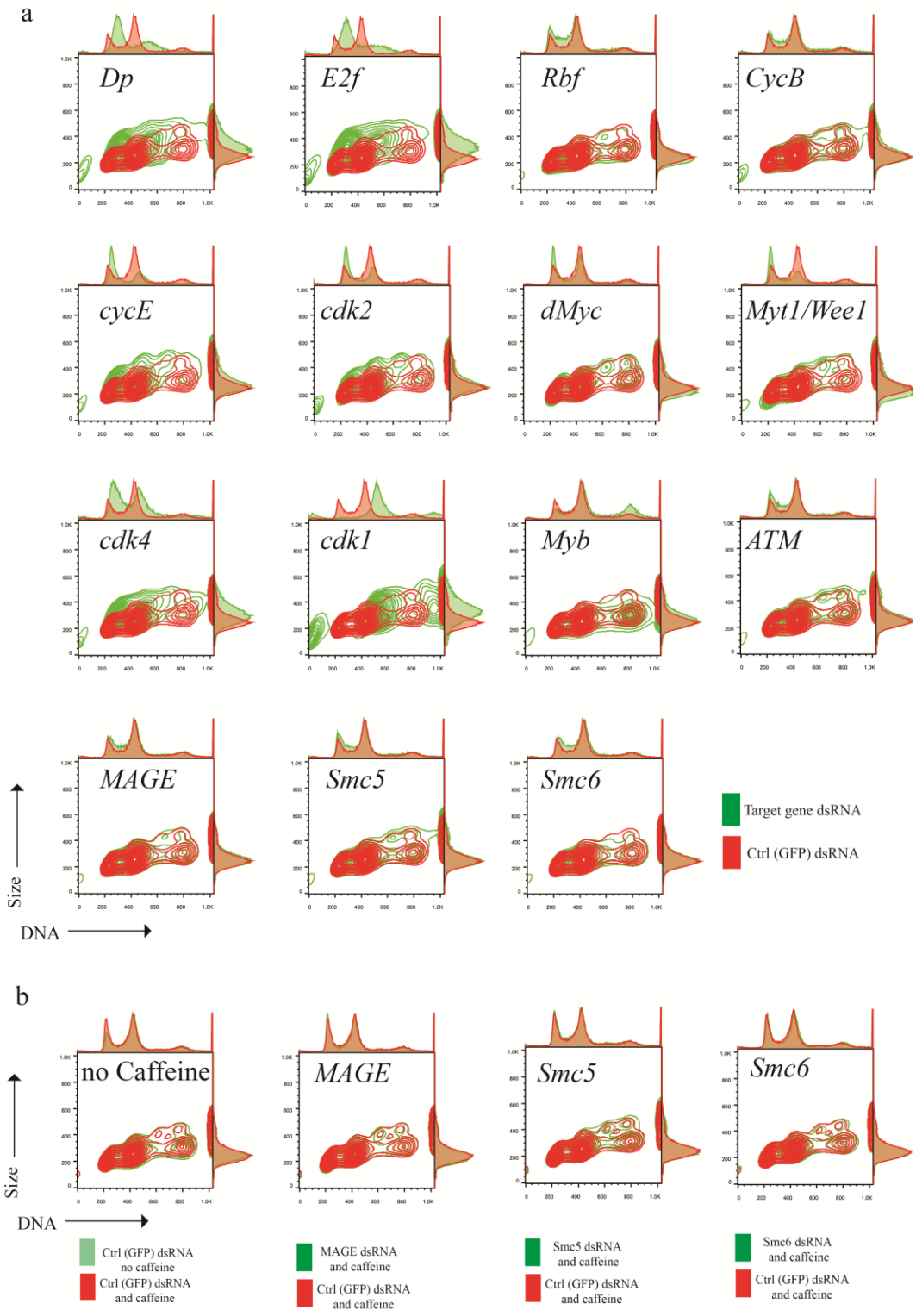
a
Dp
E2f
Rbf
CycB
cycE
cdk2
dMyc
Myt1/Wee1
cdk4
cdk1
Myb
ATM
MAGE
Smc5
Smc6
Size
DNA
Target gene dsRNA
Ctrl (GFP) dsRNA
b
no Caffeine
MAGE
Smc5
Smc6
Size
DNA
Ctrl (GFP) dsRNA no caffeine
Ctrl (GFP) dsRNA and caffeine
MAGE dsRNA and caffeine
Ctrl (GFP) dsRNA and caffeine
Smc5 dsRNA and caffeine
Ctrl (GFP) dsRNA and caffeine
Smc6 dsRNA and caffeine
Ctrl (GFP) dsRNA and caffeine

Figure 3-2 Flow cytometry analysis of S2 cells with depletion of *MAGE/Smc5/6* and other cell cycle and DNA damage repair genes.

a&b. S2 cells were treated with dsRNAs for 3 days. Caffeine was then added into the culture medium to a concentration of 2 mM 24 hours before harvest (no caffeine was added for experiments in a). Three replicate experiments were done for each gene. Data from one representative replicate are shown.

a. DNA content profiles of S2 cells with individual gene depleted (Green, target gene dsRNAs) are overlaid to a DNA content profile of control S2 cells (Red, GFP dsRNA).

b. DNA content profiles of S2 cells with *MAGE*, *Smc5,* or *Smc6* depleted when 2 mM caffeine is present in the culture medium. Left: A DNA content profile of S2 cells cultured without caffeine (Green, GFP dsRNA, no caffeine) overlaid with a DNA content profile of S2 cell cultured with caffeine in the culture medium (Red, GFP dsRNA, 2 mM caffeine); Right, DNA content profiles of S2 cells with *MAGE*, *Smc5*, or *Smc6* depleted with caffeine in the culture medium (Green, target gene dsRNAs, 2mM caffeine) overlaid with a control DNA content profile of cells with 2 mM caffeine (Red, GFP dsRNA, 2mM caffeine).

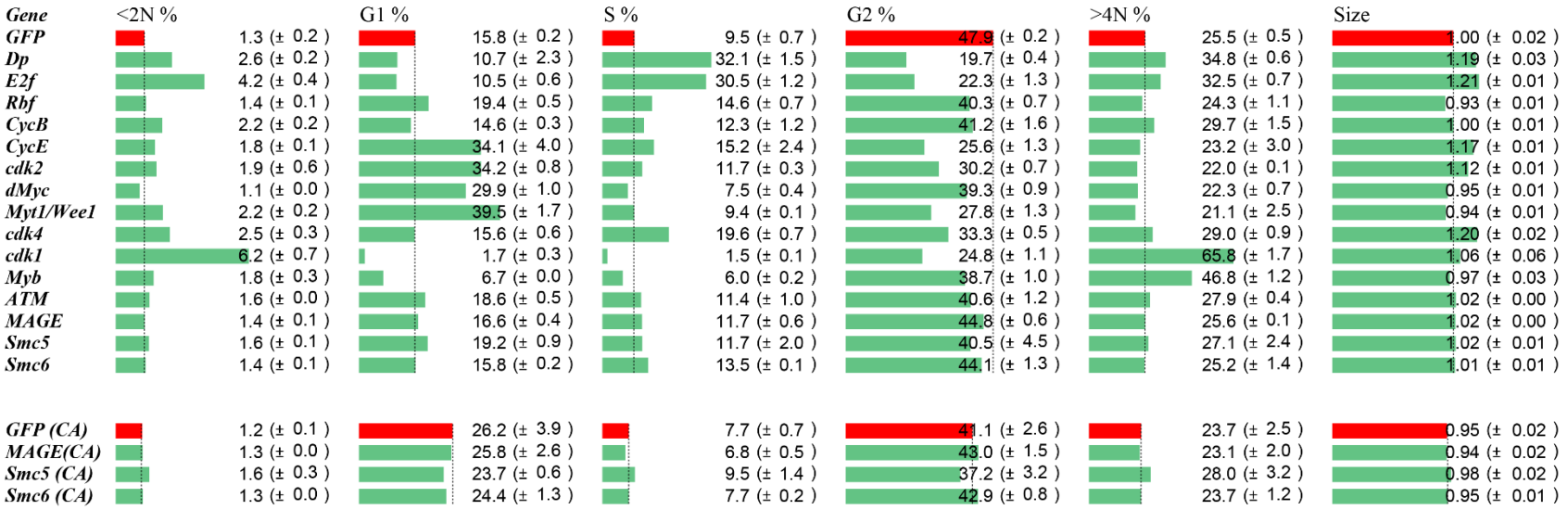

Gene	<2N %	G1 %	S %	G2 %	>4N %	Size
GFP	1.3 (± 0.2)	15.8 (± 0.2)	9.5 (± 0.7)	47.9 (± 0.2)	25.5 (± 0.5)	1.00 (± 0.02)
Dp	2.6 (± 0.2)	10.7 (± 2.3)	32.1 (± 1.5)	19.7 (± 0.4)	34.8 (± 0.6)	1.19 (± 0.03)
E2f	4.2 (± 0.4)	10.5 (± 0.6)	30.5 (± 1.2)	22.3 (± 1.3)	32.5 (± 0.7)	1.21 (± 0.01)
Rbf	1.4 (± 0.1)	19.4 (± 0.5)	14.6 (± 0.7)	40.3 (± 0.7)	24.3 (± 1.1)	0.93 (± 0.01)
CycB	2.2 (± 0.2)	14.6 (± 0.3)	12.3 (± 1.2)	41.2 (± 1.6)	29.7 (± 1.5)	1.00 (± 0.01)
CycE	1.8 (± 0.1)	34.1 (± 4.0)	15.2 (± 2.4)	25.6 (± 1.3)	23.2 (± 3.0)	1.17 (± 0.01)
cdk2	1.9 (± 0.6)	34.2 (± 0.8)	11.7 (± 0.3)	30.2 (± 0.7)	22.0 (± 0.1)	1.12 (± 0.01)
dMyc	1.1 (± 0.0)	29.9 (± 1.0)	7.5 (± 0.4)	39.3 (± 0.9)	22.3 (± 0.7)	0.95 (± 0.01)
Myt1/Wee1	2.2 (± 0.2)	39.5 (± 1.7)	9.4 (± 0.1)	27.8 (± 1.3)	21.1 (± 2.5)	0.94 (± 0.01)
cdk4	2.5 (± 0.3)	15.6 (± 0.6)	19.6 (± 0.7)	33.3 (± 0.5)	29.0 (± 0.9)	1.20 (± 0.02)
cdk1	6.2 (± 0.7)	1.7 (± 0.3)	1.5 (± 0.1)	24.8 (± 1.1)	65.8 (± 1.7)	1.06 (± 0.06)
Myb	1.8 (± 0.3)	6.7 (± 0.0)	6.0 (± 0.2)	38.7 (± 1.0)	46.8 (± 1.2)	0.97 (± 0.03)
ATM	1.6 (± 0.0)	18.6 (± 0.5)	11.4 (± 1.0)	40.6 (± 1.2)	27.9 (± 0.4)	1.02 (± 0.00)
MAGE	1.4 (± 0.1)	16.6 (± 0.4)	11.7 (± 0.6)	44.8 (± 0.6)	25.6 (± 0.1)	1.02 (± 0.00)
Smc5	1.6 (± 0.1)	19.2 (± 0.9)	11.7 (± 2.0)	40.5 (± 4.5)	27.1 (± 2.4)	1.02 (± 0.01)
Smc6	1.4 (± 0.1)	15.8 (± 0.2)	13.5 (± 0.1)	44.1 (± 1.3)	25.2 (± 1.4)	1.01 (± 0.01)
GFP (CA)	1.2 (± 0.1)	26.2 (± 3.9)	7.7 (± 0.7)	41.1 (± 2.6)	23.7 (± 2.5)	0.95 (± 0.02)
MAGE(CA)	1.3 (± 0.0)	25.8 (± 2.6)	6.8 (± 0.5)	43.0 (± 1.5)	23.1 (± 2.0)	0.94 (± 0.02)
Smc5 (CA)	1.6 (± 0.3)	23.7 (± 0.6)	9.5 (± 1.4)	37.2 (± 3.2)	28.0 (± 3.2)	0.98 (± 0.02)
Smc6 (CA)	1.3 (± 0.0)	24.4 (± 1.3)	7.7 (± 0.2)	42.9 (± 0.8)	23.7 (± 1.2)	0.95 (± 0.01)

Figure 3-3 Quantification of cell cycle profiles of S2 cells following depletion of *MAGE, Smc5,* or *Smc6* and cell cycle and DNA damage repair genes.

The analysis used the same experimental data described in Figure 3-2. The numbers in parentheses represent SD. The size values are derived from the G1 populations and calculated by normalizing the average raw values against the average raw value of the three *GFP* samples.

3.4.2 MAGE over-expression changes cell cycle profile of S2 cells

Over-expression of *NDN* in mammalian cell lines leads to cell cycle arrest. To test whether over-expression of the Drosophila *MAGE* also interferes with cell cycle regulation, we generated a S2 cell line (S2-Mage) in which expression of a V5-epitope-tagged Mage protein (Mage-V5) is inducible when $CuSO_4$ is added in the culture. In uninduced S2-Mage cultures, Mage-V5 expression was evident in less than 1% of cells as measured by immunofluorescence analysis. The cell line had been selected and maintained in hygromycin B containing medium, but not all cells were expressing Mage under induced conditions. This is probably because the MAGE cDNA was on a separate vector to that containing hygromycin resistance, and had been lost in some cells in the process of integration to the genome during the drug selection process. Nevertheless, in induced cultures, the proportion Mage-V5 expressing cells ranged from 9% to 25%. We were thus able to directly compare *MAGE* over-expressing (referred to as Mage+) cells with those expressing only endogenous levels of *MAGE* (referred to as Mage= cells*)* in the same culture.

We examined the cell cycle profile of Mage+ *vs* Mage= cells by measuring the DNA content by flow cytometry. In the culture shown in Figure 3-4 (a-d), while 18.7% of Mage= cells had DNA that suggested polyploidy (i.e. >4N), 34.3% of Mage+ cells were in the polyploid range for DNA content (Figure 3-4b-c, overlay in Figure 3-4d). We also measured the mitotic index of Mage+ *vs* Mage= cells in a second induced culture. In the culture shown in (Figure 3-4e-f), 11.3% of cells were Mage+ as measured by anti-V5 staining (Figure 3-4e). By co-immunostaining with anti-phospho-histone 3 (PH3), we were able to visualize and define a mitotic cell population (≥4N DNA content and high PH3 staining, Figure 3f), which consisted of 3.11% of the total population. In these mitotic cells, 22.5% were Mage+ cells (in Figure 3-4f). Therefore, Mage+ cells are about two fold over-represented in the mitotic population compared to the whole population. Thus, cells over-expressing *MAGE* were more likely to be in mitosis compared to cells expressing only endogenous levels of *MAGE*. Within the <4N population, a significant proportion of Mage+ cells are in early S phase (Figure 3-4d). More cells in S and M phases could mean that the cells progress more slowly through S/M phases or simply that more cells are proliferating. It is less likely that more cells are proliferating as we also observed that the

proportion of Mage+ cells dropped over time after induction and did not detect increased cleaved caspase 3 (CP3) staining in Mage+ cells. Overall, these data suggest that MAGE over-expression delays exit from mitosis, promoting entry into a polyploid state.

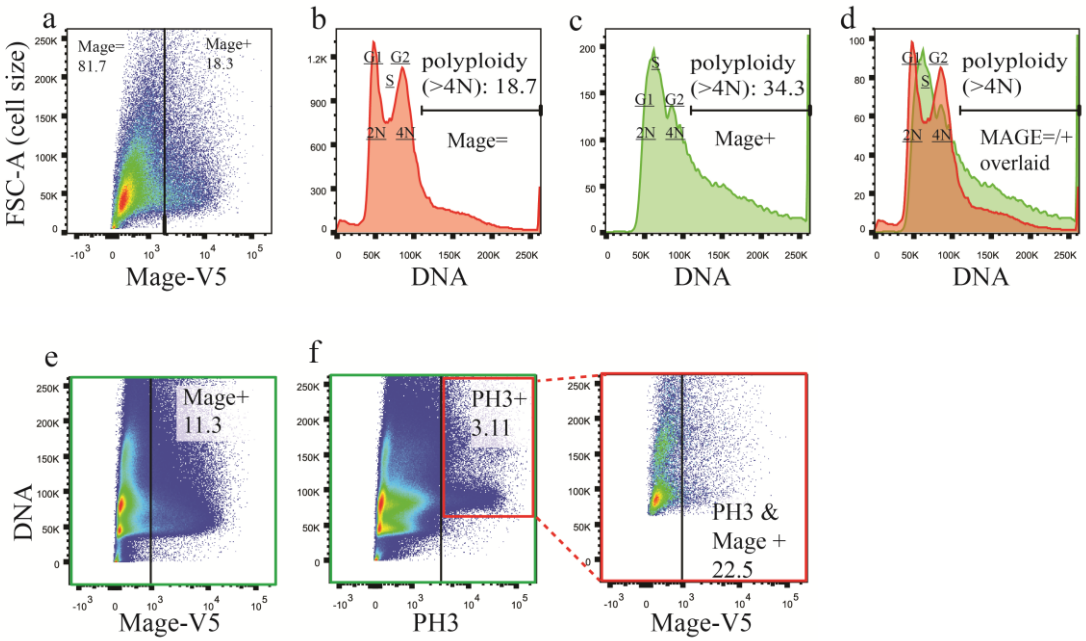
a
Mage=
81.7
Mage+
18.3
FSC-A (cell size)
Mage-V5
b
G1
G2
S
2N
4N
polyploidy
(>4N): 18.7
Mage=
DNA
c
S
G1
G2
2N
4N
polyploidy
(>4N): 34.3
Mage+
DNA
d
G1
G2
S
2N
4N
polyploidy
(>4N)
MAGE=/+
overlaid
DNA
e
Mage+
11.3
DNA
Mage-V5
f
PH3+
3.11
PH3
PH3 &
Mage +
22.5
Mage-V5

Figure 3-4 Increased S-phase, M-phase and polyploid cells in the Mage over-expressing population of cells.

a-f. Cells were harvested for flow cytometry analysis 24 hours after induction by adding $CuSO_4$ to the culture medium to a concentration of 500 μM. Mage+ populations were defined by limiting Mage+ cells to less than 1% of the total population in unstained cell controls in the same experiments.

a. After induction, 18.3% of the total cell population expresses V5-tagged Mage protein (Mage+, labelled with Cy3)

b-c. Within Mage= cells expressing only endogenous *MAGE*, 18.7% are polyploid as defined by DNA content (>4N) (b), while in the Mage+ cells, 34.3% are polyploid (c).

d. Overlay of b&c shows that within the ≤4N population (i.e. the G1, S and G2 populations), more Mage+ cells are in S phase while the G1 (2N) and G2 (4N) cells populations were reduced.

e. After induction, 11.3% of the total cell population in this experiment are Mage+ (labelled with Alexa 488).

f. A mitotic cell population is defined by high phospho-histone H3 staining (labelled with Alexa 647) and high DNA content (4N or 8N) (labelled with FxCycle Violet). Compared to the total population where 11.3 % are Mage+ (e), 22.5% are Mage+ within the mitotic cell population.

3.4.3 Effect of MAGE over-expression on sensitivity to DNA damaging agents.

Loss of Smc5/6 components, including Mage, sensitize the fruit fly to genotoxic agents (Li *et al.* 2013) and over-expression of MAGE genes in cancer cells contributes to resistance to chemotherapeutic drugs (Simpson *et al.* 2005). To test the robustness of MAGE over-expressing cells in response to cell cycle stresses, we first measured the sensitivity of the uninduced S2-Mage cells to camptothecin (CPT, a topoisomerase 1 inhibitor) and doxorubicin (DOX, a DNA intercalator) (Sortibran *et al.* 2006; Kondo and Perrimon 2011). Cell death was measured by activated caspase 3 (CP3) levels in uninduced S2 cultures after treatment with CPT (100 μM) or DOX (2 μM) for 24 hours (Figure 3-5a-b). The two drugs caused significant cell death, from a baseline level of 4% of cells CP3 positive in controls treated with DMSO to 45% of CPT-treated cells CP3 positive or 25% of DOX-treated cells being CP3 positive (Figure 3-5a - b). We induced *MAGE* expression by addition of $CuSO_4$ for 48 h, and added the drugs for the 24-48 hour time period. The proportion of Mage+ cells was determined by immunocytochemistry compared to DAPI stained nuclei. In control culture in which the cells were treated with DMSO, about 11% of cells were Mage+. In contrast, 35% of cells treated with CPT or 25% of cells treated with DOX were Mage+ (Figure 3-5c-d). This suggests that Mage+ cells had a survival advantage compared to cells that express only endogenous levels of *MAGE*. Mage+ cells also had a survival advantage at two lower concentrations of CPT (25 and 50 μM) (Appendix figure 5 a, d and f) where a significant increase in the number of CP3 cells were observed; however, they did not have a survival advantage when tested at two lower concentrations of doxorubicin (0.5 and 1 μM) where no increase in the number of CP3 cells were observed (Appendix figure 5 a, e and g). These data suggest that Mage+ cells have an increased resistance to cell death induced by CPT (3 fold advantage over cells expressing only endogenous *MAGE* at 100 μM) or doxorubicin (2.3 fold advantage at 2 μM). Mage+ cells also had a survival advantage when treated with etoposide (10 μM), a topoisomerase II inhibitor (Appendix figure 5 a). Therefore, *MAGE* over-expression confers a survival advantage to cells exposed to genotoxic stress. This suggests that Drosophila Mage has functional similarities to the human MAGE proteins that confer resistance to chemotherapeutic agents when over-expressed in cancer.

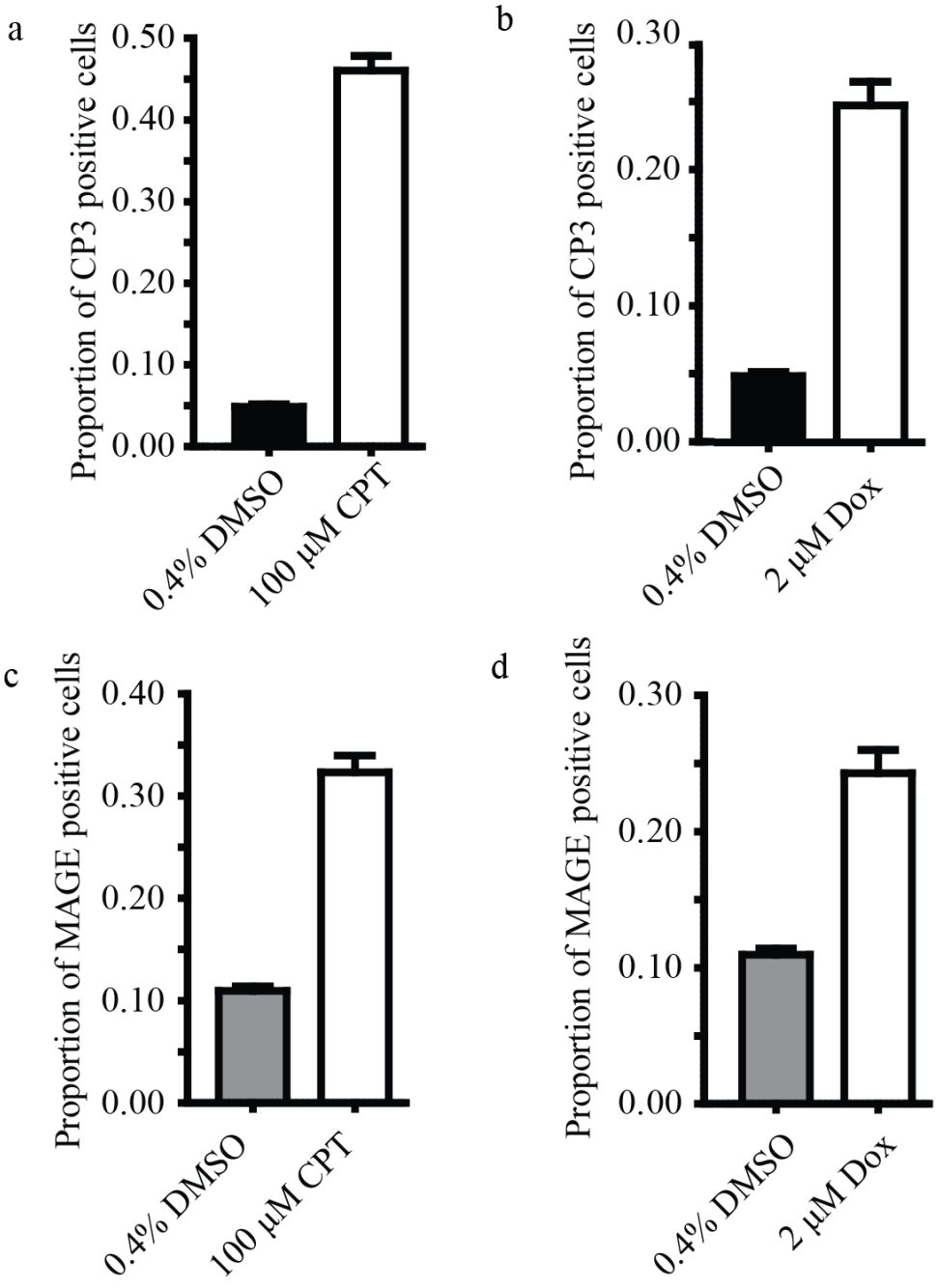
a
Proportion of CP3 positive cells
0.50
0.40
0.30
0.20
0.10
0.00
0.4% DMSO
100 μM CPT
b
Proportion of CP3 positive cells
0.30
0.20
0.10
0.00
0.4% DMSO
2 μM Dox
c
Proportion of MAGE positive cells
0.40
0.30
0.20
0.10
0.00
0.4% DMSO
100 μM CPT
d
Proportion of MAGE positive cells
0.30
0.20
0.10
0.00
0.4% DMSO
2 μM Dox

Figure 3-5 Over-expression of Mage confers resistance to DNA damage agents.

a, c. Mage protects cells from CPT induced cell death. (a) CPT (100 μM) induces apoptosis as measured by activated caspase 3 immunocytochemistry. (c) Mage expressing cells were enriched after CPT treatment.

b, d Mage protects cells from doxorubicin induced cell death. (b) DOX (2 μM) induces noticeable apoptosis and (d) Mage expressing cells were enriched at this concentration.

a-d Cells were fixed 24 hours after drug treatment (i.e. 48 hours after induction of Mage-V5 expression) and immunostained with an antibody to mark apoptotic cells or an V5 antibody to mark Mage+ cells. The proportion of Mage+ cells was determined by normalizing the number of positive cells with the total number of cells as defined by the number of DAPI stained nuclei. Error bars represent SE of the mean.

3.4.4 The MAGE over-expression phenotype could depend on the abundance of Nse1 and Nse4 proteins.

We previously showed that the Mage protein is part of the Smc5/6 complex in Drosophila, and that loss of *MAGE* causes hypersensitivity to caffeine and genotoxic agents (Li *et al.* 2013). The Smc5/6 proteins themselves, or the non-SMC components of the complex (Nse1-Nse4) may be necessary for the effect of *MAGE* over-expression on proliferation and cell cycle regulation. Alternatively, the Mage protein may act independently of the Smc5/6 complex. To assess these possibilities, we first measured the abundance of the Nse and Smc proteins in S2 cells transfected with constructs encoding epitope-tagged versions of Nse1, Nse4, Smc5 or Smc6 and an inducible form of epitope-tagged *MAGE*. Over-expression of *MAGE* in S2 cells decreased the levels of Nse1 and Smc5 proteins (Figure 3-6a). However, Mage co-expression increased the amount of Nse4 (Figure 3-6b). Next, we measured the levels of Mage protein in flies lacking Smc5 or Smc6, but found no difference in the abundance of Mage in these samples (Figure 3-6c). We then measured the endogenous Mage protein levels in two lines of flies lacking Nse1, which were created by imprecise excision of a P-element near the *Nse1* gene locus. Similar to flies lacking other Smc5/6 components, *Nse1* mutants are indistinguishable from control flies when raised on standard media, but are hypersensitive to caffeine in the culture media (Appendix figure 1 and Appendix table 1). Interestingly, Mage protein is almost undetectable in flies lacking *Nse1*, but is present in Nse1 heterozygous flies (Figure 3-6d). These results suggest that the relative abundance of the proteins in the Nse1/Mage (Nse3)/Nse4 complex is tightly regulated in cells and in flies.

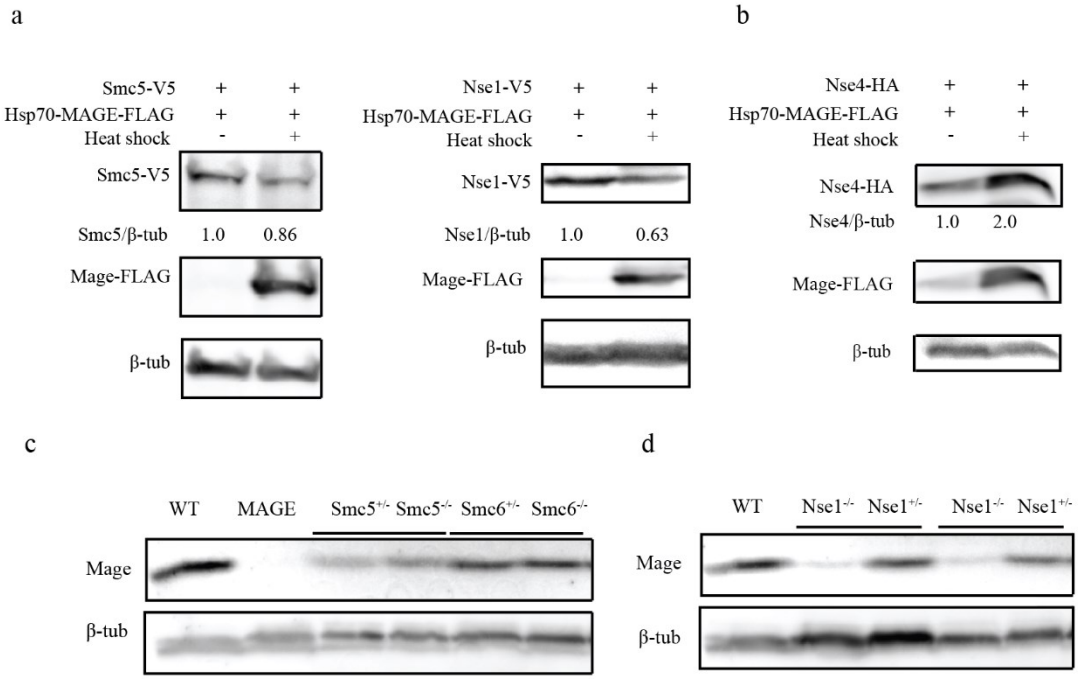
a
Smc5-V5 + +
Hsp70-MAGE-FLAG + +
Heat shock - +
Smc5-V5
Smc5/β-tub 1.0 0.86
Mage-FLAG
β-tub
Nse1-V5 + +
Hsp70-MAGE-FLAG + +
Heat shock - +
Nse1-V5
Nse1/β-tub 1.0 0.63
Mage-FLAG
β-tub
b
Nse4-HA + +
Hsp70-MAGE-FLAG + +
Heat shock - +
Nse4-HA
Nse4/β-tub 1.0 2.0
Mage-FLAG
β-tub
c
WT MAGE Smc5+/- Smc5-/- Smc6+/- Smc6-/-
Mage
β-tub
d
WT Nse1-/- Nse1+/- Nse1-/- Nse1+/-
Mage
β-tub

Figure 3-6 Interaction of Smc5/6/Mage/Nse1/Nse4 protein levels.

a. Over-expression of Mage reduces Smc5 levels (left) and Nse1 levels (right). S2 cells were co-transfected with hsp70-MAGE-FLAG (induced by heat shock at 37°C) and pMT-Smc5-V5 (induced with 500 μM $CuSO_4$ 24h after transfection) or pMT-Nse1-V5 (induced with 500 μM $CuSO_4$ 24h after transfection). Forty-four hours after transfection, cells were divided to two equal samples. One sample was heat shocked for 30 minutes then returned to 25°C and the other sample was kept at 25°C. At 48 h, cells were collected for immunoblot analysis for Smc5 or Nse1 levels, which are represented by protein/β-tubulin ratios in the figure.

b. Over-expression of Mage increases Nse4 levels. As in 5a, except that S2 cells were co-transfected with hsp70-MAGE-FLAG (induced by heat shock at 37°C) and pUAST-Nse4-HA (induced by co-transfection with ubi-GAL4).

c. Similar amounts of Mage protein are present in flies with heterozygous (+/-) or homozygous (-/-) *Smc5* or *Smc6* loss of function alleles.

d. Reduced amounts of Mage protein in homozygous (-/-) loss of function *Nse1* flies compared to heterozygous (+/-) control flies.

c-d. Lysate of a single male Drosophila of w^{1118}, $MAGE^{XL/XL}$, $Smc5^{P7E8/+}$, $Smc5^{P7E8/P7E8}$, $Smc6^{X1/+}$, $Smc6^{X1/X1}$ (in c) $w^{1118,}$ $Nse1^{XL1/XL1}$, $Nse1^{XL1/+}$, $Nse1^{XL2/XL2,}$ and $Nse1^{XL2/+}$ (in d) were used in each lane, respectively. The horizontal lines indicate corresponding two flies sibling pairs.

3.4.5 Nse4 interacts with p53, linking the Mage/Nse1/Nse4 complex to the p53 DNA damage response pathway.

Functional relationships between MAGE proteins and p53 have been reported in vertebrates (Yang *et al.* 2007; Ladelfa *et al.* 2012) but not in flies. We first tested the relationship between Mage and p53 in S2 cells transfected with constructs encoding FLAG tagged Mage (MAGE-FLAG) and V5 epitope tagged p53 (p53-V5). Over-expression of *MAGE* reduced the amount of p53 to 54-87% of the control levels (a representative experiment is shown in Figure 3-7a). Interaction between Mage-FLAG and p53-V5 was not detected by co-immunoprecipitation of protein lysates from similarly co-transfected cells. We then co-expressed HA tagged Nse4 (Nse4-HA) with p53-V5. p53-V5 was not detectable in the soluble lysates in either induced or uninduced conditions; however, p53-V5 was readily detectable in experiments where whole cell lysates were analyzed by immunoblotting (Figure 3-7a), suggesting that this protein was mainly in the insoluble fraction. The co-IP procedure concentrated all soluble p53-V5 proteins in the lysates of induced or uninduced cells where a much lower level of p53-V5 was present due to a leaky expression from the metallothionein promoter. Nse4-HA was co-immunoprecipitated with p53-V5 from the soluble lysate from the induced cells. A lower amount of Nse4-HA was co-immunoprecipitated with the much lower p53-V5 in the un-induced cells (Figure 3-7b). Thus, we conclude that Nse4-HA was co-immunoprecipitated with p53-V5 in a dose dependent manner. These data suggest that p53 and Nse4 can form a complex in S2 cells. This result is consistent with previous data showing that Drosophila p53 interacts with Nse4 but not with Mage (Lin 2006).

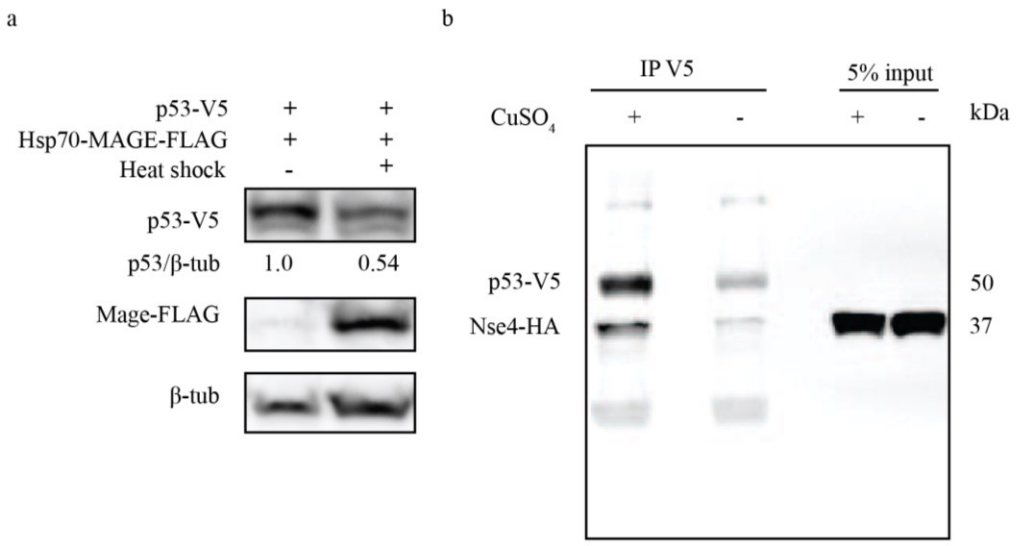

Figure 3-7 . Interactions between Mage and p53

a. Co-expression of Mage reduces the abundance of p53 in transfected cells. S2 cells were co-transfected with hsp70-MAGE-FLAG (inducible by heat shock at 37°C) and pMT-p53-V5 (inducible by adding 500 µM $CuSO_4$). $CuSO_4$ was added to induce p53 expression at 24 hours after transfection; at 44 h, cells were divided into two equal samples. One sample was heat shocked for 30 minutes then returned to 25°C and the other sample was kept at 25°C. At 48 h, cells were collected for immunoblot analysis for p53 levels, which are represented by protein/β-tubulin ratios in the figure.

b. Nse4 interacts with p53. S2 cells were co-transfected with hsp70-Nse4-HA (inducible by heat shock at 37°C) and pMT-p53-V5 (inducible by adding 500 µM $CuSO_4$). Copper was added to induce p53-V5 expression at 24 hours after transfection. At 44 hours, cells were divided into two equal samples. The two samples were heat shocked for 30 minutes to induce Nse4-HA expression then returned to 25°C. At 48 hours, cells were collected for co-immunoprecipitation experiments. a,b Experiments were done once.

3.5 Discussion

3.5.1 MAGE and the cell cycle

In the expanded mammalian *MAGE* family, some MAGE proteins, like Necdin, play a role in cell proliferation. Necdin interacts with E2F proteins (Nakada *et al.* 1998; Kobayashi *et al.* 2002) and Bmi1 to suppress neural precursor cell proliferation by down-regulating expression of *cdk1* and up-regulating a Cdk inhibitor, p16. (Kurita *et al.* 2006; Minamide *et al.* 2014). Another mammalian MAGE, MAGE-A11, interacts with both E2F and Rb proteins (Su *et al.* 2013). In flies, depletion of *MAGE* expression by RNA interference (RNAi) in brains led to over-proliferation, although no direct interaction between Mage and E2f was observed (Nishimura et al., 2008). In our study, we examined the potential cell cycle function of *MAGE* by depletion or over-expression in Drosophila S2 cells. We found that depletion of *MAGE* expression increases the G1/S phase populations and decreases the G2/M phase population. Although these effects are not as dramatic as those produced by the depletion of the major cell cycle regulators that were tested in the same experiment, this cell cycle phenotype is consistent for *MAGE*, *Smc5* and *Smc6* genes depletions. Together, these data suggest that the Smc5/6 DNA damage complex also plays a role in cell cycle regulation. This is consistent with the recent finding that depletion of Smc5 or Smc6 leads to delayed replication in human cells under unchallenged conditions (Gallego-Paez *et al.* 2014).

In humans, both MAGE proteins and their interaction partners, the Nse4 homologs, interact with the Rb-E2F pathways (Maclellan *et al.* 2000). The *MAGE*-depletion phenotype we observed also resembled that of *Rbf* depletion. However, it is unlikely that depletion of *MAGE* directly reduces Rbf activity as *Rbf* depletion also resulted in smaller cell size and this phenotype was not the case with *MAGE* depletion (Figure 3-2a and Figure 3-3).

The *MAGE*-depletion phenotype shown here also resembled that produced by depletion of *ATM*. We previously showed *MAGE* and *Smc6* genetically interact with *ATM* (Li *et al.* 2013). It would be interesting to see the effect of depletion of both *ATM* and *Smc5/6/MAGE* in S2 cells on the cell cycle profile.

In flow cytometry analysis, DNA content analysis can serve as a surrogate marker for cell death through the proportion of sub-2N cell populations. For example, *cdk1* depletion increased the proportion of dying cells (Figure 3-2a and Figure 3-3). We did not observe any increase in cell death in *MAGE, Smc5* or *Smc6* depleted cells. This result is consistent with our previous observation that *MAGE, Smc5* or *Smc6* mutant flies are viable and phenotypically normal in unchallenged conditions (Li *et al.* 2013). When grown on caffeine food, the mutants die in the presence of caffeine (0.5 – 2 mM) and proliferating cells are especially sensitive to caffeine and undergo apoptosis. When 2 mM caffeine was present in the culture medium, an accumulation of S2 cells in the G1 phase was observed (Figure 3-2b and Figure 3-3). No increased cell death was induced by caffeine for the control cells. Since we observed synthetic lethality by caffeine and loss of *Smc5*, *Smc6* or *MAGE* in flies, we were expecting to observe increased cell death in *MAGE, Smc5* or *Smc6* depleted cells when challenged with caffeine. To our surprise, no change in cell death was observed for *MAGE, Smc5* or *Smc6* depleted cells when 2 mM caffeine was present in the culture medium. The discrepancy could be explained by the short term exposure for S2 cells to caffeine and/or a more stringent requirement for these genes during specific developmental stages to handle caffeine induced cell cycle stress in whole organisms, as opposed to cells grown in culture.

MAGE over-expression produces a more striking cell cycle change. The accumulation of cells in the S phase partially resembled the *E2f* or *Dp depletion* (Figure 3-2a and Figure 3-4d). Further experiments are needed to determine whether the *MAGE* over-expression decrease E2f-Dp activities. The results from the depletion experiment suggest that Mage could act together with Smc5 and Smc6 in regulating the cell cycle. It would therefore be interesting to examine the cell cycle profiles of cells over-expressing Smc5 or Smc6 to determine whether their over-expression would recapitulate the *MAGE*-over-expression phenotype. Furthermore, it would also be important to examine the cell cycle progression of Mage+ cells with Smc5 or Smc6 depleted to determine whether they are required for the *MAGE*- over-expression phenotype.

3.5.2 MAGE over-expression and cell survival under genotoxic stress

Using a S2 cell line where a portion of cells over-express *MAGE*, we found that Mage+ cells were enriched in the population under lethal doses of DNA damaging drugs. This suggested that Mage could promote cell survival under genotoxic stress. There are three possible mechanisms through which this could be achieved. First, as a component of the Smc5/6 complex, Mage could enhance the efficiency of the complex in repairing DNA damage and therefore promote survival. Indeed, we found that Mage could stabilize Nse4 (Figure 3-6b). Further, we could test this possibility by knocking-down other components of this complex in this line. For example, we could knock-down *Smc6* and compare the survival rate of Mage+ Smc6- , Mage= Smc6-, Mage+ Smc6+, and Mage= Smc6- cells. If Mage promotes survival by enhancing the activity of the Smc5/6 complex, we expect that after removing the apparently essential component of Smc6, the survival rate of Mage+ Smc6- cells should be similar to that of the Mage= Smc6- cells; If Mage+ acts independently, the survival rate of Mage+ Smc6- cells should still be greater than that of Mage= Smc6- . Secondly, Mage could influence cell death by interacting with p53 directly or indirectly to repress its activity. p53 is not expressed in S2 cells in normal culture conditions as its expression was not detected by immunoblotting using an anti-p53 antibody. We would first examine whether p53 is induced by the treatment with the drugs. If it is indeed induced, then the hypothesis can be tested by knocking-down p53 expression (or to prevent it from being translated) using dsRNA and comparing the survival rate of Mage+ p53- and Mage= p53- cells. If this hypothesis is true, we expect that the survival rate of Mage+ p53- cells should be equal to that of Mage= p53- cells. These two possibilities may not be mutually exclusive since p53 could interact with the Nse4, the intimate interaction partner of Mage. Third, as MAGE over-expression slows down the cell cycle, Mage could reduce DNA damage by slowing down the cell cycle and therefore promote survival. Similar experiments can also be done in flies where one can over-express Mage in WT, a *p53* null or p53 over-expression background and examine Drosophila phenotypes at normal or challenged conditions. We started to work with a Drosophila line that was stated to over-express MAGE (Nishimura *et al.* 2008) but found out that it was not actually a *MAGE* transgene. The MAGE line referenced by Nishimura et al. appears to no longer exist (Yoshikawa, personal communication), so experiments that make use of such a Drosophila line would have to be constructed.

3.5.3 MAGE and p53

MAGE proteins and p53 are tightly connected. Multiple MAGE proteins interact with p53 to regulate its activity through different mechanisms (Ladelfa *et al.* 2012) and p53 targets MAGE at a transcriptional level and at a post-transcriptional level via miR-34a (Liu *et al.* 2009b; Weeraratne *et al.* 2011; Lafontaine *et al.* 2012). Our co-transfection experiment showed that *MAGE* over-expression in S2 cells moderately lowered p53 levels. The result is interesting because one mechanism by which MAGE proteins regulate p53 is by recruiting E3 RING ubiquitin ligases to target p53 for degradation. A homologue of one of these ubiquitin ligases (TRIM28) in Drosophila, *bonus*, negatively regulates p53 (Allton *et al.* 2009). Thus, Mage could target p53 by interacting with Bonus. We did not detect an interaction between Mage and p53 in our co-immunoprecipitation experiment, but we did observe that the Mage interaction partner, Nse4, interacted with p53. The next step would be to test whether their interaction is functional. This can be achieved by testing whether p53 transcriptional activity is altered when it is co-expressed with Nse4 either through a reporter assay, or by directly testing whether p53 target gene (*Reaper, hid, sickle, and Grim*) expression is changed. We also found that Mage could stabilize Nse4 levels via an unknown mechanism and Nse1 is required for MAGE protein expression in flies. We found the Smc5 and 6 protein levels are also altered by MAGE over-expression although the change was not drastic and needs to be replicated. Taken together, this suggests an interdependency between the Smc5/6 complex components and that Mage is linked to p53 function by Nse4 in Drosophila. Future studies could make use of the Drosophila mutants generated (*Smc5, 6, MAGE,* and *Nse1*) to test whether the expression of p53 target genes is changed by quantitative RT-PCR analysis.

Our study reveals that Mage regulates the cell cycle in unchallenged conditions and promotes cell survival under genotoxic stress. The study also provides evidence that Mage's functions are tightly linked to the Smc5/6 complex. Our study supports the hypothesis that some of the diverse functions of the MAGE family proteins such as regulating cell cycle, cell survival and interacting with p53 are at least conserved at functional levels from humans to flies. The study will help to understand how this expanded protein family in humans play such versatile roles in cancer and development.

Chapter 4 Conclusions

4.1 The Drosophila Mage/Smc5/6 complex

At the beginning of the study, based on sequence similarity to the yeast Smc5/6 complex proteins, we identified potential Drosophila Smc5/6 genes (*Smc5*, *Smc6*, *Nse1*, *Nse2*, *MAGE*, and *Nse4*) (Table 2-4). We were able to generate null mutants for *Smc5*, *Smc6*, *MAGE* and *Nse1* (Figure 2-4; Appendix figure 1; Appendix table 1) and showed that all the mutants share phenotypes including sensitivity to caffeine and genotoxic agents (Figure 2-2, Figure 2-9 and Figure 2-10) and a maternal effect affecting hatch rate of eggs from mutant females (Appendix table 2). In addition, co-immunoprecipitation and *in vitro* pull down experiments showed that Mage, Nse1, and Nse4 form a complex (Figure 2-7). Further, using RNAi to knock-down expression of *Smc5*, *Smc6*, *Nse1*, *Nse2*, *MAGE*, and *Nse4* in the developing eye discs resulted in a caffeine dependent small and rough eye phenotype (Appendix figure 2 and Figure 2-3a). Thus, all the Drosophila genes identified in Table 2-4 are indeed functional components of the Smc5/6 complex. Like the Smc5/6 in yeast and humans, our results suggest a role of the Drosophila Smc5/6 complex in the HR based DNA repair pathway.

Homologs of Nse5 and Nse6 in yeast have not been identified in other species. In fact, the Nse5 or Nse6 are functional homologs and no sequence similarity is shared between the counterparts of the fission and the budding yeasts. Thus, it is likely that additional components of the Smc5/6 complex that do not necessarily share sequence similarity with their yeast counterparts, exist in other species, including Drosophila. The *ddt* allele described in Chapter 2 may represent such a gene. The caffeine dependent eye phenotype created by depletion of the Smc5/6 genes through RNAi could potentially provide a robust tool to use in a reverse genetic screen in Drosophila to identify additional components or functionally related genes in the Smc5/6 pathway.

4.2 Potential roles of Mage/Smc5/6 complex outside DNA repair

The MAGE homology domain is conserved from yeast to humans. Accumulating evidence shows that the expanded human MAGE family of proteins play critical roles in cell cycle regulation, differentiation and survival. There is only one *MAGE* gene in *Drosophila melanogaster*. This provided us with a chance to examine the phenotypes

produced by loss of all MAGE activity in a multicellular organism. At the beginning of this project, we predicted that Mage in Drosophila is required for viability for the following reasons: 1) In Drosophila, Mage is expressed broadly in maternal, embryonic, and various larval and adult tissues (Nishimura *et al.* 2007); and 2) depletion of Mage using RNAi produces neuronal proliferation defects and embryonic lethality (Nishimura *et al.* 2008). 3) In yeast, *Nse3 (MAGE)* is an essential gene (Pebernard *et al.* 2004). To our surprise, as described in chapter 2, *MAGE* null mutants are completely viable. Therefore, the lethality phenotype by *MAGE* RNAi reported earlier by Nishimura et al. could result from an off-target effect from the RNAi treatment. We have not determined if the MAGE mutant exhibit the same neural precursor over-proliferation phenotype as reported for the RNAi knock-down. However, using the same RNAi MAGE transgenes to deplete the MAGE expression in the developing wing discs of Drosophila, we observed larger adult wings while there was no difference in wing size between *MAGE* homozygous and heterozygous flies (Appendix figure 3). Therefore, the over-proliferation phenotype could be unrelated to MAGE. Thus, also in light of the *MAGE* mutant having a defect in memory formation (Personal communications with Dr. François Bolduc), whether MAGE plays a role in neural proliferation or any other role in the nervous system is worth further scrutiny.

Similar arguments about the phenotypes in unchallenged conditions for the *Smc5* and *Smc6* function can be made. Like the yeast Nse3 (MAGE), Smc5 or Smc6 are also required for viability in yeasts. Early attempts to use an RNAi transgene to deplete Smc6 ubiquitously resulted in lethality in Drosophila (personal observation). Further, depletion of Smc5 or Smc6 using RNAi in Drosophila tissue culture cells resulted in heterochromatin bridges in 50% of mitotic cells (Chiolo *et al.* 2011), suggesting that the *Smc5* or *Smc6* genes would be essential for cellular viability. The discrepancy here could be explained again by an off-target effect of RNAi and/or differential requirements of Smc5/6 functions between whole organism and the cultured cells. *Smc5* and *Smc6* in *Caenorhabditis elegans* are dispensable for viability (Bickel *et al.* 2010). Chicken DT40 cells with deficient *Smc5* by targeted knockout are viable (Stephan *et al.* 2011a). In cultured human cells, depletion of different Smc5/6 complex components using siRNA does not result in obvious defects in cell proliferation or viability but *Smc6* knockout mice are embryonic lethal (Ju *et al.*

2013). Therefore, in multicellular organisms, the Smc5/6 complex is not essential for cell viability but the requirement during development varies.

Does the Drosophila Mage/Smc5/6 complex have a role in unchallenged conditions? First, as described above, Mage and by extension the Mage/Smc5/6 complex could have a role in the nervous system. The results from this study also provide some supporting evidence. As described in Chapter 3, depletion of *MAGE*, *Smc5* or *Smc6* by RNAi in S2 cells produced noticeable cell cycle shifts, suggesting a role in proliferation. This result is consistent with the recent finding that depletion of Smc5 or Smc6 leads to delayed replication in human cells under-unchallenged condition (Gallego-Paez *et al.* 2014). As an important protein complex required for HR dependent repair for DSBs, the Drosophila Mage/Smc5/6 complex could play a role in meiosis where programed DSBs are created and need to be repaired (Lake and Hawley 2012). When crossed to wild-type males, homozygous females bearing *MAGE*, *Nse1*, *Smc5*, or *Smc6* mutations produced eggs with lower hatch rates (8~77%) (Appendix table 2). Removing *mei-W68,* the Drosophila Spo11 homolog required for DSB formation, in flies deficient for meiotic DSB repair partially rescued an infertility defect (Mckim and Hayashi-Hagihara 1998; Liu *et al.* 2002). My attempt to examine whether the hatch defect can be rescued by removing mei-W68 failed because the *mei-W68* allele obtained from the stock center was homozygous lethal. A viable allele is needed to complete this experiment. Therefore, it is unclear at this stage whether this defect is caused by an inability to properly fix the programmed DSBs during meiosis in the females. Alternatively, a low hatch rate could be explained by a maternal requirement of the Mage/Smc5/6 complex for the robustness of embryonic development. *Smc5* and *Smc6* in *Caenorhabditis elegans* are dispensable for viability; however, *Smc5* or *Smc6* mutants become sterile over generations, presumably by accumulation of chromosome defects in the germ line, due to genome instability resulting from a failure to repair meiotic DSBs properly (Bickel *et al.* 2010). In principle, the two alternative explanations could be distinguished by examining whether the hatch rate would drop for the Drosophila mutants maintained as homozygous stock over many generations. Drosophila has two Nse2 homologs (Dmel\qjt\Nse2a and Dmel\cerv\Nse2b). Nse2b is ubiquitously expressed while Nse2a's expression is restricted in testis (Figure 2-6), implying a testis specific role of the Drosophila Smc5/6 complex. Knock-down of Nse2a

and 2b expression by an RNAi in developing wing discs induced extra mechano-sensory organ formation (Appendix figure 4). While this phenotype, suggesting a potential role for Nse2b in the nervous system, is intriguing, additional experiments should be done to verify this is not an off-target effect by the RNAi.

Our study showed that *MAGE* mutants shared phenotypes with *Smc5/6/Nse1* mutants in caffeine/genotoxic stress sensitivity and the maternal effect and depletion of *MAGE*, *Smc5*, or *Smc6* in S2 cells produced similar cell cycle profile shifts. Therefore, loss of function studies so far do not suggest a SMC5/6 complex independent role for Mage. We also showed that over-expression of Mage in S2 cells stabilized Nse4 and loss of Nse1 but not Smc5 or Smc6 significantly reduced the endogenous levels of Mage. Thus, Mage could have "Smc5/6 proteins" independent functions but any additional functions are likely to be connected with the Nse1-MAGE-Nse4 subcomplex.

4.3 New MAGE interaction partners?

Consistent with the previous studies in yeast and humans, our studies showed that in the Smc5/6 complex, MAGE directly interacts with the E3 ubiquitin ligase Nse1 and the kleisin family protein Nse4. Recent studies may suggest that some of the human MAGE interactions are likely evolved via diversification from or preservation of these two ancient interactions (Doyle *et al.* 2010; Hudson *et al.* 2011). Consistent with previous individual studies, Doyle et al, by using a tandem affinity purification approach to systematically identify MAGE interaction partners, found that both type I and II human MAGE proteins physically interact with at least one of the E3 RING ubiquitin ligases including Nse1, TRIM28, TRIM27, LNX1, and Praja-1. Hudson et al. reported that despite the expansion of family members, the human Nse4 paralogs (Nse4a, Nse4b, EID1, EID2, and EID2b) still interact with type I and II MAGE proteins. Similarly, in this study, we found that MAGE can interact with itself *in vitro*. This result is consistent with the findings that human Necdin homodimerizes and heterodimerizes with MAGED1 (Tcherpakov *et al.* 2002). This leaves the question whether other human MAGE interactions are conserved in Drosophila? Perhaps, human MAGE proteins have gained many new interaction partners and functions that would not be shared by Drosophila Mage. However, in addition to Nse4/EID, different families of human MAGEs share common interaction partners such as

p53, HDACs, p75NTR, E2Fs, and PIAS (Figure 1-4). Many of these interactions are mediated via the MHD and could reflect an ancestral interaction of MAGE. Therefore, some of these interactions could also be conserved in the fruit flies. The role of Mage in proliferation and survival observed in this study could reflect one of these interactions. Human p53 is physically and functionally interconnected with different groups of MAGE proteins (Figure 1-4 and discussion on page 112). In this study, we provided preliminary evidence to show that the Drosophila p53 is connected with the Mage. Co- over-expression studies showed that Mage moderately influences the p53 level. We also showed the physical interaction between Mage and p53 may not be conserved, however, there could exist a functional connection between MAGE and p53 via Nse4 in Drosophila.

In addition to p53, Drosophila homologs of p75NTR and E2F1 proteins are also attractive interaction partners of Mage, because these two proteins interact with different members of the human MAGEs (Figure 1-4) and also interact with the chicken MAGE (Lopez-Sanchez *et al.* 2007). Unbiased identification of new interaction partners by Tandem affinity purification (TAP) coupled to mass spectrometry has proven particularly useful in identifying new MAGE complex components in humans (Doyle *et al.* 2010; Hao *et al.* 2013). The TAP method has been established in the Drosophila system as well (Veraksa *et al.* 2005) and should be easily applied to the Drosophila Mage protein.

4.4 Concluding remarks

The results of these studies are summarized in Figure 4-1. The studies showed that Mage is an integral part of the Smc5/6 complex in Drosophila. And as expected, loss of Smc5/6 genes including *MAGE*, *Smc5, Smc6,* and *Nse1* confers upon flies sensitivity to genotoxic stress, presumably due to the essential role in HR based DNA repair. The caffeine sensitivity produced by the mutations and RNAi depletions confirmed that the genes identified by the sequence similarity are indeed functional counterparts of Nse1, Nse2, MAGE, Nse4, Smc5, and Smc6 in humans and yeast. A maternal phenotype, effects of over-expression on the cell cycle and resistance to genotoxic drugs, and an effect by RNAi depletion on the cell cycle are also observed, suggesting additional roles in addition to DNA repair. A possible interaction of Nse4 with p53 is also observed, suggesting a potential connection between p53 and the Smc5/6 complex.

Our studies have perhaps raised more questions than answers. The role of MAGE in the Smc5/6 complex remains largely unknown in any species. It could function as an Nse1-MAGE-Nse4 E3 ubiquitin ligase complex. But what are the targets of this complex? Mage can interact with itself *in vitro* (Figure 2-7C). Does this interaction have any physiological significance? What pathways, transcriptional factors, or cellular partners regulate Mage? The maternal effect manifested by lower hatch rate of eggs from mutant females still wait for an explanation. Much data presented in chapter 3 are preliminary. The effect of over-expression of Mage in mediating resistance to genotoxic drugs is reproducible but the mechanism underlining the resistance needs further dissection as discussed in chapter 3. The effect of over-expression on cell cycle needs to be followed up by examining the cell cycle progression using live cell imaging. Since many human MAGE proteins regulate the cell cycle and cell survival, it would be interesting to examine whether overexpressing some of these human MAGE proteins in the Drosophila S2 cell recapitulates the Drosophila Mage over-expression. Finally, the identification of the potential interaction of Nse4 with p53 is particularly encouraging and worth following up.

Although MAGEG1 is thought to be the Nse3 component in the human Smc5/6 complex, other human MAGEs do have the ability to interact with Nse4 or Nse1 and likely contribute to the function of the Smc5/6 complex in humans. Thus, with only one MAGE and Nse4 homolog, Drosophila should continue to be a useful model to help answer some of the questions raised, especially with the constructs, cell lines, and mutants generated in this study. Also, as mentioned previously, the caffeine sensitivity displayed by the Smc5/6 mutants and the powerful Drosophila genetic tools available would make identification of additional genes closely related to Smc5/6/Mage function possible.

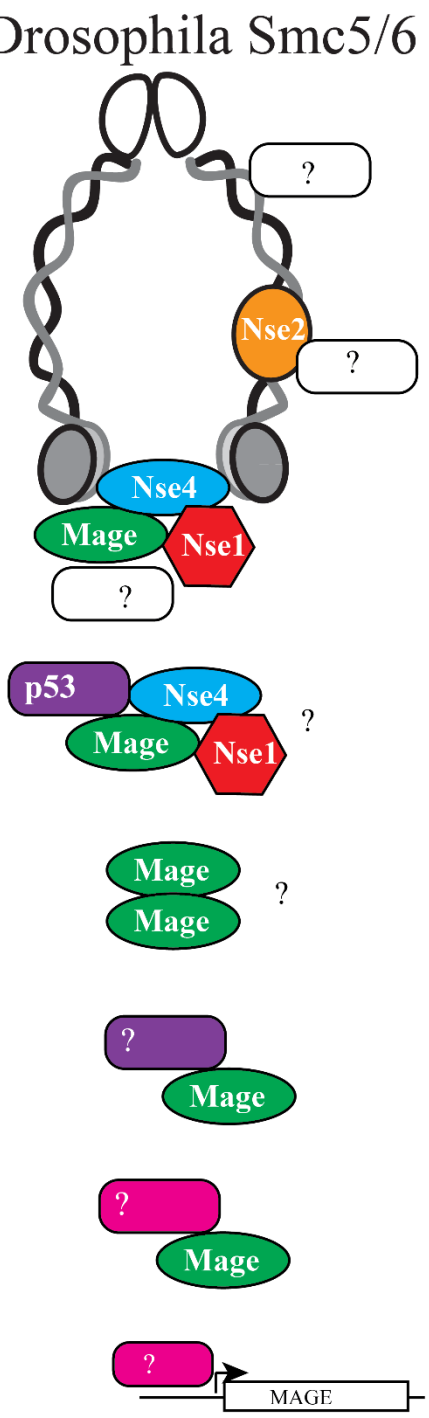

Figure 4-1 A model for Drosophila Smc5/6/Mage complex

References

Aebischer, J., R. Sturny, D. Andrieu, A. Rieusset, F. Schaller *et al.*, 2011 Necdin protects embryonic motoneurons from programmed cell death. PLoS One 6**:** e23764.

Aizawa, T., K. Maruyama, H. Kondo and K. Yoshikawa, 1992 Expression of necdin, an embryonal carcinoma-derived nuclear protein, in developing mouse brain. Brain Res Dev Brain Res 68**:** 265-274.

Albrecht, D. E., and S. C. Froehner, 2004 DAMAGE, a novel alpha-dystrobrevin-associated MAGE protein in dystrophin complexes. J Biol Chem 279**:** 7014-7023.

Allton, K., A. K. Jain, H. M. Herz, W. W. Tsai, S. Y. Jung *et al.*, 2009 Trim24 targets endogenous p53 for degradation. Proc Natl Acad Sci U S A 106**:** 11612-11616.

Almeida, L. G., N. J. Sakabe, A. R. Deoliveira, M. C. Silva, A. S. Mundstein *et al.*, 2009 CTdatabase: a knowledge-base of high-throughput and curated data on cancer-testis antigens. Nucleic Acids Res 37**:** D816-819.

Ampatzidou, E., A. Irmisch, M. J. O'connell and J. M. Murray, 2006 Smc5/6 is required for repair at collapsed replication forks. Mol Cell Biol 26**:** 9387-9401.

Andrieu, D., F. Watrin, M. Niinobe, K. Yoshikawa, F. Muscatelli *et al.*, 2003 Expression of the Prader-Willi gene Necdin during mouse nervous system development correlates with neuronal differentiation and p75NTR expression. Gene Expr Patterns 3**:** 761-765.

Asai, T., Y. Liu, S. Di Giandomenico, N. Bae, D. Ndiaye-Lobry *et al.*, 2012 Necdin, a p53 target gene, regulates the quiescence and response to genotoxic stress of hematopoietic stem/progenitor cells. Blood 120**:** 1601-1612.

Askew, E. B., S. Bai, A. J. Blackwelder and E. M. Wilson, 2010 Transcriptional synergy between melanoma antigen gene protein-A11 (MAGE-11) and p300 in androgen receptor signaling. J Biol Chem 285**:** 21824-21836.

Askew, E. B., S. Bai, A. T. Hnat, J. T. Minges and E. M. Wilson, 2009 Melanoma antigen gene protein-A11 (MAGE-11) F-box links the androgen receptor NH2-terminal transactivation domain to p160 coactivators. J Biol Chem 284**:** 34793-34808.

Atanackovic, D., Y. Hildebrandt, A. Jadczak, Y. Cao, T. Luetkens *et al.*, 2010 Cancer-testis antigens MAGE-C1/CT7 and MAGE-A3 promote the survival of multiple myeloma cells. Haematologica 95**:** 785-793.

Bai, J., R. Binari, J. Q. Ni, M. Vijayakanthan, H. S. Li *et al.*, 2008 RNA interference screening in Drosophila primary cells for genes involved in muscle assembly and maintenance. Development 135**:** 1439-1449.

Bai, J., K. J. Sepp and N. Perrimon, 2009 Culture of Drosophila primary cells dissociated from gastrula embryos and their use in RNAi screening. Nat Protoc 4**:** 1502-1512.

Bai, S., B. He and E. M. Wilson, 2005 Melanoma antigen gene protein MAGE-11 regulates androgen receptor function by modulating the interdomain interaction. Mol Cell Biol 25**:** 1238-1257.

Barker, P. A., and A. Salehi, 2002 The MAGE proteins: emerging roles in cell cycle progression, apoptosis, and neurogenetic disease. J Neurosci Res 67**:** 705-712.

Bermudez-Lopez, M., A. Ceschia, G. De Piccoli, N. Colomina, P. Pasero *et al.*, 2010 The Smc5/6 complex is required for dissolution of DNA-mediated sister chromatid linkages. Nucleic Acids Res 38**:** 6502-6512.

Bertrand, M. J., R. S. Kenchappa, D. Andrieu, M. Leclercq-Smekens, H. N. Nguyen *et al.*, 2008 NRAGE, a p75NTR adaptor protein, is required for developmental apoptosis in vivo. Cell Death Differ 15**:** 1921-1929.

Bettencourt-Dias, M., and G. Goshima, 2009 RNAi in Drosophila S2 cells as a tool for studying cell cycle progression. Methods Mol Biol 545**:** 39-62.

Bhan, S., A. Chuang, S. S. Negi, C. A. Glazer and J. A. Califano, 2012 MAGEA4 induces growth in normal oral keratinocytes by inhibiting growth arrest and apoptosis. Oncol Rep 28**:** 1498-1502.

Bhan, S., S. S. Negi, C. Shao, C. A. Glazer, A. Chuang *et al.*, 2011 BORIS binding to the promoters of cancer testis antigens, MAGEA2, MAGEA3, and MAGEA4, is associated with their transcriptional activation in lung cancer. Clin Cancer Res 17**:** 4267-4276.

Bhatia, N., T. Z. Xiao, K. A. Rosenthal, I. A. Siddiqui, S. Thiyagarajan *et al.*, 2013 MAGE-C2 promotes growth and tumorigenicity of melanoma cells, phosphorylation of KAP1, and DNA damage repair. J Invest Dermatol 133**:** 759-767.

Bhatia, N., B. Yang, T. Z. Xiao, N. Peters, M. F. Hoffmann *et al.*, 2011 Identification of novel small molecules that inhibit protein-protein interactions between MAGE and KAP-1. Arch Biochem Biophys 508**:** 217-221.

Bickel, J. S., L. Chen, J. Hayward, S. L. Yeap, A. E. Alkers *et al.*, 2010 Structural maintenance of chromosomes (SMC) proteins promote homolog-independent recombination repair in meiosis crucial for germ cell genomic stability. PLoS Genet 6**:** e1001028.

Bischof, J. M., M. Ekker and R. Wevrick, 2003 A MAGE/NDN-like gene in zebrafish. Dev Dyn 228**:** 475-479.

Bischof, J. M., C. L. Stewart and R. Wevrick, 2007 Inactivation of the mouse Magel2 gene results in growth abnormalities similar to Prader-Willi syndrome. Hum Mol Genet 16**:** 2713-2719.

Blasina, A., B. D. Price, G. A. Turenne and C. H. Mcgowan, 1999 Caffeine inhibits the checkpoint kinase ATM. Curr Biol 9**:** 1135-1138.

Boccaccio, I., H. Glatt-Deeley, F. Watrin, N. Roeckel, M. Lalande *et al.*, 1999 The human MAGEL2 gene and its mouse homologue are paternally expressed and mapped to the Prader-Willi region. Hum Mol Genet 8**:** 2497-2505.

Boyd, J. B., M. D. Golino, T. D. Nguyen and M. M. Green, 1976 Isolation and characterization of X-linked mutants of Drosophila melanogaster which are sensitive to mutagens. Genetics 84**:** 485-506.

Branzei, D., J. Sollier, G. Liberi, X. Zhao, D. Maeda *et al.*, 2006 Ubc9- and mms21-mediated sumoylation counteracts recombinogenic events at damaged replication forks. Cell 127**:** 509-522.

Brodsky, M. H., J. J. Sekelsky, G. Tsang, R. S. Hawley and G. M. Rubin, 2000 mus304 encodes a novel DNA damage checkpoint protein required during Drosophila development. Genes Dev 14**:** 666-678.

Bush, J. R., and R. Wevrick, 2008 The Prader-Willi syndrome protein necdin interacts with the E1A-like inhibitor of differentiation EID-1 and promotes myoblast differentiation. Differentiation 76**:** 994-1005.

Bush, J. R., and R. Wevrick, 2012 Loss of the Prader-Willi obesity syndrome protein necdin promotes adipogenesis. Gene 497**:** 45-51.

Castro, F., B. Leal, A. Denny, R. Bahar, S. Lampkin *et al.*, 2009 Vaccination with Mage-b DNA induces CD8 T-cell responses at young but not old age in mice with metastatic breast cancer. Br J Cancer 101**:** 1329-1337.

Chibuk, T. K., J. M. Bischof and R. Wevrick, 2001 A necdin/MAGE-like gene in the chromosome 15 autism susceptibility region: expression, imprinting, and mapping of the human and mouse orthologues. BMC Genet 2**:** 22.

Chintapalli, V. R., J. Wang and J. A. Dow, 2007 Using FlyAtlas to identify better Drosophila melanogaster models of human disease. Nat Genet 39**:** 715-720.

Chiolo, I., A. Minoda, S. U. Colmenares, A. Polyzos, S. V. Costes *et al.*, 2011 Double-strand breaks in heterochromatin move outside of a dynamic HP1a domain to complete recombinational repair. Cell 144**:** 732-744.

Cho, H. J., O. L. Caballero, S. Gnjatic, V. C. Andrade, G. W. Colleoni *et al.*, 2006 Physical interaction of two cancer-testis antigens, MAGE-C1 (CT7) and NY-ESO-1 (CT6). Cancer Immun 6**:** 12.

Chomez, P., O. De Backer, M. Bertrand, E. De Plaen, T. Boon *et al.*, 2001 An overview of the MAGE gene family with the identification of all human members of the family. Cancer Res 61**:** 5544-5551.

Chong, C. E., K. P. Lim, C. P. Gan, C. A. Marsh, R. B. Zain *et al.*, 2012 Over-expression of MAGED4B increases cell migration and growth in oral squamous cell carcinoma and is associated with poor disease outcome. Cancer Lett 321**:** 18-26.

Cimprich, K. A., and D. Cortez, 2008 ATR: an essential regulator of genome integrity. Nat Rev Mol Cell Biol 9**:** 616-627.

Cuylen, S., and C. H. Haering, 2011 Deciphering condensin action during chromosome segregation. Trends Cell Biol 21**:** 552-559.

Cypess, A. M., H. Zhang, T. J. Schulz, T. L. Huang, D. O. Espinoza *et al.*, 2011 Insulin/IGF-I regulation of necdin and brown adipocyte differentiation via CREB- and FoxO1-associated pathways. Endocrinology 152**:** 3680-3689.

Czornak, K., S. Chughtai and K. H. Chrzanowska, 2008 Mystery of DNA repair: the role of the MRN complex and ATM kinase in DNA damage repair. J Appl Genet 49**:** 383-396.

De Carvalho, F., A. L. Vettore and G. W. Colleoni, 2012 Cancer/Testis Antigen MAGE-C1/CT7: new target for multiple myeloma therapy. Clin Dev Immunol 2012**:** 257695.

De Faveri, L. E., C. D. Hurst, F. M. Platt, C. F. Taylor, J. A. Roulson *et al.*, 2013 Putative tumour suppressor gene necdin is hypermethylated and mutated in human cancer. Br J Cancer 108**:** 1368-1377.

De Piccoli, G., J. Torres-Rosell and L. Aragon, 2009 The unnamed complex: what do we know about Smc5-Smc6? Chromosome Res 17**:** 251-263.

Deng, H., S. C. Hughes, J. B. Bell and A. J. Simmonds, 2009 Alternative requirements for Vestigial, Scalloped, and Dmef2 during muscle differentiation in Drosophila melanogaster. Mol Biol Cell 20**:** 256-269.

Deponti, D., S. Francois, S. Baesso, C. Sciorati, A. Innocenzi *et al.*, 2007 Necdin mediates skeletal muscle regeneration by promoting myoblast survival and differentiation. J Cell Biol 179**:** 305-319.

Devos, J., S. V. Weselake and R. Wevrick, 2011 Magel2, a Prader-Willi syndrome candidate gene, modulates the activities of circadian rhythm proteins in cultured cells. J Circadian Rhythms 9**:** 12.

Di Certo, M. G., N. Corbi, T. Bruno, S. Iezzi, F. De Nicola *et al.*, 2007 NRAGE associates with the anti-apoptotic factor Che-1 and regulates its degradation to induce cell death. J Cell Sci 120**:** 1852-1858.

Dorsett, D., and L. Strom, 2012 The ancient and evolving roles of cohesin in gene expression and DNA repair. Curr Biol 22**:** R240-250.

Downey, M., R. Houlsworth, L. Maringele, A. Rollie, M. Brehme *et al.*, 2006 A genome-wide screen identifies the evolutionarily conserved KEOPS complex as a telomere regulator. Cell 124**:** 1155-1168.

Doyle, J. M., J. Gao, J. Wang, M. Yang and P. R. Potts, 2010 MAGE-RING protein complexes comprise a family of E3 ubiquitin ligases. Mol Cell 39**:** 963-974.

Du, Q., Y. Zhang, X. X. Tian, Y. Li and W. G. Fang, 2009 MAGE-D1 inhibits proliferation, migration and invasion of human breast cancer cells. Oncol Rep 22**:** 659-665.

Duan, X., Y. Yang, Y. H. Chen, J. Arenz, G. K. Rangi *et al.*, 2009 Architecture of the Smc5/6 Complex of Saccharomyces cerevisiae Reveals a Unique Interaction between the Nse5-6 Subcomplex and the Hinge Regions of Smc5 and Smc6. J Biol Chem 284**:** 8507-8515.

Feng, Y., J. Gao and M. Yang, 2011 When MAGE meets RING: insights into biological functions of MAGE proteins. Protein Cell 2**:** 7-12.

Feng, Z., K. Li, M. Liu and C. Wen, 2010 NRAGE is a negative regulator of nerve growth factor-stimulated neurite outgrowth in PC12 cells mediated through TrkA-ERK signaling. J Neurosci Res 88**:** 1822-1828.

Francois, S., C. D'orlando, T. Fatone, T. Touvier, P. Pessina *et al.*, 2012 Necdin enhances myoblasts survival by facilitating the degradation of the mediator of apoptosis CCAR1/CARP1. PLoS One 7**:** e43335.

Fujioka, Y., Y. Kimata, K. Nomaguchi, K. Watanabe and K. Kohno, 2002 Identification of a novel non-structural maintenance of chromosomes (SMC) component of the SMC5-SMC6 complex involved in DNA repair. J Biol Chem 277**:** 21585-21591.

Fujiwara, K., K. Hasegawa, T. Ohkumo, H. Miyoshi, Y. H. Tseng *et al.*, 2012 Necdin controls proliferation of white adipocyte progenitor cells. PLoS One 7**:** e30948.

Gallego-Paez, L. M., H. Tanaka, M. Bando, M. Takahashi, N. Nozaki *et al.*, 2014 Smc5/6-mediated regulation of replication progression contributes to chromosome assembly during mitosis in human cells. Mol Biol Cell 25**:** 302-317.

Gerard, M., L. Hernandez, R. Wevrick and C. L. Stewart, 1999 Disruption of the mouse necdin gene results in early post-natal lethality. Nat Genet 23**:** 199-202.

Giot, L., J. S. Bader, C. Brouwer, A. Chaudhuri, B. Kuang *et al.*, 2003 A protein interaction map of Drosophila melanogaster. Science 302**:** 1727-1736.

Goldfine, A. B., S. Crunkhorn, M. Costello, H. Gami, E. J. Landaker *et al.*, 2006 Necdin and E2F4 are modulated by rosiglitazone therapy in diabetic human adipose and muscle tissue. Diabetes 55**:** 640-650.

Gravekamp, C., B. Leal, A. Denny, R. Bahar, S. Lampkin *et al.*, 2008 In vivo responses to vaccination with Mage-b, GM-CSF and thioglycollate in a highly metastatic mouse breast tumor model, 4T1. Cancer Immunol Immunother 57**:** 1067-1077.

Griffin, R., R. Binari and N. Perrimon, 2014 Genetic odyssey to generate marked clones in Drosophila mosaics. Proc Natl Acad Sci U S A 111**:** 4756-4763.

Guerineau, M., Z. Kriz, L. Kozakova, K. Bednarova, P. Janos *et al.*, 2012 Analysis of the Nse3/MAGE-binding domain of the Nse4/EID family proteins. PLoS One 7**:** e35813.

Gur, I., K. Fujiwara, K. Hasegawa and K. Yoshikawa, 2014 Necdin Promotes Ubiquitin-Dependent Degradation of PIAS1 SUMO E3 Ligase. PLoS One 9**:** e99503.

Han, K., 1996 An efficient DDAB-mediated transfection of Drosophila S2 cells. Nucleic Acids Res 24**:** 4362-4363.

Han, W., M. Ming and Y. Y. He, 2011 Caffeine promotes ultraviolet B-induced apoptosis in human keratinocytes without complete DNA repair. J Biol Chem 286**:** 22825-22832.

Hao, J., R. Shen, Y. Li, Y. Zhang and Y. Yin, 2014 Cancer-testis antigen HCA587/MAGE-C2 interacts with BS69 and promotes its degradation in the ubiquitin-proteasome pathway. Biochem Biophys Res Commun 449**:** 386-391.

Hao, Y. H., J. M. Doyle, S. Ramanathan, T. S. Gomez, D. Jia *et al.*, 2013 Regulation of WASH-dependent actin polymerization and protein trafficking by ubiquitination. Cell 152**:** 1051-1064.

Hartmann, S., U. Kriegebaum, N. Kuchler, G. Lessner, R. C. Brands *et al.*, 2013 Efficacy of cetuximab and panitumumab in oral squamous cell carcinoma cell lines: prognostic value of MAGE-A subgroups for treatment success. J Craniomaxillofac Surg 41**:** 623-629.

Harvey, S. H., D. M. Sheedy, A. R. Cuddihy and M. J. O'connell, 2004 Coordination of DNA damage responses via the Smc5/Smc6 complex. Mol Cell Biol 24**:** 662-674.

Hasegawa, K., T. Kawahara, K. Fujiwara, M. Shimpuku, T. Sasaki *et al.*, 2012 Necdin controls Foxo1 acetylation in hypothalamic arcuate neurons to modulate the thyroid axis. J Neurosci 32**:** 5562-5572.

Hasegawa, K., and K. Yoshikawa, 2008 Necdin regulates p53 acetylation via Sirtuin1 to modulate DNA damage response in cortical neurons. J Neurosci 28**:** 8772-8784.

Haviland, R., S. Eschrich, G. Bloom, Y. Ma, S. Minton *et al.*, 2011 Necdin, a negative growth regulator, is a novel STAT3 target gene down-regulated in human cancer. PLoS One 6**:** e24923.

Hayashi, Y., K. Matsuyama, K. Takagi, H. Sugiura and K. Yoshikawa, 1995 Arrest of cell growth by necdin, a nuclear protein expressed in postmitotic neurons. Biochem Biophys Res Commun 213**:** 317-324.

Hirano, T., 2006 At the heart of the chromosome: SMC proteins in action. Nat Rev Mol Cell Biol 7**:** 311-322.

Huang, Z., K. Fujiwara, R. Minamide, K. Hasegawa and K. Yoshikawa, 2013 Necdin controls proliferation and apoptosis of embryonic neural stem cells in an oxygen tension-dependent manner. J Neurosci 33**:** 10362-10373.

Hudson, J. J., K. Bednarova, L. Kozakova, C. Liao, M. Guerineau *et al.*, 2011 Interactions between the Nse3 and Nse4 components of the SMC5-6 complex identify evolutionarily conserved interactions between MAGE and EID Families. PLoS One 6**:** e17270.

Imai, N., H. Ikeda and H. Shiku, 2012 [Targeting cancer antigen (MAGE-A4, NY-ESO - 1) for immunotherapy]. Nihon Rinsho 70**:** 2125-2129.

Ingraham, C. A., and N. F. Schor, 2009 Necdin and TrkA contribute to modulation by p75NTR of resistance to oxidant stress. Exp Cell Res 315**:** 3532-3542.

Ingraham, C. A., L. Wertalik and N. F. Schor, 2011 Necdin and neurotrophin receptors: interactors of relevance for neuronal resistance to oxidant stress. Pediatr Res 69**:** 279-284.

Irmisch, A., E. Ampatzidou, K. Mizuno, M. J. O'connell and J. M. Murray, 2009 Smc5/6 maintains stalled replication forks in a recombination-competent conformation. EMBO J 28**:** 144-155.

Johansson, F., A. Lagerqvist, S. Filippi, F. Palitti, K. Erixon *et al.*, 2006 Caffeine delays replication fork progression and enhances UV-induced homologous recombination in Chinese hamster cell lines. DNA Repair (Amst) 5**:** 1449-1458.

Jordan, B. W., D. Dinev, V. Lemellay, J. Troppmair, R. Gotz *et al.*, 2001 Neurotrophin receptor-interacting mage homologue is an inducible inhibitor of apoptosis protein-interacting protein that augments cell death. J Biol Chem 276**:** 39985-39989.

Ju, L., J. Wing, E. Taylor, R. Brandt, P. Slijepcevic *et al.*, 2013 SMC6 is an essential gene in mice, but a hypomorphic mutant in the ATPase domain has a mild phenotype with a range of subtle abnormalities. DNA Repair (Amst) 12**:** 356-366.

Katsura, Y., and Y. Satta, 2011 Evolutionary history of the cancer immunity antigen MAGE gene family. PLoS One 6**:** e20365.

Kegel, A., and C. Sjogren, 2010 The Smc5/6 complex: more than repair? Cold Spring Harb Symp Quant Biol 75**:** 179-187.

Kim, S. H., F. Castro, D. Gonzalez, P. C. Maciag, Y. Paterson *et al.*, 2008 Mage-b vaccine delivered by recombinant Listeria monocytogenes is highly effective against breast cancer metastases. Br J Cancer 99**:** 741-749.

Kisseleva-Romanova, E., R. Lopreiato, A. Baudin-Baillieu, J. C. Rousselle, L. Ilan *et al.*, 2006 Yeast homolog of a cancer-testis antigen defines a new transcription complex. EMBO J 25**:** 3576-3585.

Klovstad, M., U. Abdu and T. Schupbach, 2008 Drosophila brca2 is required for mitotic and meiotic DNA repair and efficient activation of the meiotic recombination checkpoint. PLoS Genet 4**:** e31.

Kobayashi, M., H. Taniura and K. Yoshikawa, 2002 Ectopic expression of necdin induces differentiation of mouse neuroblastoma cells. J Biol Chem 277**:** 42128-42135.

Kondo, S., and N. Perrimon, 2011 A genome-wide RNAi screen identifies core components of the G(2)-M DNA damage checkpoint. Sci Signal 4**:** rs1.

Kozlov, S. V., J. W. Bogenpohl, M. P. Howell, R. Wevrick, S. Panda *et al.*, 2007 The imprinted gene Magel2 regulates normal circadian output. Nat Genet 39**:** 1266-1272.

Kubota, Y., M. Osawa, L. M. Jakt, K. Yoshikawa and S. Nishikawa, 2009 Necdin restricts proliferation of hematopoietic stem cells during hematopoietic regeneration. Blood 114**:** 4383-4392.

Kubu, C. J., D. G. Goldhawk, P. A. Barker and J. M. Verdi, 2000 Identification of the Translational Initiation Codon in Human MAGED1: To the Editor. Genomics 70**:** 150-152.

Kurita, M., T. Kuwajima, I. Nishimura and K. Yoshikawa, 2006 Necdin downregulates CDC2 expression to attenuate neuronal apoptosis. J Neurosci 26**:** 12003-12013.

Kuwajima, T., K. Hasegawa and K. Yoshikawa, 2010 Necdin promotes tangential migration of neocortical interneurons from basal forebrain. J Neurosci 30**:** 3709-3714.

Kuwajima, T., I. Nishimura and K. Yoshikawa, 2006 Necdin promotes GABAergic neuron differentiation in cooperation with Dlx homeodomain proteins. J Neurosci 26**:** 5383-5392.

Kuwajima, T., H. Taniura, I. Nishimura and K. Yoshikawa, 2004 Necdin interacts with the Msx2 homeodomain protein via MAGE-D1 to promote myogenic differentiation of C2C12 cells. J Biol Chem 279**:** 40484-40493.

Kuwako, K., A. Hosokawa, I. Nishimura, T. Uetsuki, M. Yamada *et al.*, 2005 Disruption of the paternal necdin gene diminishes TrkA signaling for sensory neuron survival. J Neurosci 25**:** 7090-7099.

Kuwako, K., H. Taniura and K. Yoshikawa, 2004 Necdin-related MAGE proteins differentially interact with the E2F1 transcription factor and the p75 neurotrophin receptor. J Biol Chem 279**:** 1703-1712.

Ladelfa, M. F., L. Y. Peche, M. F. Toledo, J. E. Laiseca, C. Schneider *et al.*, 2012 Tumor-specific MAGE proteins as regulators of p53 function. Cancer Lett 325**:** 11-17.

Laduron, S., R. Deplus, S. Zhou, O. Kholmanskikh, D. Godelaine *et al.*, 2004 MAGE-A1 interacts with adaptor SKIP and the deacetylase HDAC1 to repress transcription. Nucleic Acids Res 32**:** 4340-4350.

Lafontaine, J., F. Rodier, V. Ouellet and A. M. Mes-Masson, 2012 Necdin, a p53-target gene, is an inhibitor of p53-mediated growth arrest. PLoS One 7**:** e31916.

Lake, C. M., and R. S. Hawley, 2012 The molecular control of meiotic chromosomal behavior: events in early meiotic prophase in Drosophila oocytes. Annu Rev Physiol 74**:** 425-451.

Langmead, B., C. Trapnell, M. Pop and S. L. Salzberg, 2009 Ultrafast and memory-efficient alignment of short DNA sequences to the human genome. Genome Biol 10**:** R25.

Langnaese, K., D. U. Kloos, M. Wehnert, B. Seidel and P. Wieacker, 2001 Expression pattern and further characterization of human MAGED2 and identification of rodent orthologues. Cytogenetic and Genome Research 94**:** 233-240.

Laurencon, A., A. Purdy, J. Sekelsky, R. S. Hawley and T. T. Su, 2003 Phenotypic analysis of separation-of-function alleles of MEI-41, Drosophila ATM/ATR. Genetics 164**:** 589-601.

Lavi-Itzkovitz, A., M. Tcherpakov, Z. Levy, S. Itzkovitz, F. Muscatelli *et al.*, 2012 Functional consequences of necdin nucleocytoplasmic localization. PLoS One 7**:** e33786.

Lee, S., S. Kozlov, L. Hernandez, S. J. Chamberlain, C. I. Brannan *et al.*, 2000 Expression and imprinting of MAGEL2 suggest a role in Prader-willi syndrome and the homologous murine imprinting phenotype. Hum Mol Genet 9**:** 1813-1819.

Lee, S., C. L. Walker, B. Karten, S. L. Kuny, A. A. Tennese *et al.*, 2005 Essential role for the Prader-Willi syndrome protein necdin in axonal outgrowth. Hum Mol Genet 14**:** 627-637.

Lehmann, A. R., 2005 The role of SMC proteins in the responses to DNA damage. DNA Repair (Amst) 4**:** 309-314.

Li, X., S. C. Hughes and R. Wevrick 2014 Evaluation of melanoma antigen gene (MAGE) expression in human cancers using The Cancer Genome Atlas. Journal of Cancer Research and Clinical Oncology , submitted.

Li, X., R. Zhuo, S. Tiong, F. Di Cara, K. King-Jones *et al.*, 2013 The Smc5/Smc6/MAGE complex confers resistance to caffeine and genotoxic stress in Drosophila melanogaster. PLoS One 8**:** e59866.

Lin, C., 2006 The Interaction of a Novel Protein, CG13142, with DmMAGE and Dmp53 in Drosophila, pp. Southeast University.

Liu, H., J. K. Jang, N. Kato and K. S. Mckim, 2002 mei-P22 encodes a chromosome-associated protein required for the initiation of meiotic recombination in Drosophila melanogaster. Genetics 162**:** 245-258.

Liu, X., Y. Wang, Y. Zhang, W. Zhu, X. Xu *et al.*, 2009a Nogo-A inhibits necdin-accelerated neurite outgrowth by retaining necdin in the cytoplasm. Mol Cell Neurosci 41**:** 51-61.

Liu, Y., S. E. Elf, Y. Miyata, G. Sashida, Y. Liu *et al.*, 2009b p53 Regulates Hematopoietic Stem Cell Quiescence. Cell Stem Cell 4**:** 37-48.

Lopez-Sanchez, N., Z. Gonzalez-Fernandez, M. Niinobe, K. Yoshikawa and J. M. Frade, 2007 Single mage gene in the chicken genome encodes CMage, a protein with functional similarities to mammalian type II Mage proteins. Physiol Genomics 30**:** 156-171.

Lucas, S., F. Brasseur and T. Boon, 1999 A new MAGE gene with ubiquitous expression does not code for known MAGE antigens recognized by T cells. Cancer Res 59**:** 4100-4103.

Macdonald, H. R., and R. Wevrick, 1997 The necdin gene is deleted in Prader-Willi syndrome and is imprinted in human and mouse. Hum Mol Genet 6**:** 1873-1878.

Maclellan, W. R., G. Xiao, M. Abdellatif and M. D. Schneider, 2000 A novel Rb- and p300-binding protein inhibits transactivation by MyoD. Mol Cell Biol 20**:** 8903-8915.

Maggert, K. A., W. J. Gong and K. G. Golic, 2008 Methods for homologous recombination in Drosophila. Methods Mol Biol 420**:** 155-174.

Marcar, L., N. J. Maclaine, T. R. Hupp and D. W. Meek, 2010 Mage-A cancer/testis antigens inhibit p53 function by blocking its interaction with chromatin. Cancer Res 70**:** 10362-10370.

Maruyama, K., M. Usami, T. Aizawa and K. Yoshikawa, 1991 A novel brain-specific mRNA encoding nuclear protein (necdin) expressed in neurally differentiated embryonal carcinoma cells. Biochem Biophys Res Commun 178**:** 291-296.

Masuda, Y., A. Sasaki, H. Shibuya, N. Ueno, K. Ikeda *et al.*, 2001 Dlxin-1, a novel protein that binds Dlx5 and regulates its transcriptional function. J Biol Chem 276**:** 5331-5338.

Matsuda, T., H. Suzuki, I. Oishi, S. Kani, Y. Kuroda *et al.*, 2003 The receptor tyrosine kinase Ror2 associates with the melanoma-associated antigen (MAGE) family protein Dlxin-1 and regulates its intracellular distribution. J Biol Chem 278**:** 29057-29064.

Matsumoto, K., H. Taniura, T. Uetsuki and K. Yoshikawa, 2001 Necdin acts as a transcriptional repressor that interacts with multiple guanosine clusters. Gene 272**:** 173-179.

Mckim, K. S., and A. Hayashi-Hagihara, 1998 mei-W68 in Drosophila melanogaster encodes a Spo11 homolog: evidence that the mechanism for initiating meiotic recombination is conserved. Genes Dev 12**:** 2932-2942.

Meek, D. W., and L. Marcar, 2012 MAGE-A antigens as targets in tumour therapy. Cancer Lett 324**:** 126-132.

Mercer, R. E., E. M. Kwolek, J. M. Bischof, M. Van Eede, R. M. Henkelman *et al.*, 2009 Regionally reduced brain volume, altered serotonin neurochemistry, and abnormal behavior in mice null for the circadian rhythm output gene Magel2. Am J Med Genet B Neuropsychiatr Genet 150B**:** 1085-1099.

Mercer, R. E., S. D. Michaelson, M. J. Chee, T. A. Atallah, R. Wevrick *et al.*, 2013 Magel2 is required for leptin-mediated depolarization of POMC neurons in the hypothalamic arcuate nucleus in mice. PLoS Genet 9**:** e1003207.

Mercer, R. E., and R. Wevrick, 2009 Loss of magel2, a candidate gene for features of Prader-Willi syndrome, impairs reproductive function in mice. PLoS One 4**:** e4291.

Minamide, R., K. Fujiwara, K. Hasegawa and K. Yoshikawa, 2014 Antagonistic interplay between necdin and Bmi1 controls proliferation of neural precursor cells in the embryonic mouse neocortex. PLoS One 9**:** e84460.

Minges, J. T., S. Su, G. Grossman, A. J. Blackwelder, E. A. Pop *et al.*, 2012 Melanoma antigen-A11 (MAGE-A11) Enhances Transcriptional Activity by Linking Androgen Receptor Dimers. J Biol Chem 288**:** 1939-1952.

Miranda, E. I., 2010 MAGE, biological functions and potential clinical applications. Leuk Res 34**:** 1121-1122.

Miyabe, I., T. Morishita, T. Hishida, S. Yonei and H. Shinagawa, 2006 Rhp51-dependent recombination intermediates that do not generate checkpoint signal are accumulated in Schizosaccharomyces pombe rad60 and smc5/6 mutants after release from replication arrest. Mol Cell Biol 26**:** 343-353.

Monte, M., M. Simonatto, L. Y. Peche, D. R. Bublik, S. Gobessi *et al.*, 2006 MAGE-A tumor antigens target p53 transactivation function through histone deacetylase

recruitment and confer resistance to chemotherapeutic agents. Proc Natl Acad Sci U S A 103**:** 11160-11165.

Mou, D. C., X. S. Leng, J. R. Peng, L. Zhao, W. X. Wang *et al.*, 2004 [Expression of MAGE-B genes in hepatocellular carcinoma]. Zhonghua Zhong Liu Za Zhi 26**:** 40-42.

Mouri, A., A. Sasaki, K. Watanabe, C. Sogawa, S. Kitayama *et al.*, 2012 MAGE-D1 regulates expression of depression-like behavior through serotonin transporter ubiquitylation. J Neurosci 32**:** 4562-4580.

Murray, J. M., and A. M. Carr, 2008 Smc5/6: a link between DNA repair and unidirectional replication? Nat Rev Mol Cell Biol 9**:** 177-182.

Muscatelli, F., D. N. Abrous, A. Massacrier, I. Boccaccio, M. Le Moal *et al.*, 2000 Disruption of the mouse Necdin gene results in hypothalamic and behavioral alterations reminiscent of the human Prader-Willi syndrome. Hum Mol Genet 9**:** 3101-3110.

Nagashima, H., N. Sadanaga, K. Mashino, K. Yamashita, H. Inoue *et al.*, 2001 Expression of MAGE-B genes in esophageal squamous cell carcinoma. Jpn J Cancer Res 92**:** 167-173.

Nakada, Y., H. Taniura, T. Uetsuki, J. Inazawa and K. Yoshikawa, 1998 The human chromosomal gene for necdin, a neuronal growth suppressor, in the Prader-Willi syndrome deletion region. Gene 213**:** 65-72.

Nardiello, T., A. A. Jungbluth, A. Mei, M. Diliberto, X. Huang *et al.*, 2011 MAGE-A inhibits apoptosis in proliferating myeloma cells through repression of Bax and maintenance of survivin. Clin Cancer Res 17**:** 4309-4319.

Nghiem, P., P. K. Park, Y. Kim, C. Vaziri and S. L. Schreiber, 2001 ATR inhibition selectively sensitizes G1 checkpoint-deficient cells to lethal premature chromatin condensation. Proc Natl Acad Sci U S A 98**:** 9092-9097.

Nguyen, T. H., M. J. Bertrand, C. Sterpin, Y. Achouri and O. R. De Backer, 2010 Maged1, a new regulator of skeletal myogenic differentiation and muscle regeneration. BMC Cell Biol 11**:** 57.

Nishimura, I., J. Y. Sakoda and K. Yoshikawa, 2008 Drosophila MAGE controls neural precursor proliferation in postembryonic neurogenesis. Neuroscience 154**:** 572-581.

Nishimura, I., S. Shimizu, J. Y. Sakoda and K. Yoshikawa, 2007 Expression of Drosophila MAGE gene encoding a necdin homologous protein in postembryonic neurogenesis. Gene Expr Patterns 7**:** 244-251.

Palecek, J., S. Vidot, M. Feng, A. J. Doherty and A. R. Lehmann, 2006 The Smc5-Smc6 DNA repair complex. bridging of the Smc5-Smc6 heads by the KLEISIN, Nse4, and non-Kleisin subunits. J Biol Chem 281**:** 36952-36959.

Pandey, U. B., and C. D. Nichols, 2011 Human disease models in Drosophila melanogaster and the role of the fly in therapeutic drug discovery. Pharmacol Rev 63**:** 411-436.

Papadopoulos, J. S., and R. Agarwala, 2007 COBALT: constraint-based alignment tool for multiple protein sequences. Bioinformatics 23**:** 1073-1079.

Papageorgio, C., R. Brachmann, J. Zeng, R. Culverhouse, W. Zhang *et al.*, 2007 MAGED2: a novel p53-dissociator. Int J Oncol 31**:** 1205-1211.

Pebernard, S., W. H. Mcdonald, Y. Pavlova, J. R. Yates, 3rd and M. N. Boddy, 2004 Nse1, Nse2, and a novel subunit of the Smc5-Smc6 complex, Nse3, play a crucial role in meiosis. Mol Biol Cell 15**:** 4866-4876.

Pebernard, S., J. Wohlschlegel, W. H. Mcdonald, J. R. Yates, 3rd and M. N. Boddy, 2006 The Nse5-Nse6 dimer mediates DNA repair roles of the Smc5-Smc6 complex. Mol Cell Biol 26**:** 1617-1630.

Peche, L. Y., M. Scolz, M. F. Ladelfa, M. Monte and C. Schneider, 2012 MageA2 restrains cellular senescence by targeting the function of PMLIV/p53 axis at the PML-NBs. Cell Death Differ 19**:** 926-936.

Pessina, P., V. Conti, R. Tonlorenzi, T. Touvier, R. Meneveri *et al.*, 2012 Necdin enhances muscle reconstitution of dystrophic muscle by vessel-associated progenitors, by promoting cell survival and myogenic differentiation. Cell Death Differ 19**:** 827-838.

Pold, M., A. Pold, H. J. Ma, N. N. Sjak-Shieb, R. A. Vescio *et al.*, 2000 Cloning of the first invertebrate MAGE paralogue: an epitope that activates T-cells in humans is highly conserved in evolution. Dev Comp Immunol 24**:** 719-731.

Pold, M., J. Zhou, G. L. Chen, J. M. Hall, R. A. Vescio *et al.*, 1999 Identification of a new, unorthodox member of the MAGE gene family. Genomics 59**:** 161-167.

Potts, P. R., and H. Yu, 2005 Human MMS21/NSE2 is a SUMO ligase required for DNA repair. Mol Cell Biol 25**:** 7021-7032.

Potts, P. R., and H. Yu, 2007 The SMC5/6 complex maintains telomere length in ALT cancer cells through SUMOylation of telomere-binding proteins. Nat Struct Mol Biol 14**:** 581-590.

Rai, R., S. P. Varma, N. Shinde, S. Ghosh, S. P. Kumaran *et al.*, 2011 Small ubiquitin-related modifier ligase activity of Mms21 is required for maintenance of chromosome integrity during the unperturbed mitotic cell division cycle in Saccharomyces cerevisiae. J Biol Chem 286**:** 14516-14530.

Reddy, E. M., S. T. Chettiar, N. Kaur, R. Ganeshkumar, V. Shepal *et al.*, 2011 Dlxin-1, a member of MAGE family, inhibits cell proliferation, invasion and tumorigenicity of glioma stem cells. Cancer Gene Ther 18**:** 206-218.

Reddy, E. M., S. T. Chettiar, N. Kaur, V. Shepal and A. Shiras, 2010 Dlxin-1, a MAGE family protein, induces accelerated neurite outgrowth and cell survival by enhanced and early activation of MEK and Akt signalling pathways in PC12 cells. Exp Cell Res 316**:** 2220-2236.

Rogers, S. L., and G. C. Rogers, 2008 Culture of Drosophila S2 cells and their use for RNAi-mediated loss-of-function studies and immunofluorescence microscopy. Nat Protoc 3**:** 606-611.

Ross, M. T., D. V. Grafham, A. J. Coffey, S. Scherer, K. Mclay *et al.*, 2005 The DNA sequence of the human X chromosome. Nature 434**:** 325-337.

Saburi, S., D. Nadano, T. O. Akama, K. Hirama, K. Yamanouchi *et al.*, 2001 The trophinin gene encodes a novel group of MAGE proteins, magphinins, and regulates cell proliferation during gametogenesis in the mouse. J Biol Chem 276**:** 49378-49389.

Sakurai, T., K. Itoh, H. Higashitsuji, T. Nagao, K. Nonoguchi *et al.*, 2004 A cleaved form of MAGE-A4 binds to Miz-1 and induces apoptosis in human cells. J Biol Chem 279**:** 15505-15514.

Salehi, A. H., P. P. Roux, C. J. Kubu, C. Zeindler, A. Bhakar *et al.*, 2000 NRAGE, a novel MAGE protein, interacts with the p75 neurotrophin receptor and facilitates nerve growth factor-dependent apoptosis. Neuron 27**:** 279-288.

Sang, M., Y. Lian, X. Zhou and B. Shan, 2011a MAGE-A family: attractive targets for cancer immunotherapy. Vaccine 29**:** 8496-8500.

Sang, M., L. Wang, C. Ding, X. Zhou, B. Wang *et al.*, 2011b Melanoma-associated antigen genes - an update. Cancer Lett 302**:** 85-90.

Sarkaria, J. N., E. C. Busby, R. S. Tibbetts, P. Roos, Y. Taya *et al.*, 1999 Inhibition of ATM and ATR kinase activities by the radiosensitizing agent, caffeine. Cancer Res 59**:** 4375-4382.

Sasaki, A., L. Hinck and K. Watanabe, 2005 RumMAGE-D the members: structure and function of a new adaptor family of MAGE-D proteins. J Recept Signal Transduct Res 25**:** 181-198.

Sasaki, A., Y. Masuda, K. Iwai, K. Ikeda and K. Watanabe, 2002 A RING finger protein Praja1 regulates Dlx5-dependent transcription through its ubiquitin ligase activity for the Dlx/Msx-interacting MAGE/Necdin family protein, Dlxin-1. J Biol Chem 277**:** 22541-22546.

Schaller, F., F. Watrin, R. Sturny, A. Massacrier, P. Szepetowski *et al.*, 2010 A single postnatal injection of oxytocin rescues the lethal feeding behaviour in mouse newborns deficient for the imprinted Magel2 gene. Hum Mol Genet 19**:** 4895-4905.

Sekelsky, J. J., M. H. Brodsky and K. C. Burtis, 2000 DNA repair in Drosophila: insights from the Drosophila genome sequence. J Cell Biol 150**:** F31-36.

Sepp, K. J., P. Hong, S. B. Lizarraga, J. S. Liu, L. A. Mejia *et al.*, 2008 Identification of neural outgrowth genes using genome-wide RNAi. 4**:** e1000111.

Sergeant, J., E. Taylor, J. Palecek, M. Fousteri, E. A. Andrews *et al.*, 2005 Composition and architecture of the Schizosaccharomyces pombe Rad18 (Smc5-6) complex. Mol Cell Biol 25**:** 172-184.

Silva, E., S. Tiong, M. Pedersen, E. Homola, A. Royou *et al.*, 2004 ATM is required for telomere maintenance and chromosome stability during Drosophila development. Curr Biol 14**:** 1341-1347.

Silva, E. A., B. J. Lee, L. S. Caceres, D. Renouf, B. R. Vilay *et al.*, 2006 A novel strategy for identifying mutations that sensitize Drosophila eye development to caffeine and hydroxyurea. Genome 49**:** 1416-1427.

Simpson, A. J., O. L. Caballero, A. Jungbluth, Y. T. Chen and L. J. Old, 2005 Cancer/testis antigens, gametogenesis and cancer. Nat Rev Cancer 5**:** 615-625.

Singh, M., I. Ramos, D. Asafu-Adjei, W. Quispe-Tintaya, D. Chandra *et al.*, 2013 Curcumin improves the therapeutic efficacy of Listeria(at)-Mage-b vaccine in correlation with improved T-cell responses in blood of a triple-negative breast cancer model 4T1. Cancer Med 2**:** 571-582.

Sollier, J., R. Driscoll, F. Castellucci, M. Foiani, S. P. Jackson *et al.*, 2009 The Saccharomyces cerevisiae Esc2 and Smc5-6 proteins promote sister chromatid junction-mediated intra-S repair. Mol Biol Cell 20**:** 1671-1682.

Sortibran, A. N., M. G. Tellez and R. Rodriguez-Arnaiz, 2006 Genotoxic profile of inhibitors of topoisomerases I (camptothecin) and II (etoposide) in a mitotic recombination and sex-chromosome loss somatic eye assay of Drosophila melanogaster. Mutat Res 604**:** 83-90.

Srinivasan, M., P. Mehta, Y. Yu, E. Prugar, E. V. Koonin *et al.*, 2011 The highly conserved KEOPS/EKC complex is essential for a universal tRNA modification, t6A. EMBO J 30**:** 873-881.

St Johnston, D., 2013 Using mutants, knockdowns, and transgenesis to investigate gene function in Drosophila. Wiley Interdiscip Rev Dev Biol 2**:** 587-613.

Stephan, A. K., M. Kliszczak, H. Dodson, C. Cooley and C. G. Morrison, 2011a Roles of vertebrate Smc5 in sister chromatid cohesion and homologous recombinational repair. Mol Cell Biol.

Stephan, A. K., M. Kliszczak, H. Dodson, C. Cooley and C. G. Morrison, 2011b Roles of vertebrate Smc5 in sister chromatid cohesion and homologous recombinational repair. Mol Cell Biol 31**:** 1369-1381.

Stephan, A. K., M. Kliszczak and C. G. Morrison, 2011c The Nse2/Mms21 SUMO ligase of the Smc5/6 complex in the maintenance of genome stability. FEBS Lett 585**:** 2907-2913.

Stone, B., M. Schummer, P. J. Paley, M. Crawford, M. Ford *et al.*, 2001 MAGE-F1, a novel ubiquitously expressed member of the MAGE superfamily. Gene 267**:** 173-182.

Stowers, R. S., and T. L. Schwarz, 1999 A genetic method for generating Drosophila eyes composed exclusively of mitotic clones of a single genotype. Genetics 152**:** 1631-1639.

Su, S., A. J. Blackwelder, G. Grossman, J. T. Minges, L. Yuan *et al.*, 2012 Primate-specific melanoma antigen-A11 regulates isoform-specific human progesterone receptor-B transactivation. J Biol Chem 287**:** 34809-34824.

Su, S., J. T. Minges, G. Grossman, A. J. Blackwelder, J. L. Mohler *et al.*, 2013 Proto-oncogene activity of melanoma antigen-A11 (MAGE-A11) regulates retinoblastoma-related p107 and E2F1 proteins. J Biol Chem 288**:** 24809-24824.

Sullivan, W., M. Ashburner and R. S. Hawley, 2000 *Drosophila protocols*. Cold Spring Harbor Laboratory Press, Cold Spring Harbor, N.Y.

Sutcliffe, J. S., M. Han, S. L. Christian and D. H. Ledbetter, 1997 Neuronally-expressed necdin gene: an imprinted candidate gene in Prader-Willi syndrome. Lancet 350**:** 1520-1521.

Sypniewska, R. K., L. Hoflack, M. Tarango, S. Gauntt, B. Z. Leal *et al.*, 2005 Prevention of metastases with a Mage-b DNA vaccine in a mouse breast tumor model: potential for breast cancer therapy. Breast Cancer Res Treat 91**:** 19-28.

Takazaki, R., I. Nishimura and K. Yoshikawa, 2002 Necdin is required for terminal differentiation and survival of primary dorsal root ganglion neurons. Exp Cell Res 277**:** 220-232.

Taniguchi, N., H. Taniura, M. Niinobe, C. Takayama, K. Tominaga-Yoshino *et al.*, 2000 The postmitotic growth suppressor necdin interacts with a calcium-binding protein (NEFA) in neuronal cytoplasm. J Biol Chem 275**:** 31674-31681.

Taniura, H., K. Matsumoto and K. Yoshikawa, 1999 Physical and functional interactions of neuronal growth suppressor necdin with p53. J Biol Chem 274**:** 16242-16248.

Taniura, H., N. Taniguchi, M. Hara and K. Yoshikawa, 1998 Necdin, a postmitotic neuron-specific growth suppressor, interacts with viral transforming proteins and cellular transcription factor E2F1. J Biol Chem 273**:** 720-728.

Taniura, H., and K. Yoshikawa, 2002 Necdin interacts with the ribonucleoprotein hnRNP U in the nuclear matrix. J Cell Biochem 84**:** 545-555.

Taylor, E. M., A. C. Copsey, J. J. Hudson, S. Vidot and A. R. Lehmann, 2008 Identification of the proteins, including MAGEG1, that make up the human SMC5-6 protein complex. Mol Cell Biol 28**:** 1197-1206.

Taylor, E. M., J. S. Moghraby, J. H. Lees, B. Smit, P. B. Moens *et al.*, 2001 Characterization of a novel human SMC heterodimer homologous to the Schizosaccharomyces pombe Rad18/Spr18 complex. Mol Biol Cell 12**:** 1583-1594.

Tcherpakov, M., F. C. Bronfman, S. G. Conticello, A. Vaskovsky, Z. Levy *et al.*, 2002 The p75 neurotrophin receptor interacts with multiple MAGE proteins. J Biol Chem 277**:** 49101-49104.

Tennese, A. A., C. B. Gee and R. Wevrick, 2008 Loss of the Prader-Willi syndrome protein necdin causes defective migration, axonal outgrowth, and survival of embryonic sympathetic neurons. Dev Dyn 237**:** 1935-1943.

Tennese, A. A., and R. Wevrick, 2011 Impaired hypothalamic regulation of endocrine function and delayed counterregulatory response to hypoglycemia in Magel2-null mice. Endocrinology 152**:** 967-978.

Thomas, B. J., and S. L. Zipursky, 1994 Early pattern formation in the developing Drosophila eye. Trends Cell Biol 4**:** 389-394.

Tian, X. X., D. Rai, J. Li, C. Zou, Y. Bai *et al.*, 2005 BRCA2 suppresses cell proliferation via stabilizing MAGE-D1. Cancer Res 65**:** 4747-4753.

Toba, G., T. Ohsako, N. Miyata, T. Ohtsuka, K. H. Seong *et al.*, 1999 The gene search system. A method for efficient detection and rapid molecular identification of genes in Drosophila melanogaster. Genetics 151**:** 725-737.

Torres-Rosell, J., F. Machin, S. Farmer, A. Jarmuz, T. Eydmann *et al.*, 2005 SMC5 and SMC6 genes are required for the segregation of repetitive chromosome regions. Nat Cell Biol 7**:** 412-419.

Tsai, T. F., D. Armstrong and A. L. Beaudet, 1999 Necdin-deficient mice do not show lethality or the obesity and infertility of Prader-Willi syndrome. Nat Genet 22**:** 15-16.

Tseng, H. Y., L. H. Chen, Y. Ye, K. H. Tay, C. C. Jiang *et al.*, 2012 The melanoma-associated antigen MAGE-D2 suppresses TRAIL receptor 2 and protects against TRAIL-induced apoptosis in human melanoma cells. Carcinogenesis 33**:** 1871-1881.

Tseng, Y. H., A. J. Butte, E. Kokkotou, V. K. Yechoor, C. M. Taniguchi *et al.*, 2005 Prediction of preadipocyte differentiation by gene expression reveals role of insulin receptor substrates and necdin. Nat Cell Biol 7**:** 601-611.

Uetsuki, T., K. Takagi, H. Sugiura and K. Yoshikawa, 1996 Structure and expression of the mouse necdin gene. Identification of a postmitotic neuron-restrictive core promoter. J Biol Chem 271**:** 918-924.

Van Der Bruggen, P., C. Traversari, P. Chomez, C. Lurquin, E. De Plaen *et al.*, 1991 A gene encoding an antigen recognized by cytolytic T lymphocytes on a human melanoma. Science 254**:** 1643-1647.

Veraksa, A., A. Bauer and S. Artavanis-Tsakonas, 2005 Analyzing protein complexes in Drosophila with tandem affinity purification-mass spectrometry. Dev Dyn 232**:** 827-834.

Verkade, H. M., S. J. Bugg, H. D. Lindsay, A. M. Carr and M. J. O'connell, 1999 Rad18 is required for DNA repair and checkpoint responses in fission yeast. Mol Biol Cell 10**:** 2905-2918.

Wang, X., J. Tang, L. Xing, G. Shi, H. Ruan *et al.*, 2010 Interaction of MAGED1 with nuclear receptors affects circadian clock function. EMBO J 29**:** 1389-1400.

Wang, Y., L. Y. Geer, C. Chappey, J. A. Kans and S. H. Bryant, 2000 Cn3D: sequence and structure views for Entrez. Trends Biochem Sci 25**:** 300-302.

Watanabe, K., M. Pacher, S. Dukowic, V. Schubert, H. Puchta *et al.*, 2009 The STRUCTURAL MAINTENANCE OF CHROMOSOMES 5/6 Complex Promotes Sister Chromatid Alignment and Homologous Recombination after DNA Damage in Arabidopsis thaliana. Plant Cell 21**:** 2688-2699.

Waterhouse, A. M., J. B. Procter, D. M. Martin, M. Clamp and G. J. Barton, 2009 Jalview Version 2--a multiple sequence alignment editor and analysis workbench. Bioinformatics 25**:** 1189-1191.

Weeraratne, S. D., V. Amani, A. Neiss, N. Teider, D. K. Scott *et al.*, 2011 miR-34a confers chemosensitivity through modulation of MAGE-A and p53 in medulloblastoma. Neuro Oncol 13**:** 165-175.

Wen, C. J., B. Xue, W. X. Qin, M. Yu, M. Y. Zhang *et al.*, 2004 hNRAGE, a human neurotrophin receptor interacting MAGE homologue, regulates p53 transcriptional activity and inhibits cell proliferation. FEBS Lett 564**:** 171-176.

Williams, M. E., P. Strickland, K. Watanabe and L. Hinck, 2003 UNC5H1 induces apoptosis via its juxtamembrane region through an interaction with NRAGE. J Biol Chem 278**:** 17483-17490.

Wong, K. M., T. J. Hudson and J. D. Mcpherson, 2011 Unraveling the genetics of cancer: genome sequencing and beyond. Annu Rev Genomics Hum Genet 12**:** 407-430.

Wu, N., and H. Yu, 2012 The Smc complexes in DNA damage response. Cell Biosci 2**:** 5.

Xiao, T. Z., N. Bhatia, R. Urrutia, G. A. Lomberk, A. Simpson *et al.*, 2011 MAGE I transcription factors regulate KAP1 and KRAB domain zinc finger transcription factor mediated gene repression. PLoS One 6**:** e23747.

Yang, B., S. M. O'herrin, J. Wu, S. Reagan-Shaw, Y. Ma *et al.*, 2007 MAGE-A, mMage-b, and MAGE-C proteins form complexes with KAP1 and suppress p53-dependent apoptosis in MAGE-positive cell lines. Cancer Res 67**:** 9954-9962.

Zhao, X., and G. Blobel, 2005 A SUMO ligase is part of a nuclear multiprotein complex that affects DNA repair and chromosomal organization. Proc Natl Acad Sci U S A 102**:** 4777-4782.

Zhao, Z., F. Lu, F. Zhu, H. Yang, Y. Chai *et al.*, 2002 Cloning and biological comparison of Restin, novel member of Mage superfamily. Sci China C Life Sci 45**:** 412-420.

Zhu, N. L., J. Wang and H. Tsukamoto, 2010 The Necdin-Wnt pathway causes epigenetic peroxisome proliferator-activated receptor gamma repression in hepatic stellate cells. J Biol Chem 285**:** 30463-30471.

Appendices

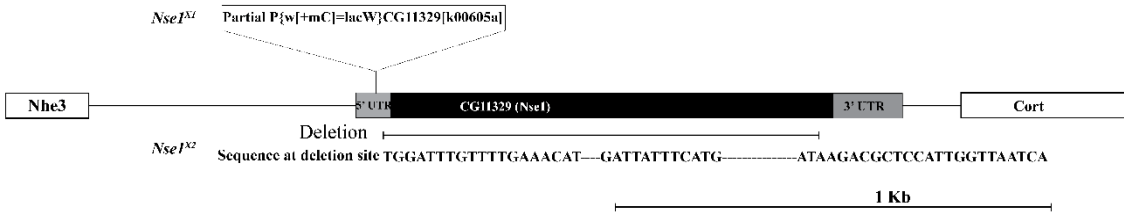

Appendix figure 1 *Nse1* mutants

Two *Nse1* alleles were produced by imprecise excision of *P{w[+mC]=lacW}CG11329[k00605a]* (BDSC 10480, the second site lethal (*l(2)k00605b[k00605b]*) linked to the P in this line was crossed out before the excision experiment was carried out). For the *X1* allele, the p element was partially removed at C terminus, leaving a fragment in the 5' regulatory sequence of the gene. For the *X2* allele, the entire coding sequence was largely removed.

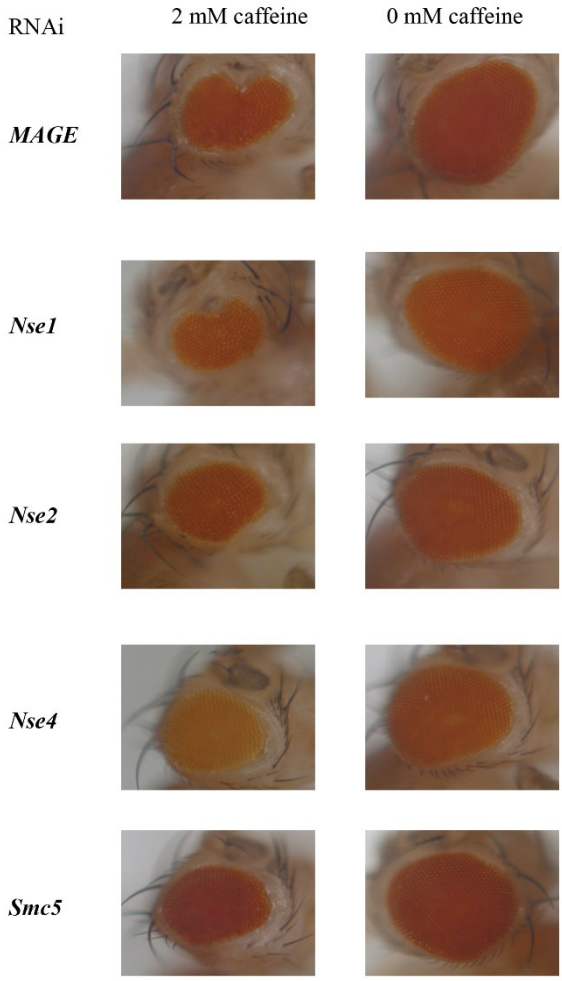

Appendix figure 2 Depletion of Smc5/6 genes in developing eye discs results in a caffeine dependent small eye phenotype.

UASRNAi flies were crossed to Drc2/Drc2; ey-GAL4/ey-GAL4 flies and the progeny were raised in caffeine or no caffeine food. Representative eyes for each gene are shown. UASRNAi flies were obtained from DGRC or VDRC: *MAGE (10865), Nse2 (55291), Nse4 (24511),* and *Smc5 (38969).*

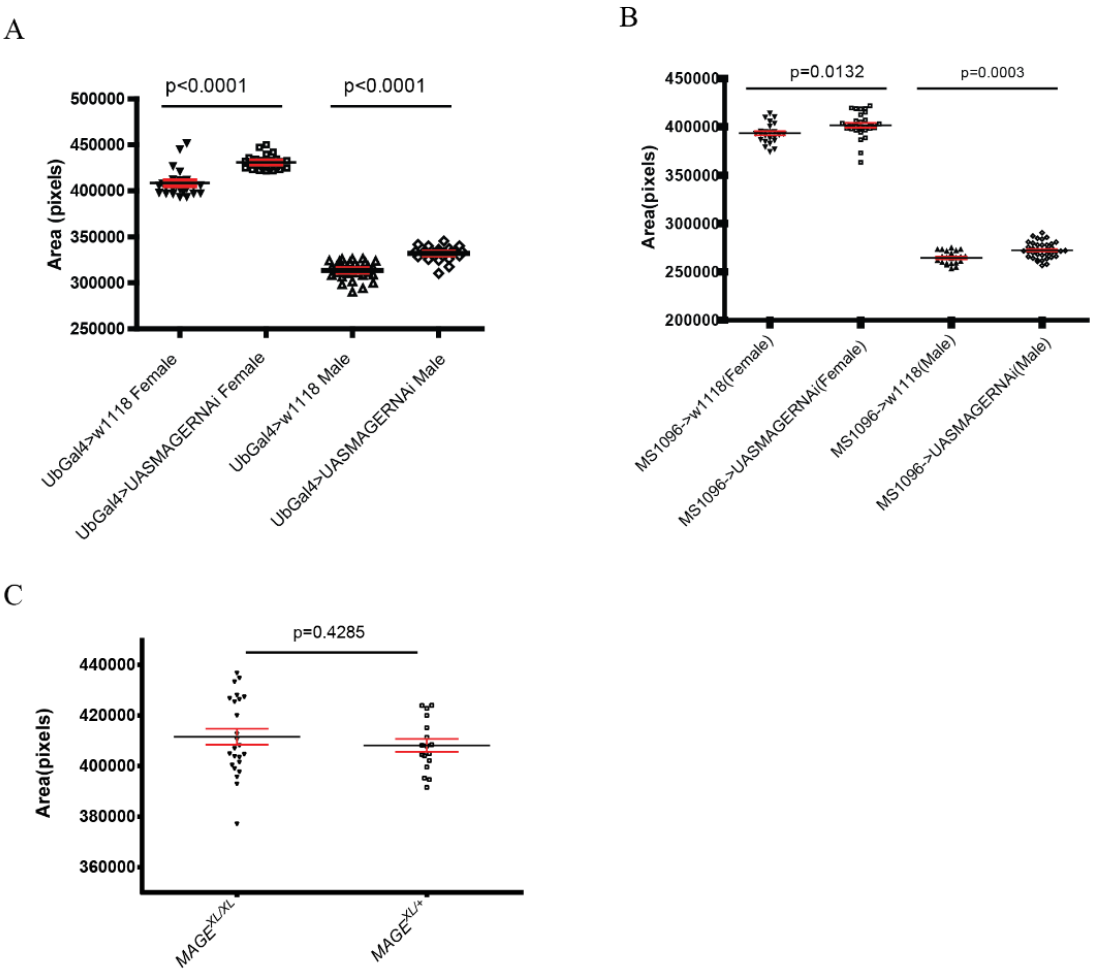

Appendix figure 3 (A) Wing size of *UbiGAL4>MAGE_RNAi*, (B) *MS1096GAL4 >MAGE_RNAi* and (C*) MAGE*$^{XL/XL}$

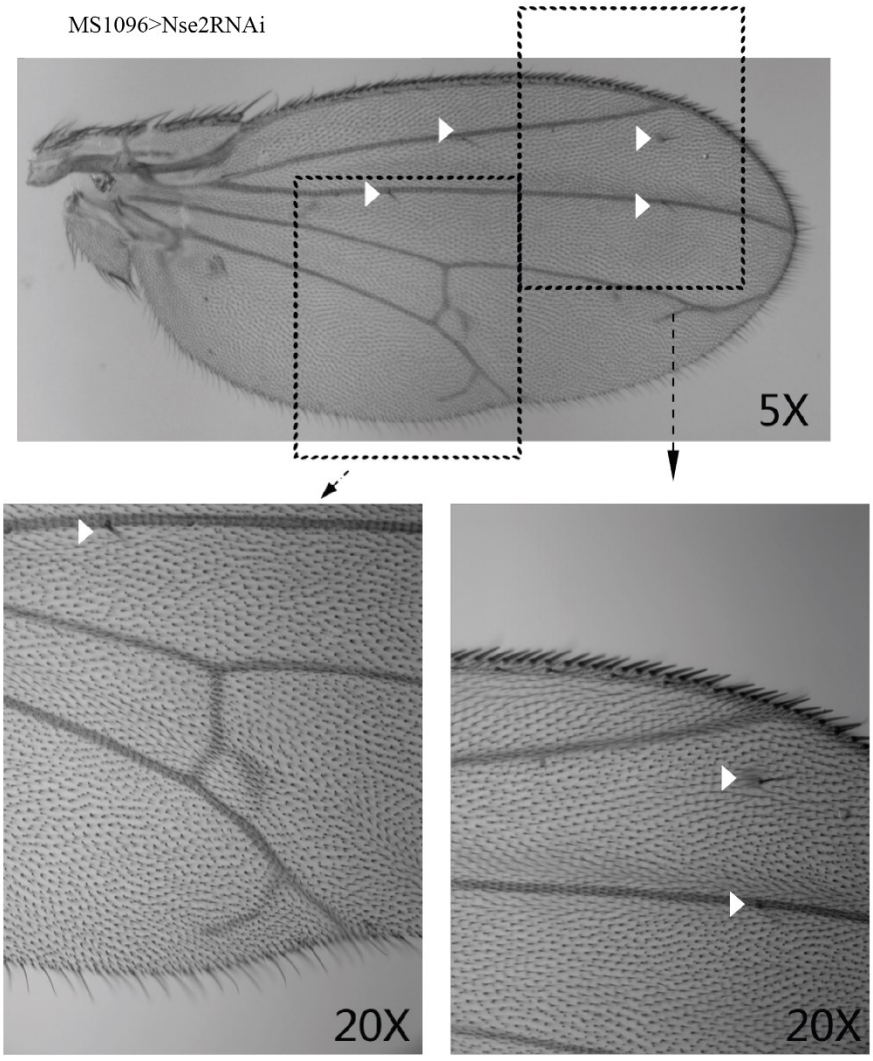

Appendix figure 4 Depletion of Nse2 using RNAi in the developing wing discs produces ectopic mechanosensory bristles (white triangles) in adult wings. The Nse2 RNAi line (20206) was obtained from VDRC.

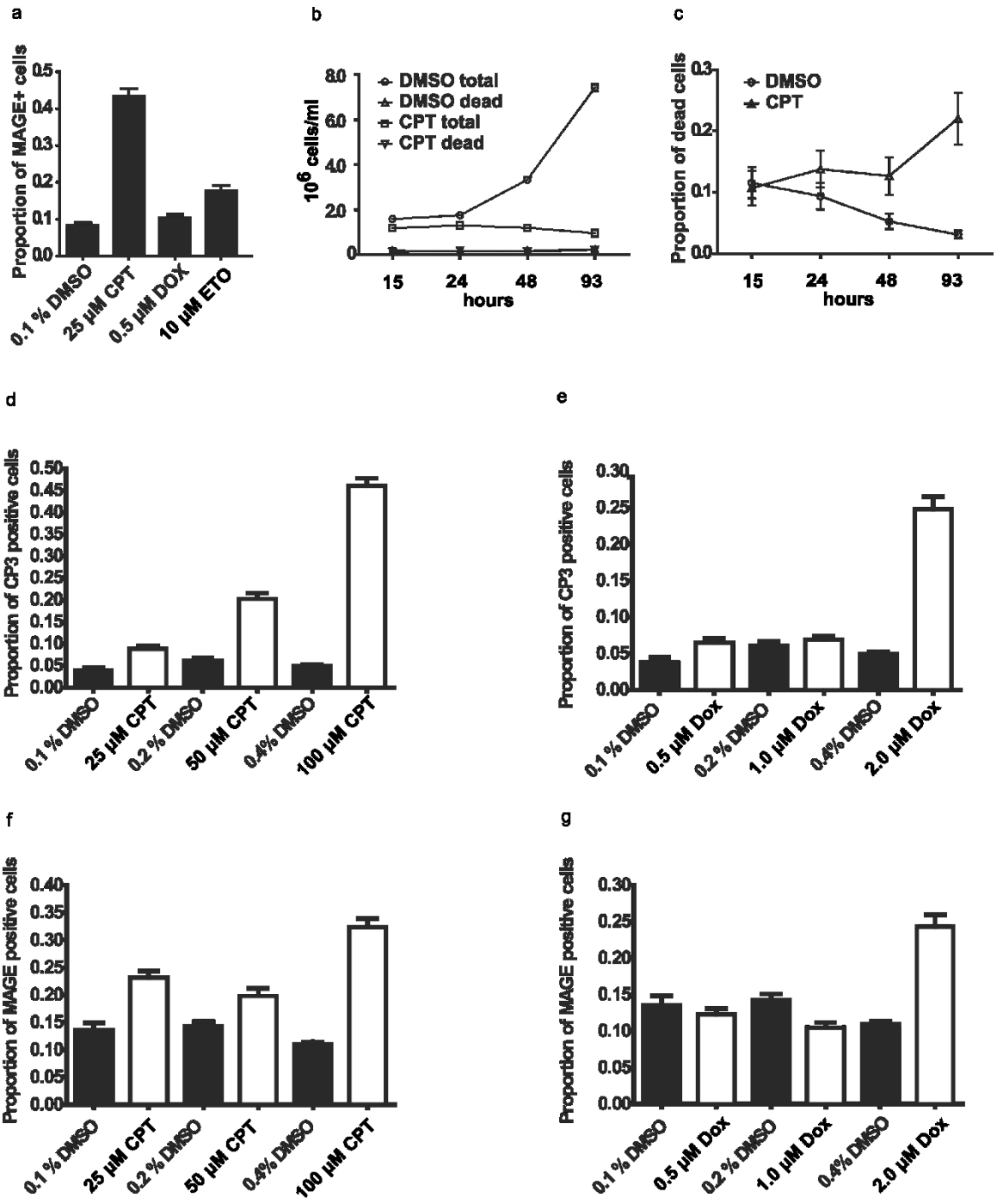
a
Proportion of MAGE+ cells
0.5
0.4
0.3
0.2
0.1
0.0
0.1 % DMSO
25 µM CPT
0.5 µM DOX
10 µM ETO
b
10^6 cells/ml
8.0
6.0
4.0
2.0
0
DMSO total
DMSO dead
CPT total
CPT dead
15
24
48
93
hours
c
Proportion of dead cells
0.3
0.2
0.1
0.0
DMSO
CPT
15
24
48
93
hours
d
Proportion of CP3 positive cells
0.50
0.45
0.40
0.35
0.30
0.25
0.20
0.15
0.10
0.05
0.00
0.1 % DMSO
25 µM CPT
0.2 % DMSO
50 µM CPT
0.4% DMSO
100 µM CPT
e
Proportion of CP3 positive cells
0.30
0.25
0.20
0.15
0.10
0.05
0.00
0.1 % DMSO
0.5 µM Dox
0.2 % DMSO
1.0 µM Dox
0.4% DMSO
2.0 µM Dox
f
Proportion of MAGE positive cells
0.40
0.35
0.30
0.25
0.20
0.15
0.10
0.05
0.00
0.1 % DMSO
25 µM CPT
0.2 % DMSO
50 µM CPT
0.4% DMSO
100 µM CPT
g
Proportion of MAGE positive cells
0.30
0.25
0.20
0.15
0.10
0.05
0.00
0.1 % DMSO
0.5 µM Dox
0.2 % DMSO
1.0 µM Dox
0.4% DMSO
2.0 µM Dox

Appendix figure 5 Over-expression of Mage confers resistance to DNA damage agents.

a. Mage+ cells are enriched among live cells treated with camptothecin (CPT, 25 μM), and etoposide (ETO, 10 μM) but not doxorubicin (DOX, 0.5 μM). Drugs were added into media 24 hours after induction of Mage-V5 expression. Cell re-attachment was measured after another 24 hours. To measure cell reattachment, cells were detached by pipetting the culture up and down. An aliquot of the cell suspension was added to 200-500 μl of fresh SFX medium on a coverslip placed in a well of a 6-well culture plate. Cells were allowed to settle and reattach for 30 min. Cells that were unable to reattach were removed by pipetting the medium off the coverslip. A solution of 2% paraformaldehyde in PBS was added into the well to gently cover the coverslip to fix the cells.

b, c. CPT inhibits cell proliferation and induces cell death. Equal amount of S2 cells were plated at 0 hour and CPT or the vehicle (DMSO) were added into the media. The number of cells per ml was determined by hemocytometer counting at the indicated time pointed. Dead cells were defined by the inability to exclude trypan blue. Numbers represent the average of three replicates.

d, f . Mage protects cells from CPT induced cell death. (d) CPT (25, 50 or 100 μM) induces apoptosis in a dose-dependent manner as measured by activated caspase 3 immunocytochemistry. (f) Mage+ cells were enriched after CPT treatment also in a dose-dependent manner.

e, g Mage protects cells from DOX induced cell death. (b) DOX induces noticeable apoptosis at a higher concentration (2 μM) but not at two lower concentration (0.5 and 1.0 μM) and (d) Mage+ cells were enriched at the concentration but not at the two lower concentration.

d-g Cells were resuspended and fixed 24 hours after drug treatment (i.e. 48 hours after induction of Mage-V5 expression).

a, d-g Fixed cells were immunostained with an antibody to mark apoptotic cells (d-g) or an V5 antibody (a, d-g) to mark Mage+ cells. The proportion of Mage+ cells was determined by normalizing the number of positive cells with the total number of cells as defined by the number of DAPI stained nuclei. Error bars represent SE of the mean.

Genotype	caffeine (0 mM)	caffeine (0.25 mM)	caffeine (0.5 mM)	Water	MMS (0.005%)	HU (4 mM)
Nse1 $^{X1/df}$	104	36	0	138	3	45
Nse1 $^{X1/+}$	121	124	134	123	93	108
	caffeine (0 mM)	caffeine (0.125 mM)	caffeine (0.25 mM)	DMSO	CPT (25 mM)	
Nse1 $^{X2/X2}$	350	200	4	707	228	
Nse1 $^{X2/+}$	642	1241	797	666	800	

Appendix table 1 *Nse1* mutants are sensitive to caffeine, MMS, HU and CPT.

Female genotype	Hatch rate of eggs produced by females	SE	N
$Smc5^{p7/p5}$	70.4%	3.4%	179
$Smc5^{p5/df}$	77.0%	2.6%	265
w^{1118}	85.3%	2.6%	190
$Smc5^{p7/df}$	74.0%	4.4%	100
$Smc5^{df/+}$	87.0%	3.4%	100
$Smc5^{p7/+}$	90.0%	3.0%	100
$Smc6^{X1/R1}$	72.0%	4.5%	100
$Smc6^{X1/+}$	99.0%	1.0%	100
$Nse1^{X1/df}$	8.0%	2.7%	100
$Nse1^{X1/+}$	99.0%	1.0%	100
$Nse1^{X1/df}$	27.0%	4.4%	100
$Nse1^{X1/+}$	90.0%	3.0%	100
$Nse1^{X2/df}$	12.4%	3.3%	100
$MAGE^{XL/RZ}$	69.2%	1.9%	614
$MAGE^{XL/XL}$	32.1%	1.9%	611
w^{1118}	89.3%	1.2%	625

Appendix table 2 Embryos from *Smc5*, *Smc6*, *Nse1*, and *MAGE* mutant mothers have reduced hatch rate.

Two to four day old virgin females were crossed to w^{1118} males and allowed to lay eggs on apple juice agar plate supplemented with yeast paste. Hatch rate was scored 26~48 hours after egg laying.